Standard solar models, with and without helium diffusion, and the solar neutrino problem

J. N. Bahcall

School of Natural Sciences, Institute for Advanced Study, Princeton, New Jersey 08540

M. H. Pinsonneault

Department of Astronomy, Yale University, New Haven, Connecticut 06511

We first show that, with the same input parameters, the standard solar models of Bahcall and Ulrich; of Sienkiewicz, Bahcall, and Paczyński; of Turck-Chièze, Cahen, Cassé, and Doom; and of the current Yale code all predict event rates for the chlorine experiment that are the same within ±0.1 SNU (solar neutrino units), i.e., approximately 1% of the total calculated rate. We then construct new standard solar models using the Yale stellar evolution computer code supplemented with a more accurate (exportable) nuclear energy generation routine, an improved equation of state, recent determinations of element abundances, and the new Livermore (OPAL) opacity calculations. We evaluate the individual effects of different improvements by calculating a series of precise models, changing only one aspect of the solar model at a time. We next add a new subroutine that calculates the diffusion of helium with respect to hydrogen with the aid of the Bahcall-Loeb formalism. Finally, we compare the neutrino fluxes computed from our best solar models constructed with and without helium diffusion. We find that helium diffusion increases the predicted event rates by about 0.8 SNU, or 11% of the total rate, in the chlorine experiment; by about 3.5 SNU, or 3%, in the gallium experiments; and by about 12% in the Kamiokande and SNO experiments. The best standard solar model including helium diffusion and the most accurate nuclear parameters, element abundances, radiative opacity, and equation of state predicts a value of 8.0±3.0 SNU for the ^{37}Cl experiment and 132^{+21}_{-17} SNU for the ^{71}Ga experiment. The quoted errors represent the total theoretical range and include the effects on the model predictions of 3σ errors in measured input parameters. All 15 calculations since 1968 of the predicted rate in the chlorine experiment given in this series of papers are consistent with both the range estimated in the present work and the 1968 best-estimate value of 7.5±2.3 SNU. Including the effects of helium diffusion and the other improvements in the description of the solar interior that are implemented in this paper, the inferred primordial solar helium abundance is $Y=0.273$. The calculated depth of the convective zone is $R=0.707R_\odot$, in agreement with the value of $0.713R_\odot$ inferred by Christensen-Dalsgaard, Gough, and Thompson from a recent analysis of the observed p-mode oscillation frequencies. Including helium diffusion increases the calculated present-day hydrogen surface abundance by about 4%, decreases the helium abundance by approximately 11%, and increases the calculated heavy-element abundance by about 4%. In the Appendix, we present detailed numerical tables of our best standard solar models computed both with and without including helium diffusion. In the context of the MSW (Mikheyev-Smirnov-Wolfenstein) or other weak-interaction solutions of the solar neutrino problem, the numerical models can be used to compute the influence of the matter in the sun on the observed neutrino fluxes.

CONTENTS

I. Introduction 885
A. The plan of this paper 886
B. Solar neutrino experiments in progress 887
C. New physics? 889
II. Nuclear Energy Generation 890
A. Energy generation subroutine 890
B. Some individual reaction rates 890
1. Comparison of different cross-section factors 890
2. The *pp* rate 890
3. The *hep* rate 892
C. Comparison of nuclear rates in different stellar evolution codes 893
1. Bahcall and Ulrich 893
2. Sienkiewicz *et al.* 893
3. Turck-Chièze *et al.* 893
4. Sackmann, Boothroyd, and Fowler 894
III. Other Input Data 894
A. Opacities 895
B. Equations of state 896
IV. Comparison of Neutrino Production in Standard Models 896
A. Models with the same nuclear parameters 896
B. Comparison with Turck-Chièze *et al.* 898
C. Comparison with Sackmann *et al.* 899
D. Summary 899
V. Opacities and Heavy-Element Mixtures 899
A. Heavy-element abundances 899
B. Radiative opacities 900
C. Neutrino fluxes with different abundances and opacities 900
1. Results of model calculations 900
2. Uncertainties due to abundances and opacities 901
VI. Best Solar Model without Element Diffusion 902
A. Some important model results 903
B. Detailed numerical models 904
VII. Best Solar Model with Helium Diffusion 904
A. Basic equations for helium diffusion 904
B. Method 905
C. Results with diffusion 905
VIII. Uncertainties 907
IX. The Maximum Rate Model 909
X. Discussion 910
Acknowledgments 911
Appendix: Numerical solar models 912
References 924

I. INTRODUCTION

This paper presents new results on solar neutrinos and other solar interior properties. The best estimates of cal-

culated quantities are derived from stellar models that include the diffusion of helium within the solar interior and also make use of improved input data for radiative opacities, element abundances, and nuclear reaction rates. In this introduction, we first describe in Sec. I.A the plan of the paper, emphasizing the astronomical context of the solar neutrino problem. In Sec. I.B we describe the solar neutrino experiments that are in progress, and in Sec. I.C we discuss the relation of the models and the experiments to the question of whether the solar neutrino problem is revealing new physics. This paper is the fifth in a series of related papers in *Reviews of Modern Physics* dealing with the physics and astronomy of solar neutrinos (see Bahcall, 1978, 1987; Bahcall *et al.*, 1982; Bahcall and Ulrich, 1988).

A. The plan of this paper

Approximately every five years for the past quarter century, there has been a flurry of interest in possible differences between neutrino fluxes computed with different stellar evolution codes. The cause of these differences has been identified in nearly all cases (see, for example, Bahcall and Sears, 1972 and Bahcall, 1989) as being due to differences in input parameters, although there have occasionally been differences that were caused by a lack of accuracy in a computer calculation. Because of the revival of interest in the precision of results of neutrino fluxes from different solar models, we have compared our calculated fluxes with those obtained recently by other authors who have made detailed calculations. For the same input parameters and physical assumptions, we find numerical agreement between our models and the standard solar models of Bahcall and Ulrich (1988), of Turck-Chièze *et al.* (1988), and of Sienkiewicz, Bahcall, and Paczyński (1990). The difference between the Turck-Chièze *et al.* (1988) result and the results obtained by the other three groups that have recently computed precise solar models to determine solar neutrino fluxes is due to different choices by Turck-Chièze *et al.* for two input values of nuclear cross sections (and an overestimate for an opacity effect), as is shown in Tables III and IV of this paper.

Having established the agreement among different solar evolution codes, we turn our attention to improvements in the input physics. Helium and the heavy elements sink relative to hydrogen in the radiative interior of a star because of gravitational settling and thermal diffusion. This slow physical process has generally been omitted in previous calculations of precise standard solar models and, in particular, is not included in any of the solar models cited in the previous paragraph. Diffusion can affect the chemical abundances and the radiative opacity in the outer layers of a star, where the time scale for diffusion is shortest. Hence diffusion is potentially important for helioseismology. Diffusion also affects the elemental abundances and the radiative opacity in the stellar core, altering the calculated solar neutrino fluxes. Quantitative estimates of other effects usually neglected in solar models suggest (see Bahcall, 1989) that for solar neutrino calculations the diffusion of helium is the most significant, well-understood phenomenon that is not included in standard models. We have therefore developed an exportable numerical code for including helium diffusion in the calculation of precise stellar models.

The calculations of solar neutrino emission and of solar p-mode oscillation frequencies require high precision for comparison with experiments. The primary reason for neglecting diffusion in previous calculations is that earlier studies (Eddington, 1926; Aller and Chapman, 1960; Vauclair, Vauclair, and Pamjatnikh, 1974; Montmerle and Michaud, 1976; Noerdlinger, 1977, 1978; Vauclair, Vauclair, and Michaud, 1978; Fontaine and Michaud, 1979a, 1979b; Wambsganss, 1988; Cox, Guzik, and Kidman, 1989) all showed that element diffusion is a relatively unimportant process in the cores of dwarf stars. Indeed, for the conditions believed to be typical of the solar interior, the characteristic time to diffuse a solar radius is of order 6×10^{13} yr (Bahcall and Loeb, 1990). Diffusion in the outermost layers of the sun could be even longer than indicated by these estimates, since it may be inhibited by meridional circulation or by turbulence driven by hydrodynamic rotational instabilities. An additional reason that diffusion has been neglected is that diffusion complicates conventional stellar evolution codes, since both space and time derivatives appear in the same equations. Because the space and time derivatives are treated separately in most existing stellar evolution codes, the elapsed time required to write and test the new subroutines describing diffusion is measured in years. The effects of element diffusion on the calculated frequencies of the solar p modes and g modes are discussed in a separate paper that is in preparation.

Wambsganss (1988) calculated the effect of hydrogen and helium diffusion on the central temperature and the primordial solar helium abundance in some illustrative solar models. The diffusion velocities used by Wambsganss are larger than those calculated by Noerdlinger (1977) and by Bahcall and Loeb (1990). In addition, the nuclear reaction rates that were employed in the calculations of Wambsganss were not specified in his paper, and an older version of the Los Alamos opacity tables was used. In the results given by Wambsganss, it is difficult to separate the effect of diffusion on neutrino fluxes from the possibly larger effects of using older reaction rates and opacity tables. A frontal attack on the problem of diffusion in solar models was carried out by Cox, Guzik, and Kidman (1989), who evaluated the effect of diffusion on the helioseismological frequencies of a standard solar model by solving numerically a set of 23 coupled partial differential equations. They used an older set of nuclear reaction rates (taken from the review of Fowler, Caughlan, and Zimmerman, 1975), an equation of state that yielded pressures that they suggest are slightly too large, and an opacity at the base of the convective zone that was adjusted to give improved agreement between calculated and measured solar p-mode fre-

quencies. The results of Cox *et al.* (1989) were used by Bahcall and Loeb (1990) to make, with the aid of approximate formulas of the dependence of neutrino fluxes on central temperature, an estimate of the differential effect of diffusion on the predicted event rates in solar neutrino experiments.

Since the calculated ^{7}Be and ^{8}B neutrino fluxes are sensitive to the conditions in the interior of a solar model, the best way to determine the effect of element diffusion on calculated neutrino fluxes is to construct precise solar models with and without diffusion using the same computer code and the same input parameters. In order to ensure that our diffusion calculations were embedded in a precise solar model, we developed a new (exportable) subroutine for evaluating the rates of nuclear reactions and of the related solar neutrino fluxes. We have incorporated this improved nuclear reaction subroutine into the standard Yale stellar evolution code and, in the process, have uncovered some minor errors in previous calculations.

In Sec. II we describe and compare the nuclear cross-section factors that are used in the studies of Bahcall and Ulrich (1988), of Turck-Chièze, Cahen, Cassé, and Doom (1988), of Sienkiewicz, Bahcall, and Paczyński (1990), of Sackmann, Boothroyd, and Fowler (1990), and in this paper. In Sec. III we discuss opacities, equations of state, and other input data used in the different stellar evolution codes. In Sec. IV we compare the neutrino fluxes and event rates calculated from the five different codes of Bahcall and Ulrich (1988), Turck-Chièze *et al.* (1988), Sinekiewicz *et al.* (1990), Sackmann *et al.* (1990), and this paper. The results are summarized in Table V. We explore in Sec. VI the effects of different opacity codes and of different heavy-element mixtures on the calculated solar neutrino fluxes and the predicted event rates in different experiments. In Sec. VII we describe our treatment of helium diffusion and compare the neutrino fluxes and other solar parameters that are calculated in standard solar models with and without diffusion. We discuss in Sec. VIII the uncertainties in the calculated neutrino fluxes and the experimental event rates. We calculate the uncertainties using 3σ errors for all measured quantities, as described in Chap. 7 of Bahcall (1989) or in Bahcall and Ulrich (1988). We present in Sec. IX the predictions of a Maximum Rate Model, a nonstandard solar model that can be used, together with nonstandard neutrino physics such as the MSW (Mikheyev-Smirnov-Wolfenstein) effect, to estimate the maximum changes in neutrino properties that might be inferred from solar neutrino experiments. In Sec. X we summarize the main results of this paper. In the Appendix, we present tables of the derived physical characteristics as a function of radius for our best standard solar models. These tables can be used to make detailed calculations of the solar MSW effect.

B. Solar neutrino experiments in progress

Four solar neutrino experiments are currently taking data; two other experiments are being constructed. Two additional experiments are undergoing feasibility tests. We summarize briefly here the main features of all these experiments and provide basic references to the original literature, from which more detailed information and additional references can be derived. More extensive summaries of all the experiments can also be found in Bahcall (1989).

The first, and for two decades the only, solar neutrino experiment uses a radiochemical chlorine detector to observe electron-type neutrinos via the reaction (Davis 1964; Pontecorvo 1946)

$$\nu_e + {}^{37}\mathrm{Cl} \rightarrow e^- + {}^{37}\mathrm{Ar} \ . \tag{1}$$

The ^{37}Ar atoms produced by neutrino capture are extracted chemically from the 0.6 kilotons of fluid, C_2Cl_4, in which they were created, and are then counted using their characteristic radioactivity in small, gaseous proportional counters. The threshold energy is 0.8 MeV. The chlorine solar neutrino experiment is described by Davis (1978, 1987) and Rowley, Cleveland, and Davis (1985). The experimental capture rate is (Davis, Harmer, and Hoffman, 1968; Davis, 1978, 1987, 1989; Rowley, Cleveland, and Davis, 1985; Davis *et al.*, 1990)

$$\text{capture rate} = (2.2 \pm 0.2) \text{ SNU} \ , \tag{2}$$

where the quoted experimental error is the 1σ uncertainty and an SNU (solar neutrino unit) is defined as 10^{-36} events per target atom per second. A number of authors have discussed the possibility that the capture rate in the chlorine experiment is not constant in time, but the event rate is too small to permit definitive statistics (see Davis, 1987, 1989; Davis *et al.* 1990, and references therein). The calculated capture rate derived in this paper is much larger than the observed rate,

$$\text{theoretical capture rate} = 8.0 \pm 3.0 \text{ SNU} \ , \tag{3}$$

where the uncertainty in the theoretical value takes account of 3σ errors in all of the input experimental quantities. All 14 previous calculations of the chlorine capture rate carried out in this series of investigations since 1968 lie within the quoted errors given in Eq. (3) (see Fig. 1.2 of Bahcall, 1989). During the past two decades, the discrepancy between the various contemporaneous versions of Eqs. (2) and (3) produced the "solar neutrino problem" and gave rise to a number of suggestions that either the standard theory of stellar evolution is in error or that new physical ideas are required in addition to the standard model of electroweak interactions (Glashow, 1961; Weinberg, 1967; Salam, 1968). The experiments described below are designed to discriminate between these two possibilities and to provide details about the new physics or new astronomy that is required to resolve the solar neutrino problem.

The second solar neutrino experiment to have been performed, Kamiokande II, is based upon the neutrino-electron-scattering reaction,

$$\nu + e \rightarrow \nu' + e' \ , \tag{4}$$

which occurs inside the fiducial mass of 0.68 kilotons of ultrapure water. Only ^{8}B solar neutrinos are detectable in the Kamiokande II experiment, for which the lowest published value for the detection threshold is 7.5 MeV. In the Kamiokande II experiment, the electrons are detected by the Čerenkov light that they produce while moving through the water. Neutrino-scattering experiments provide information that is not available from radiochemical detectors, including the direction from which the neutrinos come, the precise arrival times for individual events, information about the energy spectrum of the neutrinos, and some sensitivity to muon and tau neutrinos.

The result of the Kamiokande experiments is (Hirata *et al.*, 1989, 1990a, 1990b, 1991)

$$\langle \phi(^8\mathrm{B})_{\mathrm{obs}} \rangle = [0.47 \pm 0.05(\mathrm{stat}) \pm 0.06(\mathrm{syst})] \phi_{\mathrm{calc}}(^8\mathrm{B}) , \tag{5}$$

when expressed in terms of the flux of ^{8}B neutrinos calculated with our best standard solar model (see Sec. VII). The direction of the recoiling electrons shows that the incoming neutrinos originate in the sun. No time dependence of the signal has been observed over a period of almost three years.

The Super-Kamiokande experiment (Totsuka, 1990) will have a fiducial volume for neutrino-electron scattering of 22 000 tons of water, more than 30 times the current detector, and will make possible accurate diagnostic experiments beginning in 1996.

There are two experiments in progress, GALLEX (Kirsten, 1986, 1991) and SAGE (Gavrin *et al.*, 1990; Abazov *et al.*, 1991a, 1991b), that provide the first observational information about the low-energy neutrinos from the basic proton-proton reaction. The GALLEX and SAGE experiments make use of neutrino absorption by gallium,

$$\nu_e + {}^{71}\mathrm{Ga} \rightarrow e^- + {}^{71}\mathrm{Ge} , \tag{6}$$

which has a threshold of only 0.23 MeV for the detection of electron-type neutrinos. This low threshold makes possible the detection of the low-energy neutrinos from the proton-proton (or *pp*) reaction; the *pp* reaction initiates the nuclear fusion chain in the sun by producing neutrinos with a maximum energy of only 0.42 MeV.

Both the SAGE and the GALLEX experiments use radiochemical procedures to extract and count a small number of atoms from a large detector, similar to what is done in the chlorine experiment. There are differences in the chemical form of the two gallium detectors (SAGE uses liquid metallic gallium; GALLEX uses an aqueous solution of gallium chloride and hydrochloric acid), their sizes (the first results from SAGE use 30 tons of gallium, but this has recently been increased to 60 tons; GALLEX uses 30 tons), their locations (SAGE is positioned in an underground laboratory in the Baksan Valley in the Northern Caucasus; GALLEX is situated in the Gran Sasso Underground Laboratory in Italy), and in the detailed construction and operation of the gaseous proportional counters that measure the extracted ^{71}Ge.

The initial results from the GALLEX experiment are (Anselmann *et al.*, 1992):

$$^{71}\mathrm{Ga\ capture\ rate} = [83 \pm 19(\mathrm{stat}) \pm 8(\mathrm{syst})]\ \mathrm{SNU} , \tag{7a}$$

and from the SAGE experiment are (Abazov *et al.*, 1991a, 1991b; Gavrin, 1992):

$$^{71}\mathrm{Ga\ capture\ rate} = [58^{+17}_{-24} \pm 14(\mathrm{syst})]\ \mathrm{SNU} . \tag{7b}$$

The capture rate predicted by the standard model for a ^{71}Ga experiment is relatively precise. Approximately half of the predicted rate is contributed by the basic *pp* neutrinos, whose flux can be evaluated accurately within the context of the standard model. The estimated uncertainties due to the other neutrino fluxes are also relatively small (see Bahcall *et al.*, 1982; Bahcall and Ulrich, 1988). The result obtained in this paper (and in previous papers in this series) disagrees with Eq. (7), although the statistical uncertainties are large. We calculate in this paper a best-estimate rate of

$$\Sigma(\phi\sigma)_{\mathrm{Ga}} = 132^{+21}_{-17}\ \mathrm{SNU} , \tag{8}$$

where the theoretical uncertainties include 3σ errors on measured input parameters. The minimum expected event rate is (Bahcall, 1989) 80 SNU, provided only that nothing happens to neutrinos while they are traveling inside the sun or on their way to the Earth.

The next solar neutrino experiment to be performed, SNO, will use 1 kiloton of heavy water, D_2O, and larger photomultiplier coverage to observe Čerenkov light from recoil electrons produced by three different reactions. The charged current reaction,

$$\nu_e + d \rightarrow p + p + e^- , \tag{9}$$

will permit an accurate measurement of the energy spectrum of the electron neutrinos. Nearly all of the energy possessed by the incoming neutrinos is transferred to the outgoing electrons, although the protons take up much of the incoming momentum. The SNO detector will also be sensitive to neutrino-electron scattering, Eq. (4), in the heavy water. In addition, the total neutrino flux, irrespective of neutrino type, can be measured by the neutral-current reaction,

$$\nu + d \rightarrow \nu + p + n , \tag{10}$$

which has a threshold of 2.2 MeV. The neutrons will be captured by ^{35}Cl from NaCl dissolved in D_2O, producing light from electrons when the gamma rays from the neutron capture (with energies up to 8.6 MeV) are stopped in the D_2O. The cross section for Eq. (10) is independent of the flavor of the incident neutrino. Comparison of the flux of electron-type neutrinos inferred by measurements of the charged current, Eq. (9), with the total flux of neutrinos determined by observing the neutral-current disintegration of the neutrino, Eq. (10), will constitute a test of the standard electroweak model that is independent of

solar models. If the standard electroweak model is correct, the flux of electron-type neutrinos will equal the flux of all neutrinos measured by the neutral current. Details of the SNO experiments have been described by Aardsma *et al.* (1987) and Ewan *et al.* (1987). The experiment is expected to begin operation in 1995.

Two additional experiments, one designed to detect ^{7}Be neutrinos and one designed to detect *pp* neutrinos, are currently being tested for feasibility. The ^{7}Be experiment is known as Borexino (Raghavan, 1990; Arpasella *et al.*, 1991) and will observe the scattering of neutrinos by electrons in an ultrapure liquid scintillator (design purity of 10^{-16} g of uranium and thorium per g) with a total mass of only 0.1 kiloton. The event rate per day (~ 50) in this small detector is expected to be comparable to the event rate per year in the operating chlorine, Kamiokande, and gallium experiments, because of the predicted high flux of ^{7}Be solar neutrinos and because of the high luminosity of the liquid scintillator. A real-time detector of *pp* neutrinos, proposed by Lanou, Maris, and Seidel (1987), would observe neutrinos scattered in liquid helium by detecting rotons produced by the scattering.

C. New physics?

Solar neutrino experiments test the combined predictions of the standard electroweak model and the standard solar model. In principle, discrepancies between the calculated event rates and the observations can be explained in terms of nonstandard neutrino physics or nonstandard solar models, or both. In fact, many examples of nonstandard models of both types have been proposed to account for the results of the chlorine solar neutrino experiment (see ideas and references in Chaps. 5 and 9 of Bahcall, 1989).

In the last few years, almost all of the theoretical work has been devoted to nonstandard models of neutrino physics. We therefore present a brief introduction to these new ideas. A full discussion of nonstandard particle physics models would require at least one independent and complete article in the Reviews of Modern Physics and is beyond the scope of this paper. We note that future developments in helioseismology will permit observational tests of many of the nonstandard solar models (see, e.g., Leibacher *et al.*, 1985; Libbrecht, 1988; Gough and Toomre, 1991).

To buttress this choice of emphasis on nonstandard physics rather than on nonstandard solar models, we note that Bahcall and Bethe (1990) have argued that the combined results of the chlorine and the Kamiokande experiments cannot be explained plausibly without new physics. The argument is based upon the fact that the spectrum shape of neutrinos from a given nuclear source is, to measurable accuracy, independent of conditions in the sun (Bahcall, 1991). Thus, if the standard electroweak model is correct, one can convert the event rate from ^{8}B neutrinos that is observed in the Kamiokande II experiment into an expected event rate in the chlorine experiment; this converted ^{8}B rate is by itself somewhat larger than the total observed chlorine rate. In addition, there are significant contributions to the chlorine rate from the *pep* and the ^{7}Be neutrinos, whose calculated fluxes are much less sensitive to conditions in the stellar models than is the ^{8}B neutrino flux. Assuming the validity of the standard electroweak model (i.e., the invariance of the shape of the energy spectrum of ^{8}B neutrinos), the observed rate in the Kamiokande II experiment, and the relative precision with which the flux of ^{7}Be neutrinos can be calculated (compared to the much larger uncertainties in the stellar calculation of the ^{8}B neutrino flux), a rate larger than that observed is predicted for the chlorine experiment. The most plausible conclusion, according to Bahcall and Bethe (1990), is that the shape of the energy spectrum of electron-type neutrinos from ^{8}B has been altered by physical processes that require an extension of the standard electroweak model.

The conjecture that new physics is required by solar neutrino experiments is supported by the initial results from the SAGE (gallium) experiment (Abazov *et al.* 1991a, 1991b; Gavrin, 1992) and the GALLEX experiment (Anselmann *et al.*, 1992), although the statistical uncertainties in the experiments are large.

There are a variety of suggested explanations for the solar neutrino problem that require new physics; these explanations involve modifications, either minor or major, of the standard electroweak model. The most frequently discussed explanation, and the one for which the most precise calculations have been performed, is some form of the MSW effect (Wolfenstein, 1978, 1979; Bethe, 1986; Haxton, 1986; Kolb, Turner, and Walker, 1986; Mikheyev and Smirnov, 1986a, 1986b, 1986c; Parke, 1986; Rosen and Gelb, 1986; see also the excellent reviews by Kuo and Pantaleone, 1989 and Mikheyev and Smirnov, 1989), according to which neutrinos of the electron type are converted to muon or tau neutrinos via their interactions with electrons in the sun. The MSW effect involves simpler changes in existing theory than most of the other proposed modifications. For the MSW effect, the suggested changes involve relatively natural extensions of the standard electroweak model. Oscillations in vacuum are a possible but unlikely solution because of the fine-tuning that is required in the neutrino parameters (see Gribov and Pontecorvo, 1969; Bahcall and Frautschi, 1969; Glashow and Krauss, 1987). An alternative possibility (see especially Voloshin, Vysotskii, and Okun, 1986a, 1986b) is that the electron neutrino possesses a magnetic moment many orders of magnitude larger than implied by the standard electroweak model, in fact, just barely smaller than existing physics and astrophysics limits. This large magnetic moment could cause the neutrino spin to flip in the solar convective zone, resulting in right-handed neutrinos that would not be detected. This idea has been generalized to include the possibility that the spin is flipped in the solar interior by a combination of neutral and charged current scattering of neutrinos that have large magnetic moment interactions (see Akhmedov and Khlopov, 1988; Lim and

Marciano, 1988).

Many other elegant and intriguing modifications of the standard electroweak model have been proposed to account for the discrepancy between the calculated and the observed rates in solar neutrino experiments. The experiments that are in progress or are under development will eliminate many of these models. But, the number of neutrino parameters that have to be determined is so large, and the imaginations of theoretical physicists so fertile, that it seems likely that additional experiments will be required before a unique solution of the solar neutrino problem can be inferred with confidence.

II. NUCLEAR ENERGY GENERATION

In this section we discuss the rates of nuclear reactions as they appear in different stellar evolution codes, including the changes and corrections made in the course of the development of a new energy generation subroutine. In Sec. II.A we describe the new exportable subroutine for calculating nuclear energy generation and solar neutrino fluxes, and in Sec. II.B we comment upon individual nuclear reaction rates. We compare in Sec. II.C the constants adopted in different stellar evolution codes that have been used recently to calculate solar neutrino fluxes.

A. Energy generation subroutine

For the work discussed in this paper, one of us (JNB) wrote an essentially new nuclear energy subroutine with the same structure as the original Yale subroutine. The new subroutine, which contains an addition to calculate the neutrino fluxes, also has extensive annotations explaining the origin of the various terms and the numerical expressions. The code is written in FORTRAN in a style that facilitates the use of revised rate parameters as new experimental data become available. A copy of the nuclear energy generation and neutrino code can be obtained by writing to one of us (JNB).

Surviving unscathed many years of revision of other parts of the Yale stellar evolution code, the constants describing nuclear reactions in the previous Yale subroutine for energy generation (Prather, 1976) were taken mainly from Fowler, Caughlan, and Zimmerman (1975) and, for the crucial ^{7}Be and ^{8}B rates, from Bahcall and Sears (1972). The revised subroutine, which was used for calculating, nearly all of the Yale models described in this paper, employs reaction rates similar to those of Bahcall and Ulrich (1988) and Bahcall (1989), except for the *hep* reaction. For all of the reactions important for solar neutrino calculations, the current best-estimate cross-section factors differ significantly from what they were in the original Yale code (which was not designed to perform solar neutrino calculations). In a few cases, numerical errors (not due to revisions in the nuclear data) were corrected in the original code. In a small number of other places, the original version contained physically incorrect descriptions of nuclear processes, each of which has been corrected.

We expect that these changes in the nuclear reaction rates, while important for the solar neutrino problem, will lead to only minor revisions in the Yale isochrones, since the latter are not sensitive to details of the nuclear reaction rates of the major reactions and are insensitive to even relatively large changes in the minor reactions.

Electron screening in the Yale code is computed according to the prescriptions for weak and intermediate screening given by DeWitt, Graboske, and Cooper (1973) and Graboske *et al.* (1973). For the initial comparisons with Bahcall and Ulrich (1988) and Sienkiewicz, Bahcall, and Paczyński (1990), we considered only weak screening, since Bahcall and Ulrich inadvertently omitted intermediate screening.

Neutrino energy loss in the new Yale code is calculated accurately according to the prescription of Bahcall and Ulrich (1988; see their Table XXI), which is also used in the Bahcall-Ulrich code and in the Sienkiewicz *et al.* (1990) code.

B. Some individual reaction rates

We discuss in this section the nuclear cross-section factors adopted for the *pp* chain by different authors (Sec. II.B.1) and then describe the current situation with the *pp* rate (Sec. II.B.2). and the *hep* rate (Sec. II.B.3).

1. Comparison of different cross-section factors

Table I summarizes, for the most important nuclear reactions, the values for the low-energy cross-section factors [defined, e.g., in Eq. (3.7) of Bahcall, 1989] that have been adopted by authors who have recently calculated precise standard solar models. This table highlights the similarities and the differences among the adopted values. The values listed under column 4, "Bahcall-Ulrich (1988)," and column 9, "This work (1992)," are taken primarily from the review articles of Parker (1986), Bahcall and Ulrich (1988), Parker and Rolfs (1991), and Johnson, Kolbe, Koonin, and Langanke (1992). Note that the S_0 value for the ^{7}Be$(p,\gamma)^8$B reaction has been reduced by 8.5% as a result of the comprehensive analysis by Johnson *et al.* (1992); the estimated uncertainty in this crucial quantity remains large, approximately 28% at the effective 3σ level. Cross-section factors for other, less crucial reactions, and the best-estimate derivatives of the cross-section factors, are given in Tables 3.2 and 3.4 of Bahcall (1989).

In the following two subsections, we summarize the recent developments that have led to our adoption of revised values for the cross-section factors for the *pp* and the *hep* reaction rates.

2. The *pp* rate

The effective cross section for the proton-proton (*pp*) reaction can be written (Bahcall and May, 1969)

$$S_{\rm eff}=S(0)[1+0.417\tau^{-1}+12.6\tau^{-2}+36.6\tau^{-3}]\ , \quad (11)$$

where $\tau=33.80T_6^{-1/3}$ and T_6 is the temperature in units of 10^6 K. The first two terms in the brackets are independent of the nuclear reaction cross section, and the last two terms in the brackets of Eq. (11) are proportional to the logarithmic derivative, $(S^{-1}dS/dE)_{E=0}$, of the cross-section factor S at zero energy. The numerical value given by Bahcall and May (1969) for the correction associated with the logarithmic derivative has been confirmed by independent calculations of Bargholtz (1979), and therefore the bracketed term shown in Eq. (11) has been incorporated without change in standard solar model calculations. The cross section for the *pp* reaction was first estimated by Bethe and Critchfield (1938); Blin-Stoyle and Papageorgiou (1965) first discussed meson exchange corrections in this context.

Much work has been done since 1969 on three important quantities that determine the numerical value of the low-energy cross-section factor $S(0)$. The quantities of interest are the square of the overlap integral in the impulse approximation, $\Lambda^2(0)$ [see Eq. (8) of Bahcall and May, 1969 or Eq. (15) of Salpeter, 1952]; the ratio G_A/G_V of the axial vector to the vector coupling constant; and the fractional correction δ to the nuclear matrix element due to exchanges of π and ρ mesons. For theoretical calculations of the strong-interaction aspects of the *pp* cross section [$\Lambda^2(0)$ and δ], see Brolley (1971); Gari and Huffman (1972); Gari (1978); Bargholtz (1979); Gould and Guessoum (1990); and Carlson, Riska, Schiavilla, and Wiringa (1991); for the relevant weak-interaction experiments, see references to the measurement of G_A/G_V in neutron decay given in the analysis of Hernández *et al.* (1990). Unfortunately, not all authors have stated explicitly what values they adopted for each of the three factors mentioned above when they were providing new results for a specific one of the quantities of interest.

The low-energy cross-section factor can be written (see Bahcall *et al.*, 1982) in terms of $\Lambda^2(0), G_A/G_V$, and δ as follows:

$$S(0)=3.78\left[\frac{\Lambda^2(0)}{7.08}\right]\left[\frac{G_A/G_V}{1.238}\right]^2(1+\delta)^2 \times 10^{-25}\ \text{MeV b}\ , \quad (12)$$

where 3.78×10^{-25} MeV b is the value obtained by Bahcall and May (1969). In considering small effects due to electromagnetic radiative corrections, it is convenient to rewrite Eq. (12) in terms of the measured *ft* values for the neutron and for the 0^+ to 0^+ decays (e.g., the beta decay of ^{14}O). A convenient form for the scaling when written in terms of nuclear beta-decay rates is given in Eq. (12) of Bahcall and May (1969).

Table II shows the values obtained or used by a number of authors for the three important quantities being discussed here. There are six published calculations for which the best estimate for $\Lambda^2(0)$ is less than or equal to

TABLE I. Comparison of some important nuclear reaction parameters.[a]

Reaction	No.	Parker (1988)	Bahcall-Ulrich (1988)	Sienkiewicz *et al.* (1990)	Sackmann *et al.*[b] (1990)	Turck-Chièze *et al.* (1988)	Parker & Rolfs (1991)	This work[c] (1992)
^{1}H($p,e^+\nu_e$)^{2}H	1	4.03E−22	4.07E−22	4.07E−22	4.07E−22	4.07E−22	4.10E−22	$4.00^{+0.19}_{-0.12}$E−22
^{1}H($p+e^-,\nu_e$)^{2}H	2	Eq. (3.17)	Eq. (3.17)	Eq. (3.17)	≈Eq. (3.17)	Eq. (3.17)	Eq. (3.17)	Eq. (3.17)
^{3}He(^{3}He,2p)^{4}He	3	5.5E+03	5.15E+03	5.15E+03	5.6E+03	5.57	5.0E+03	5.0(1±0.18)E+03
^{3}He(^{4}He,γ)^{7}Be	4	0.54	0.54	0.54	0.54	0.54	0.533	0.533(1±0.096)
^{7}Be(e^-,ν_e)^{7}Li	5	Eq. (3.18)	Eq. (3.18)	Eq. (3.18)	≈Eq. (3.18)	Eq. (3.18)	Eq. (3.18)	Eq. (3.18)
^{7}Be(p,γ)^{8}B	6	0.0243	0.0243	0.0243	0.024	0.021	0.0243	0.0224(1±0.28)[d]
^{3}He($p,e^+\nu_e$)^{4}He	7	–	8E−20	8E−20	8.1E−20	–	–	1.3E−20[e]

[a]The tabulated values of $S(0)$ are expressed in keV b. Other recommended nuclear parameters are given in Tables 3.2 and 3.4 of Bahcall (1989), which is also the source of "Eq. (3.17)" and "Eq. (3.18)."

[b]Inferred by comparing formulas in Caughlan and Fowler (1988) with standard expressions for nuclear reaction rates. Sackmann *et al.* (1990), following Caughlan-Fowler, omitted the terms involving derivatives with respect to energy, $S'(0)$ and $S''(0)$, for reactions 4, 6, and 7.

[c]The uncertainties for the cross-section factors are indicated in parentheses; they correspond to 3σ limits based upon the analyses of Bahcall and Ulrich (1988) and Parker and Rolfs (1991). The values adopted here for reactions 3 and 4 are taken from Parker and Rolfs (1991).

[d]The value adopted here is from the recent comprehensive analysis by Johnson *et al.* (1992).

[e]The value used here is from Carlson *et al.* (1991). We adopt an uncertainty of a factor of 6 in the cross-section factor (see Sec. II.B.1).

TABLE II. Parameters for the *pp* reaction.

$\Lambda^2(0)$	(G_A/G_V)	δ	Authors
7.08±0.18	1.238	0.0	Bahcall and May (1969)
...	...	0.02	Rozenblit (1970)
6.38[a]±0.05	1.247	0.0	Brolley (1971)
$7.08^{a}{}^{+0.15}_{-0.06}$	...	0.048±0.004	Gari and Huffman (1972)
...	...	0.035±0.004	Dautry, Rho, and Riska (1976)
6.91±0.17	...	0.026±0.03	Gari (1978)
6.96±0.11	...	$0.01^{+0.01}_{-0.006}$	Bargholtz (1979)
7.39(1±0.04)	1.271	0.02	Gould and Guessoum (1990)
7.04	1.262	0.0075	Carlson, Riska, Schiavilla, and Wiringa (1991)
7.08±0.18	1.261±0.004	$0.01^{+0.02}_{-0.006}$	This paper

[a]Includes vacuum polarization.

7.08; only the calculation by Gould and Guessoum (1990) gives a best estimate (7.39) that is considerably larger than this value. It is not clear what is the origin of the discrepancy between the Gould-Guessoum calculation and that of the other authors (including the recent and precise calculation of Carlson *et al.*, 1991; Carlson, 1991). The divergent value of Gould and Guessoum (1990) is particularly puzzling in light of the fact that Bargholtz (1979) noted that the effective range approximation for $\Lambda^2(0)$ agreed to within 0.3% with the result obtained from integrating the numerical solutions for four different nucleon-nucleon potentials. We use for our best solar models in this paper the value of 7.08 for $\Lambda^2(0)$, since there has not been a recent systematic redetermination of this number that uses the best available modern data. Calculations are underway (Kamionkowski and Bahcall, 1992) to reevaluate $\Lambda^2(0)$ including vacuum polarization in a self-consistent way (see below). The ratio of G_A/G_V used here, 1.262±0.004, is taken from Hernández *et al.* (1990) and represents a weighted average of four precise modern experiments. The original detailed calculations of mesonic exchange by Gari and Huffman (1972) and Gari (1978) took account of interactions with π mesons, but did not include the terms, which are more difficult to calculate, resulting from ρ-meson exchange. Bargholtz (1979) and Carlson *et al.* (1991) have shown that the effects of π- and ρ-meson exchange largely cancel; constructive interference was enforced in an earlier phenomenological calculation by Rozenblit (1970). For this paper, we adopt $\delta=0.01^{+0.02}_{-0.006}$, which is based upon the results of Bargholtz (1979) and Carlson *et al.* (1991). The error estimate that we have adopted for δ may seem somewhat large to the experts, given the good agreement between the only two calculations that include destructive interference between π and ρ exchange (see in Table II the entries due to Bargholtz, 1979 and to Carlson *et al.* 1991), but in our view more numerical explorations with plausible representations of the exchange processes are required before we can be certain that this difficult-to-calculate correction has been evaluated accurately. The effects of vacuum polarization have been included in calculations by Brolley (1971), by Gari and Huffman (1972), and by Gould (1990) and, within the context of certain assumptions, reduce the reaction rate by approximately 1%. However, it is not clear, in any of the evaluations referenced above, that the effects of vacuum polarization have been included consistently in the determination of the proton-proton-scattering phase shifts and in the derivation of the nuclear potentials, as well as in the cross-section calculations. For this reason, we include the effects of vacuum polarization on the estimated uncertainty, but not the absolute value, inferred for the low-energy cross-section factor. Calculations now under way include in a self-consistent manner both radiative corrections to the weak-interaction matrix elements and the effects of vacuum polarization on the strong-interaction matrix elements.

The value of the low-energy cross-section factor at zero energy, $S(0)$ [see Eq. (3.14) of Bahcall, 1989], that follows from Eq. (12) and the last row of Table II is

$$S(0)=4.00^{+0.19}_{-0.12}\times 10^{-22}\ \text{keV b}\ . \tag{13}$$

The value given here is less than the other values given in row 1 of Table I, because we have adopted the more recent (but uncertain) calculation of Carlson *et al.* (1991; see also Bargholtz, 1979) for the value of δ, the mesonic exchange correction. The ratio of the *pep* reaction rate to the *pp* reaction rate is unaffected by the parameter changes shown in Table II and is given by Eq. (3.17) of Bahcall (1989).

3. The *hep* rate

Three important new studies have advanced our understanding of the *hep* reaction (see Wolfs, Freedman, Nelson, Dewey, and Greene, 1989; Carlson, Riska, Schiavilla, and Wiringa, 1991; and Wervelman, Abrahams, Postma, Booten, and Van Hees, 1991). Two separate experiments (Wolfs *et al.*, 1989; Wervelman *et al.*, 1991) determined the cross section for the radiative capture of thermal neutrons on ^{3}He and obtained the same answer to within relatively small errors (11% for Wolfs *et al.*, 1989; 5% for Wervelman *et al.* 1991). However, there is a complicated relation between the measured thermal-neutron cross section and the low-

energy cross-section factor for the production of *hep* neutrinos. The most detailed published calculation (Carlson *et al.*, 1991) yields a cross-section factor of $S(0)=1.3\times10^{-20}$ keV b, which we use throughout this paper. An even more recent calculation (Schiavilla, Wiringa, Pandharipande, and Carlson, 1992) that includes Δ-isobar degrees of freedom yields values between $S(0)=1.4\times10^{-20}$ keV b and $S(0)=3.2\times10^{-20}$ keV b. Less sophisticated analyses yield very different answers (see Wolfs *et al.*, 1989; Wervelman *et al.*, 1991). We adopt a large uncertainty—essentially all from theoretical aspects of the problem—of a factor of 6 in the absolute value of the low-energy cross section. This adopted uncertainty is about a factor of 3 larger than the range found by Schiavilla *et al.* (1992), who performed several precise calculations with specific assumptions. The estimated uncertainty for the low-energy cross-section factor of this reaction could be reduced significantly if a variety of different theoretical calculations were to converge to the same numerical value.

The numerical value of the cross-section factor used here, 1.3×10^{-20} keV b, is 6.15 times smaller than the value, based upon less accurate measurements and calculations, that was used by Bahcall and Ulrich (1988), Turck-Chièze *et al.* (1988), and Sienkiewicz *et al.* (1990). Since the *hep* reaction occurs only rarely, it does not influence the rates of the other reactions, and the inferred *hep* neutrino flux is linearly proportional to $S(hep)$. For the comparisons that are carried out in Sec. IV, we have rescaled the calculated *hep* neutrino fluxes so that they all refer to the cross-section factor adopted here.

C. Comparison of nuclear rates in different stellar evolution codes

Section II.C contains comments on the nuclear reaction data used recently in different stellar evolution codes.

1. Bahcall and Ulrich

The nuclear reaction rates used in the most recent version of the Bahcall-Ulrich code were discussed in detail in Sec. II.A of Bahcall and Ulrich (1988), in Chap. 3 of Bahcall (1989), and in Ulrich and Cox (1991).

In the course of testing the energy generation and neutrino flux subroutine, one of us (JNB) discovered a programing error in the original Bahcall-Ulrich code. The bracketed term in the expression of electron capture by ^{7}Be should read [see Eq. (3.18) of Bahcall, 1989] $[1+0.004(T_6-16)]$, whereas it was programed as $[1+0.004(T_6-1.6)]$ in the Bahcall-Ulrich code. This error caused all the calculated ^{8}B fluxes previously reported by Bahcall and Ulrich to be 6% lower than they should have been for typical solar interior conditions. The programing error had no significant effect on any other solar variable ($\ll1\%$ on other neutrino fluxes and $\ll0.01\%$ on p-mode frequencies), since the ^{7}Be rate affects only the branching between ^{7}Be proton capture and ^{7}Be electron capture (the overwhelming dominant branch). The Bahcall-Ulrich ^{8}B fluxes used in this paper for comparisons with other calculations have been corrected for the programing error.

2. Sienkiewicz *et al.*

The Sienkiewicz *et al.* (1990) code uses the same nuclear reaction parameters as Bahcall and Ulrich (1988), but does not treat the CNO (carbon-nitrogen-oxygen) bicycle in full detail. The CN part of the cycle was assumed by Sienkiewicz *et al.* (1990) to be in equilibrium.

3. Turck-Chièze *et al.*

The Turck-Chièze *et al.* (1988) calculation uses values for two of the nuclear physics parameters that are significantly different from the values employed by Bahcall and Ulrich (1988), Sienkiewicz *et al.* (1990), and the current Yale code.

The most important difference between the nuclear parameters adopted by Turck-Chièze *et al.* (1988) and by Bahcall and Ulrich (1988) is in the low-energy cross-section factor for the $p+^7$Be reaction. Bahcall and Ulrich (1988) used the value of 0.0243 ± 0.0018 keV b (1σ error) determined by the experimentalists Parker (1986) and Parker and Rolfs (1991). Caughlan and Fowler (1988) and Filippone (1986) also advocated 0.024 keV b, in agreement with the value of Parker (1986) and Parker and Rolfs (1991). On the other hand, Turck-Chièze *et al.* adopted 0.021 ± 0.003 keV b, which is 14.5% lower than the value used by Bahcall and Ulrich (1988). This difference in adopted values is primarily due to the way that the measured reaction cross section is extrapolated to low relative kinetic energies. The systematic reinvestigation of this reaction by Johnson, Kolbe, Koonin, and Langanke (1992) yields a cross-section factor of 0.0224 ± 0.0021 keV b, intermediate between the values adopted by Bahcall and Ulrich (1988) and by Turck-Chièze *et al.* (1988). In this paper, we adopt the new value determined by Johnson *et al.* (1992).

For the ^{3}He-^{3}He reaction, Turck-Chièze *et al.* (1988) adopt a rate that is obtained by converting directly the low-energy measurements by Krauss *et al.* (1987) to a cross-section factor, 5.57 ± 0.32 MeV b. Parker and Rolfs (1991), following Assenbaum, Langanke, and Rolfs (1987), correct the Krauss *et al.* (1987) measurement for screening by electron clouds in the laboratory measurements and average the newer results with the previously performed Caltech experiments. The Parker-Rolfs–recommended value is 5.0 ± 0.3 MeV b (1σ error). The cross-section factor currently recommended by Parker and Rolfs (1991) is 3% less than the value used by Bahcall and Ulrich (1988) and 10% less than the value used by Turck-Chièze *et al.* (1988). For solar neutrino calculations, the choice of the rate for the ^{3}He-^{3}He reaction is much less important than the choice of the rate for the ^{7}Be$+p$ reaction.

The choices for cross-section factors made by Turck-Chièze *et al.* (1988) are within the range of uncertainties quoted by Parker (1986) and adopted by Bahcall and Ulrich (1988; Bahcall, 1989); they are also within the uncertainties determined in this paper. We show in Sec. IV that the difference in calculated event rates for the chlorine solar neutrino experiment obtained by Turck-Chièze *et al.* (1988) and Bahcall and Ulrich (1988) is due primarily to the two choices, cited above, for the low-energy nuclear cross-section factors.

4. Sackmann, Boothroyd, and Fowler

Sackmann, Boothroyd, and Fowler (1990) do not state explicitly what low-energy cross-section factors they used, but instead refer to the review by Caughlan and Fowler (1988). These latter authors also do not give the nuclear parameters in an explicit form; rather, they provide analytic expressions for the reaction rates which are valid for temperatures that can be much higher than in the sun (e.g., temperatures as high as 10^9 K). By comparing the analytic formulas quoted by Caughlan and Fowler (1988) with standard expressions for nuclear reaction rates, we have inferred the cross-section factors that are listed in Table I in the column labeled "Sackmann *et al.* (1990)." Caughlan and Fowler (1988) have omitted the cross-section derivatives in reactions 4, 6, and 7 of Table I and have used approximate fitting formulas for the rates of the electron-capture reactions *pep* and *hep*. The quantitative effect of these approximations is not obvious.

III. OTHER INPUT DATA

The numerical schemes and the basic physical descriptions used in the different codes compared in this paper were developed independently over two decades by different programers with different applications in mind. We discuss in Sec. IV results obtained with the Yale code (see Appendix A of Prather, 1986; Guenther, Jaffe, and Demarque, 1989; and Pinsonneault, Kawaler, Sofia, and Demarque, 1989); the Bahcall and Ulrich (1988) code (see also Bahcall, Huebner, Lubow, Parker, and Ulrich, 1982; and Bahcall, 1989); the Paczyński-Ratcliff-Sienkiewicz code (hereafter referred to as PRS; Paczyński, 1969, 1970; Sienkiewicz, Paczyński, and Ratcliff, 1988; Sienkiewicz, Bahcall, and Paczyński, 1990); the Turck-Chiéze *et al.* code (1988); and the Sackmann, Boothroyd, and Fowler (1990) code (see Paczyński, 1974 and Boothroyd and Sackmann, 1988). In this section, we summarize the most important input data that are used in these different codes.

To make direct comparisons possible, we use in this paper the same solar parameters as were used by Bahcall and Ulrich (1988) and by Sienkiewicz *et al.* (1990) for the solar age (4.6 Gyr), luminosity (3.86×10^{33} erg s^{-1}), and initial ^{3}He abundance (10^{-4} by mass fraction). For the comparisons discussed in Sec. IV with standard solar models calculated by other groups, we used the values compiled by Grevesse (1984) for the relative heavy-element abundances and for the total ratio of heavy elements to hydrogen. We use neutrino interaction cross sections from Bahcall and Ulrich (1988) and opacities obtained from the Los Alamos Opacity Library (Huebner *et al.* 1977; Huebner, 1986).

For our best solar models computed with and without diffusion (see Secs. VI and VII), we use the improved relative heavy-element abundances and the value of Z/X compiled by Anders and Grevesse (1989) and the radiative opacities calculated at Lawrence Livermore National Laboratory by Iglesias and Rogers (1991a, 1991b). In the Yale code, the conductive opacity is computed separately from the radiative opacity using the electron conduction calculations of Hubbard and Lampe (1969). For all our models, the helium abundance Y was fixed by the requirement that solar models with the given individual abundance ratios Z_i/X have the observed solar luminosity at the solar age. In our models, this gives a value for the heavy-element abundance in the range $Z=0.0194$ to $Z=0.0198$ for the Grevesse (1984) mixture and $Z=0.01893$ (without diffusion) and $Z=0.01958$ (with diffusion) for the Anders and Grevesse (1989) mixture. The exact value of the inferred Z depends upon the precise equation of state, opacity, and nuclear reaction rates that are used.

It is important to iterate solar models to the correct ratio of Z/X for the assumed solar mixture, especially when there is a substantial change in the surface helium abundance (see the discussion in Bahcall *et al.*, 1982; Bahcall and Ulrich, 1988). In our best models which include diffusion, precise iteration of Z/X is as important for calculating the neutrino fluxes as is helium diffusion (see Sec. VII.C). For each case, we first computed a solar model with an initial estimate for the total Z for the given mixture [0.0194 for Grevesse (1984) and 0.0188 for Anders-Grevesse (1989) and Grevesse (1991)]. We used the calibrated hydrogen abundance obtained for this model and the Z/X of the mixture to determine an improved estimate of the total Z. We then calibrated a solar model with the new estimate for Z; for each case we then had two sets of neutrino fluxes for two different values of Z/X. We used linear interpolation to determine the fluxes for the correct value of Z/X (which was intermediate between the two models and close to the second one). We carried the iteration procedure further in some cases, and found that the linear interpolation was accurate to better than 0.05% in all of the neutrino fluxes.

We used 10 initial time steps of 10^7 years (to resolve the appearance and disappearance of a small convective core) and 50 later time steps of 9×10^7 years to construct our models. By constructing sequences with doubled and halved time steps, we determined that the finite time steps caused errors of order 0.1% in the B^8 flux estimate, 0.5% in the CNO fluxes, and 0.2% in the *pp* and *pep* fluxes. We used Richardson extrapolation to correct the

errors in our fluxes arising from the finite time steps; test calculations performed for different models indicated that the time-step dependence of our results was similar for solar models with different assumed input physics.

In computing the experimental rates predicted by our best solar models for the ^{37}Cl experiment, we use the result of Garcia *et al.* (1991). According to Garcia *et al.*, the best estimate for the absorption cross section for ^{8}B neutrinos is 1.09×10^{-42} cm^2, which is about 3% larger than the value used by Bahcall and Ulrich (1988), and the best estimate for the *hep* absorption cross section is 4.26×10^{-42} cm^2, which is 9% larger than the value used by Bahcall and Ulrich (1988).

A. Opacities

The opacities that have been used for all the precise solar neutrino studies carried out prior to 1991 were constructed from the Los Alamos Astrophysical Library (Huebner, 1986), although different numerical methods were used to construct opacity tables from the same Los Alamos data. The change in opacity caused by CNO conversion was overestimated by Bahcall and Ulrich due to the limited numerical accuracy in the interpolation formula for the opacity contributions of individual species given in Huebner (1986). This overestimate was first pointed out by Cox (1990), who used the Los Alamos Astrophysical Library; Iglesias and Rogers (1991a) also found, using the Lawrence Livermore opacity code, that the CNO correction defined by Bahcall and Ulrich (1988) was negligible. A different mishap with respect to the Los Alamos opacity calculations caused Turck-Chièze *et al.* (1988) to overestimate the correction due to collective effects in the photon-electron-scattering cross section. Turck-Chièze *et al.* (1988; Turck-Chièze, 1990) followed Bahcall *et al.* (1982) and subtracted $0.07(1+X)$ from the electron-scattering opacity, but this prescription applies only to the opacities created on a special basis by the Los Alamos group for the Bahcall *et al.* (1982) paper. Subsequent Los Alamos calculations include collective effects in the numerical values of the opacities that are distributed to different computational groups (see footnote 1 in Bahcall and Ulrich, 1988).

The opacities that we have used for our best current models (see Secs. VI and VII) are produced by the Livermore opacity code, OPAL (see Iglesias and Rogers, 1991a, 1991b; Rogers and Iglesias, 1992). We have used an opacity table with a relatively small number of data points chosen to be near the locus of temperatures and densities for a solar model (Rogers and Iglesias, 1991, private communication). Opacities were calculated at the same values of temperatures, densities, and hydrogen and metal abundances as were published in Table III of Bahcall and Ulrich (1988). The opacities extend down to a minimum temperature of 10^6 K; below this minimum temperature, another opacity source must be used. We have used opacities from the Los Alamos library, for the same mixture of elements, below this temperature. The low-temperature extension of the opacity tables does not affect, to calculable accuracy, the solar neutrino fluxes.

The small number (three, in the published table of Bahcall and Ulrich, 1988; see also Ulrich and Cox, 1991) of density values at a given temperature has caused some concern about the accuracy of solar opacities (Faulkner and Swenson, 1992), especially because in a solar model the locus of temperature and density is outside the table for temperatures below approximately 4×10^6 K. However, the errors in opacity induced by the limited table size are small—and the derived opacities are probably more accurate than those derived by interpolation within a larger but coarser table. We have tested the accuracy of the table in two ways.

First, the opacity tables actually used by Bahcall and Ulrich (1988) contained six densities at a given temperature rather than the three values that were published. We compared the tabulated values for the densities that were not published with the values obtained by extrapolation from the central three values that were published by Bahcall and Ulrich. The characteristic errors were 0.5% when extrapolating by one grid point, and 1% when extrapolating by two grid points. We conclude that, for temperatures in excess of 1×10^6 K, the numerical error in the opacities is less than 1% with our table format. For calculating neutrino fluxes, the opacities in the center of the solar model are most important; in this regime, the densities and temperatures are within the table, and the numerical precision should be greater than 1%. Using the solar models evolved by Bahcall, Bahcall, and Ulrich (1969) with different opacity perturbations, we conclude that uncertainties in the numerical precision of the opacity interpolation cause errors in the neutrino fluxes that are only of order a few percent or less. The larger errors reported by Faulkner and Swenson (1992) may be a consequence of their having used linear interpolation rather than the three-point Lagrangian extrapolation used in our work.

As a further test of the numerical precision required in the opacity tables, we also computed solar models using a new set of tables with a greater range in temperature (6×10^3 K to 10^8 K) and a greater range of density at a given temperature (6 orders of magnitude rather than 0.5). These tables were also constructed using the OPAL code (Rogers and Iglesias, 1991). The new tables are provided for values of the metallicity Z from 0.0 to 0.04 and use a heavy-element mixture (Grevesse, 1991, private communication) which is similar to the Anders-Grevesse mixture with the meteoritic iron abundance. We constructed a table for the same value of Z (0.0188) as for our best solar model by cubic spline interpolation in Z from the overall set of tables. We then recalibrated our solar model and compared the neutrino fluxes with those obtained using the original table. The neutrino fluxes of the solar models with this new opacity table were almost identical to those obtained with the original model. The fluxes for the CNO neutrinos changed by about 2–3% when switching from the more compact to the more extended opacity table, while the other neutrino fluxes

differed by less than 1%. Furthermore, the location of the base of the surface convection zone changed by less than $0.001R_\odot$. This almost negligible shift is much less than the change obtained by Faulkner and Swenson (1992) and may indicate the importance of the choice of interpolation or extrapolation schemes. Even these small changes may overestimate the errors due to numerical interpolation. The original table was computed specifically for the solar value of Z, while the larger table was interpolated from a set of tables for different Z. The points at which the density was evaluated in the newer table are also farther apart than in the original table. There are also small differences in the mixtures involving the carbon and the oxygen abundances. Although the larger tables are valuable for general stellar evolution calculations, they are less accurate for solar neutrino calculations. We have therefore adopted the opacities supplied by Rogers and Iglesias (1991) in the Bahcall and Ulrich (1988) format for computing our standard solar models.

The numerical comparisons we have made show that errors of at most about 1% in the most sensitive neutrino fluxes are caused by limiting the opacity values to the tabulated entries we have used.

B. Equations of state

The equations of state used in the computer codes are slightly different, although it is known from previous studies that small differences (less than 1% in the interior pressures) between existing accurate equations of state have only a modest effect on the calculated neutrino fluxes (see Bahcall, Bahcall, and Ulrich, 1969; and Bahcall, Huebner, Lubow, Parker, and Ulrich, 1982). The Bahcall-Ulrich and PRS equations of state are described, respectively, in Bahcall *et al.* (1982) and in Sienkiewicz *et al.* (1988). The Bahcall-Ulrich code includes the Debye-Hückel correction to the pressure (see footnote 15 of Bahcall, Bahcall, and Shaviv, 1968):

$$P = P_0 \left[1 - 0.044 \frac{(3.5+X)^{3/2}}{(3+5X)} \frac{\rho^{1/2}}{T_6^{3/2}} \right] , \tag{14}$$

where P_0 is the pressure of a perfect gas including degeneracy, ρ is the density in g cm^{-3}, X is the hydrogen mass fraction, and T_6 is the temperature in units of 10^6 K. [A minor typographical error in the footnote of Bahcall *et al.* (1968) has been corrected in the above form of Eq. (14).] The Debye-Hückel correction reduces the pressure in the solar interior by an amount that is approximately constant, 1%, since $\rho \propto T^3$ in the inner regions of the sun. This reduction in pressure is compensated by a decrease in Y of about 0.01. The neglect of the Debye-Hückel correction by some authors has led to some published solar models with a primordial helium abundance that is too large.

We added the Debye-Hückel correction given in Eq. (14) to the equation-of-state subroutine of the Yale code and constructed solar models with and without this correction. Comparing these models, we established the sensitivity of the calculated neutrino fluxes to this improvement in the equation of state (cf. rows 5 and 6 of Table III in Sec. IV). The Turck-Chièze *et al.* (1988) model includes the Debye-Hückel correction; the Sackmann *et al.* (1990) code includes the correction for part, but not all, of the pressure; and the PRS code does not include the Debye-Hückel correction.

The Yale evolution code solves the Saha equation for partial ionization for temperatures less than $10^{5.5}$ K and assumes full ionization above 10^6 K. At intermediate temperatures, the ionization is determined by interpolation. The formulation and tables used in the equation-of-state calculations are described by Prather (1976).

IV. COMPARISON OF NEUTRINO PRODUCTION IN STANDARD MODELS

In Sec. IV.A we compare the neutrino fluxes and predicted event rates calculated from three different standard solar evolution codes that all use the same nuclear parameters, including neutrino absorption cross sections, as were used by Bahcall and Ulrich (1988). The fluxes for the *hep* reaction were scaled to take account of the new estimate, discussed in Sec. II.B.2, for the cross-section factor of this reaction. We summarize in Table III the results for the neutrino fluxes and for the neutrino capture rates in the chlorine and gallium experiments. For the predicted rate in the ^{37}Cl experiment, the three codes give results that, for the same input data, agree to within ± 0.05 SNU (better than 1%); they agree to within ± 0.5 SNU (better than 0.5%) for the gallium experiment. In Sec. IV.B we compare the results of the present calculations with that of Turck-Chièze *et al.* (1988), after correcting for the differences in input data. The Bahcall-Ulrich, Turck-Chièze, Sinekiewicz, and Yale codes all give the same answer to an accuracy of about 0.1 SNU for the ^{37}Cl experiment, as is shown in detail in Table IV. In Sec. IV.C we discuss the Sackmann *et al.* (1990) results. In Sec. IV.D and in Table V, we give a summary of all of the different comparisons.

The comparisons between three of the codes—Bahcall and Ulrich (1988), Sienkiewicz *et al.* (1990), and Yale (this paper)—are made directly by computing solar models with the same input data. The comparison with the results of Turck-Chièze *et al.* (1988; see Table IV below) requires (1) making corrections for different assumed cross sections for two nuclear reactions with the aid of previously published partial derivatives of neutrino fluxes with respect to nuclear cross sections (Table 7.2 of Bahcall, 1989), and (2) computing solar models for two different prescriptions for the electron-scattering opacity (Turck-Chièze, 1990).

A. Models with the same nuclear parameters

Table III compares the neutrino fluxes and the event rates (in solar neutrino units, SNU) for the chlorine and gallium experiments that were computed from a series of solar models of Yale (this paper), of Bahcall and Ulrich

TABLE III. Neutrino fluxes from different solar models.[a]

Solar model	*pp* (E10)	*pep* (E8)	*hep* (E3)	^{7}Be (E9)	^{8}B (E6)	^{13}N (E8)	^{15}O (E8)	^{17}F (E6)	Cl (SNU)	Ga (SNU)
BU[b]	6.02	1.42	1.24	4.57	5.64	5.78	4.90	4.83	7.8±2.6	131^{+20}_{-16}
SBP[b]	6.05	1.30	1.28	4.79	5.65	3.9[c]	3.9[c]	–	7.7±2.6	130^{+19}_{-16}
Old Yale	5.95	1.37	1.18	4.71	6.40	4.24	3.36	4.59	8.4±3.3	130^{+21}_{-17}
BU Opac	5.95	1.38	1.18	4.69	6.38	4.23	3.35	4.59	8.4±3.3	130^{+21}_{-17}
WScr	6.00	1.41	1.21	4.71	6.04	6.00	5.15	5.09	8.2±3.1	133^{+22}_{-18}
WScr+ DH	6.02	1.40	1.23	4.49	5.64	5.77	4.92	4.85	7.7±2.9	130^{+21}_{-17}
Compare vs BU	+0.0%	−1.3%	−1.2%	−1.7%	+0.0%	−0.3%	+0.4%	+0.3%	−1%	−1%
Interm screen	6.04	1.42	1.24	4.43	5.28	5.27	4.42	4.28	7.3±2.8	128^{+20}_{-16}

[a]The unit of flux is $cm^{-2}s^{-1}$ and is given in exponential form, $10^{10} \equiv E10$.
[b]BU represents Bahcall and Ulrich (1988); SBP represents Sienkiewicz, Bahcall, and Paczyński (1990); see also Paczyński, 1969 and Sienkiewicz, Ratcliff, and Paczyński, 1988.
[c]The CN part of the CNO bi-cycle was assumed to be in equilibrium in this calculation.

(1988), and of Sienkiewicz *et al.* (1990). Chapters 3 and 6 of Bahcall (1989) describe the nuclear reactions that give rise to each of the neutrino branches listed in Table III; Chap. 8 of the same reference gives the neutrino cross sections used to compute the rates in SNU.

The first row in Table III corresponds to the "Best" standard model of Table XIV of Bahcall and Ulrich (1988; denoted BU in Table III), when (see Sec. II.B) the small *hep* flux is multiplied by 0.163 to take account of the recently determined cross-section factor for the *hep* reaction (see Sec. II.B.2), when the ^{8}B flux is multiplied by 1.058 to take account of the programing error for the ^{7}Be reaction that was discussed in Sec. II.C, and when the unnecessary CNO opacity correction is eliminated. The CNO opacity correction was removed from the fluxes given in the Bahcall-Ulrich "Best" table entry by multiplying the "Best" fluxes by the ratio of two other entries in Table XIV ("AllNew"/"CNO Cor"), this being the ratio that accounts for the small difference between models with and without the CNO correction. The event rates for the chlorine and gallium experiments are, for this corrected "Best" model, 7.8 SNU and 131 SNU, which differ by 1% from the values of 7.9 SNU and 132 SNU given by the uncorrected "Best" model (Bahcall and Ulrich, 1988).

The second row, labeled "SBP," contains the fluxes computed for the standard solar model by Sienkiewicz, Bahcall, and Paczyński (1990), with the factor of 0.163 included for the *hep* flux. The BU and SBP fluxes agree to better than 10% for all the calculated fluxes (better than 6% for the important *pp*, ^{7}Be, and ^{8}B fluxes), except for the CNO fluxes for which Sienkiewicz *et al.* made simplifying assumptions that are described in Sec. II.C.2. Table III shows that the differences between the results obtained with the Paczyński-Ratcliff-Sienkiewicz code (Paczyński, 1969; Sienkiewicz *et al.*, 1988, 1990) and the Bahcall-Ulrich (1988) code amount to only 0.1 SNU for the chlorine experiment and 1 SNU for the gallium experiment. The results can be written symbolically for the chlorine experiment as

$$[\text{Sienkiewicz } et\ al. - (\text{Bahcall-Ulrich})]_{\text{Cl}} = -0.1 \text{ SNU} . \quad (15)$$

The third row of Table III, labeled "Old Yale," gives the results for the old Yale model before the series of improvements discussed below were made. The agreement is already surprisingly good at this stage; the sensitive ^{8}B neutrino flux obtained with the old Yale code differs by only 13% from the Bahcall and Ulrich (1988) and the Sienkiewicz *et al.* (1990) values. In row 4, we give the results that were computed with the Yale code using, instead of the individual opacity values calculated by the Yale numerical techniques, the values for individual opacities that Bahcall and Ulrich computed from the Los Alamos opacity data. The two slightly different opacity tables give essentially the same neutrino fluxes, as expected. Sienkiewicz *et al.* used an interpolation routine different from both BU and Yale.

For the models summarized in the fifth and sixth rows, the nuclear physics parameters used were the same as those in Bahcall and Ulrich (1988), including only weak screening (see Sec. II.A) and the corrected *hep* cross-section factor. The sixth row contains the results calculated by adding the Debye-Hückel correction given in Eq. (14). Comparing rows 5 and 6, we see that the Debye-Hückel correction decreases the calculated event rate in the ^{37}Cl experiment by 0.5 SNU and in the gallium experiment by 3 SNU.

The seventh row of Table III, labeled "Compare," gives the percentage difference between the neutrino fluxes computed with the Bahcall-Ulrich code and the fluxes computed with the improved Yale nuclear energy generation routine (weak screening only), including in both cases the Debye-Hückel correction. This row determines how well the fluxes from the Yale and the Bahcall-Ulrich codes agree when the input parameters are made as similar as we can make them. The agreement is excellent; the computed neutrino fluxes differ by less than 2% in all cases. Table III shows that the difference between the rates computed using the two

codes amounts to 0.1 SNU in the chlorine experiment and 1 SNU in the gallium experiment. The results can be written symbolically for the chlorine experiment as

$$[\text{Yale}-(\text{Bahcall-Ulrich})]_{\text{Cl}}=-0.1\ \text{SNU}\ . \quad (16)$$

To determine the specific effect of including intermediate screening, we computed a separate model—shown in the last row of Table III—in which intermediate electron screening was taken into account as described in Sec. II.A. The inclusion of intermediate screening lowers the ^{8}B neutrino flux by about 7% and decreases the CNO fluxes by about 10%. Intermediate screening reduces the calculated rate of the chlorine experiment by 0.4 SNU (5%), to a total rate of 7.3 SNU, and reduces the calculated rate for the gallium experiment by 2 SNU (1.5%), to a total of 128 SNU.

B. Comparison with Turck-Chièze *et al.*

Table IV compares the neutrino capture rate calculated with the Yale model that includes intermediate screening (see the last row of Table III and the discussion at the end of the previous section) with the capture rate calculated with the Turck-Chièze *et al.* (1988) model. The first and second rows of Table IV refer to the cross-section factors of the $p+^7$Be and the ^{3}He-^{3}He reactions. The second and third columns of this table list, respectively, the values used in the Yale calculation and in the Turck-Chièze *et al.* (1988) calculation. The last column of Table IV gives the difference in SNU predicted for the chlorine experiment due to the different choice of input data. The quantity ΔSNU is positive if the Yale value of the parameter causes the calculated event rate to be larger than the rate calculated with the Turck-Chièze *et al.* value.

The flux of the rare ^{8}B neutrinos is linearly proportional to the assumed value of $S_0(p+^7\text{Be})$, and no other solar neutrino fluxes (or other solar model parameters) are significantly affected by this cross-section factor. Turck-Chièze *et al.* (1988) chose a value for this cross-section factor that is 14.5% lower than the value chosen by Bahcall and Ulrich (1988; see row 6 of Table I). Because of the choice of the lower value for the cross-section factor for $S_0(p+^7\text{Be})$, the event rate calculated by Turck-Chièze *et al.* must be 0.83 SNU less than the Yale value, all other input quantities being equal. The fact that Turck-Chièze *et al.* chose a higher value for $S_0(^3\text{He}+^3\text{He})$ than Bahcall and Ulrich (1988; see row 3 of Table I) reduces their calculated event rate for the chlorine experiment by 0.2 SNU (cf. Table 7.2 of Bahcall, 1989) relative to the Yale value.

Turck-Chièze *et al.* (1988) may have overestimated (see Sec. III.A) the collective effects on the photon-electron-scattering opacity. Turck-Chièze (1990) states that she subtracted $0.07(1+X)$ from the circulated Los Alamos opacities on the assumption that the Los Alamos opacities had not been corrected for collective effects. This subtraction was not made by Bahcall and Ulrich (1988), by Sienkiewicz *et al.* (1990), or by the present authors in using the Yale code, since the Los Alamos opacities do contain a correction for collective effects (see discussion in Bahcall and Ulrich, 1988). Independent of the precise size of the collective effects, if we want to compare the results of calculations with the same input parameters, we must undo in the Turck-Chièze *et al.* (1988) calculations the effect of the subtraction made on the Los Alamos opacities. This undoing is illustrated symbolically in the third column of Table IV. According to Turck-Chièze (1990), the additional correction she used for collective effects reduces the calculated event rate by 0.6 SNU for the chlorine experiment.

Taking into account the three differences in input data shown in Table IV, the Yale and the Turck-Chièze *et al.* (1988) calculations are in excellent agreement. Symbolically, one can write

$$[\text{Yale}-(\text{Turck-Chièze})]_{\text{Cl}} = 7.3\ \text{SNU}-[5.8+0.83+0.19+0.6]\ \text{SNU}\ , \quad (17)$$

or,

$$[\text{Yale}-(\text{Turck-Chièze})]_{\text{Cl}}=-0.1\ \text{SNU}\ . \quad (18)$$

Since the Yale value is 0.1 SNU less than the Bahcall and Ulrich (1988) value for the chlorine experiment [cf. Eq. (16)], it is plausible that for the same input data

$$[(\text{Turck-Chièze})-(\text{Bahcall-Ulrich})]_{\text{Cl}}\simeq 0.0\ \text{SNU}\ . \quad (19)$$

TABLE IV. Comparison of Turck-Chièze *et al.* (1988) with the Yale (1992) model.

Input data	Bahcall and Ulrich (1988) value	Turck-Chièze *et al.* (1988) value	Δ SNU
$S_0(^7\text{Be}+p)$	0.0243 keV b	0.021 keV b	+0.83[a]
$S_0(^3\text{He}+^3\text{He})$	5.15 MeV b	5.57 MeV b	+0.19[a]
κ	κ (Los Alamos)	κ(LA)−0.07(1+X)	+0.6[c]
Total	7.3 SNU[b]	(5.8+1.6) SNU= 7.4 SNU[c]	

[a]Calculated using Table 7.2 of Bahcall (1989).
[b]Calculated with the current Yale code (see last row of Table III).
[c]A different interpretation (see Sec. IV.B) leads to an opacity correction of 0.4 SNU and a total rate of 7.2 SNU.

Most recently, Turck-Chièze (1992) kindly informed us that the opacity tape used in the calculations of Turck-Chièze *et al.* (1988) did not contain the best contemporary Los Alamos opacities, but instead represented a much earlier version. According to the interpretation of Turck-Chièze of what the earlier opacity tape actually contained, approximately 0.4 SNU (instead of 0.6 SNU) should be added to the published Turck-Chièze *et al.* (1988) rate to account for the different opacities. Making this assumption leads to a difference of 0.2 SNU (or 2%) between the calculations of Turck-Chièze *et al.* (1988) and of Bahcall and Ulrich (1988), which is still excellent agreement.

C. Comparison with Sackmann *et al.*

It would be necessary to evolve accurately a specially constructed solar model with an altered code in order to make a precisely defined comparison of the results of Sackmann, Boothroyd, and Fowler (1990) with those of Bahcall and Ulrich (1988), Yale (this paper), and Sienkiewicz *et al.* (1990). The reason is that Sackamnn *et al.* (1990) omitted (see Sec. II.C.4) the derivative corrections to the nuclear reaction cross-section factors, used approximate expressions for the rates of the *pep* and ^{7}Be electron-capture reactions, and included (see Sec. III.B) the Debye-Hückel correction only for ions but not for electrons. In addition, Boothroyd (1992) had kindly informed us of other important approximations that were embodied in the stellar evolution code that was used by Sackmann *et al.* (1990). The best standard solar model of Sackmann *et al.* (1990) predicts a capture rate of 7.7 SNU for the chlorine experiment, in agreement with the rates calculated from other precise standard solar models. However, the approximations made by Sackmann *et al.* (1990) prevent a direct, quantitative comparison with the Bahcall and Ulrich (1988), Sienkiewicz *et al.* (1990), or Turck-Chièze *et al.* (1988) calculations.

D. Summary

For the same input data, all four codes—Yale, Bahcall-Ulrich (1988), SBP, and Turck-Chièze *et al.* (1988)—yield neutrino capture rates that agree to within ± 0.1 SNU ($\approx 1\%$) for the chlorine experiment, as shown by Eqs. (15), (16), and (18). These results are summarized in Table V. In addition, Table III shows that the agreement is also excellent for the gallium experiment. The Yale, Bahcall-Ulrich, and SBP codes all agree to within 1 SNU for the same input parameters. For the gallium experiment, a direct comparison cannot be made with the Turck-Chièze *et al.* (1988) code, since Turck-Chièze (1990) did not state for gallium the effect of the overestimate of the correction on the photon-electron-scattering opacity.

The comparisons made in this section show that different stellar evolution codes, with different software architectures and with different numerical techniques, predict similar neutrino fluxes when the same input physics is used (for similar conclusions reached at earlier epochs, see Bahcall and Sears, 1972 and Bahcall *et al.* (1982). We now proceed to calculate more accurate solar models using improved input physics.

TABLE V. Predicted ^{37}Cl event rate for solar models with similar parameters.[a]

Authors	SNU
Bahcall and Ulrich (1988)	7.8
Sienkiewicz *et al.* (1990).	7.7
Yale (this paper).	7.7
Turck-Chièze *et al.* (1988).	7.4[b,c]

[a]The comparison was made after adjustments were made for known differences in input data (see discussion in Sec. IV).
[b]Could be 7.2 SNU. See last paragraph of Sec. IV.B.
[c]Should be compared with 7.3 SNU, since different input data were used (see Table IV and Sec. IV.B).

V. OPACITIES AND HEAVY-ELEMENT MIXTURES

Uncertainties in the radiative opacities and in the assumed primordial heavy-element mixture have long been recognized as major contributors to the total uncertainty in the calculated solar neutrino fluxes (see, e.g., Bahcall, Bahcall, and Ulrich, 1969; Bahcall *et al.* 1982; and Bahcall and Ulrich, 1988 for complementary discussions). In this section we evaluate the separate effects on neutrino fluxes of the assumed heavy-element abundances and of the atomic physics codes used in producing radiative opacities. We begin by reviewing in Sec. V.A the status of solar abundance determinations, and in Sec. V.B we summarize the recent improvements in the calculations of radiative opacities. In Sec. V.C we evaluate the uncertainties in the calculated neutrino fluxes that arise from uncertainties in abundance determinations and in radiative opacities.

A. Heavy-element abundances

The most recent comprehensive analysis of the relative heavy-element abundances on the surface of the sun is by Anders and Grevesse (1989), who discuss both direct measurements on the solar surface and measurements of meteorites. Many of the photospheric abundances discussed in the Anders and Grevesse paper have been improved significantly since the previous standard discussion of Grevesse (1984); the improvements are largely due to the availability of more accurate atomic transition probabilities. The most significant remaining uncertainty in the element abundances for our purposes is the difference between the meteoritic value for the iron abundance, $\log[\mathrm{Fe}]=7.51$, and the photospheric value for the iron abundance, $\log[\mathrm{Fe}]=7.67$. If the photospheric iron abundance is adopted, then the total heavy-element abundance determined by Anders and Grevesse (1989) is almost identical to the value, $Z/X=0.02765$, obtained by Grevesse (1984). However, if the meteoritic iron abundance is used, then the Anders-Grevesse value of Z is

significantly lower, $Z/X=0.02668$. In what follows, we shall present neutrino fluxes calculated for both values of the iron abundance.

For our best estimates, we use the neutrino fluxes determined for the meteoritic iron abundances, since historically the meteoritic values have most often turned out to be correct when there was a conflict between the values inferred for the photospheric and the meteoritic abundances. The choice of the lower iron abundance is supported by the recent work using Fe II lines by Holweger, Heise, and Kock (1990) and by the work on Fe I lines by Holweger, Bard, Kock, and Kock (1991) and by O'Brian, Wickliffe, Lawler, Whaling, and Brault (1991).

B. Radiative opacities

Until very recently, radiative opacities for stellar models had been taken almost exclusively from calculations performed at Los Alamos National Laboratory and made available in the Los Alamos Opacity Library (LAOL; see, for example, Cox, Stewart, and Eilers, 1965; Cox and Stewart, 1970; Huebner *et al.*, 1977; Magee, Merts, and Huebner, 1984; and Huebner, 1986). The uncertainties in the radiative opacity calculations were estimated by Bahcall *et al.* (1982), who compared neutrino fluxes computed using Los Alamos opacities with the corresponding fluxes computed using opacities obtained with a different code developed by B. Rosznyai (1980). The Rosznyai code uses a mean ion model that is based upon relativistic Hartree-Fock-Slater calculations.

In a major contribution to stellar astrophysics, a group at Lawrence Livermore National Laboratory has developed a new and independent code, called OPAL, for computing radiative opacities (see Iglesias, Rogers, and Wilson, 1987, 1990; Iglesias and Rogers, 1991a, 1991b; Rogers and Iglesias, 1992). This code removes several approximations that are present in the Los Alamos calculations for the equation of state and in the method for combining various photon absorption coefficients; the Livermore code also contains improvements in the basic atomic physics. The improvements in opacity values have already led to a better understanding of apparent discrepancies between stellar models and observations that can plausibly be attributed to inaccuracies in opacity (see, e.g., Stellingwerf, 1978; Andreasen, 1988; Andreasen and Petersen, 1988; Swenson, Stringfellow, and Faulkner, 1990; Cox, 1991; Stothers and Chin, 1991; Cox *et al.*, 1992; Moskalik and Dziembowski, 1992).

Table VI presents the solar interior opacities that we have used in our best solar models that were computed with and without including helium diffusion; these opacities were calculated by the Livermore group and generously made available for this project (Iglesias and Rogers, 1991c, private communication). The opacities were computed for the Anders and Grevesse (1989) mixture of heavy elements assuming the meteoritic iron abundance. Analogous tables were used (see Sec. V.C) in calculating solar models with the Grevesse (1984) mixture and with the Anders and Grevesse (1989) mixture that has the higher photospheric iron abundance.

For the conditions that apply in the deep interior of a solar model, the Livermore opacities are larger than the corresponding Los Alamos opacities, which leads to a higher calculated central temperature. Therefore models computed with the Livermore opacities produce, for the same element abundances, higher ^{8}B neutrino fluxes (cf. Bahcall, Bahcall, and Ulrich, 1969).

C. Neutrino fluxes with different abundances and opacities

Table VII shows the neutrino fluxes calculated for different sets of input abundances and radiative opacities. We have constructed accurate standard solar models with both sets of element mixtures, Grevesse (1984) and Anders and Grevesse (1989), using both the Los Alamos opacities and the Livermore opacities. We also present models that differ only in whether the meteoritic or the photospheric iron abundance is used. All of the models described in Table VII were computed using the same nuclear reaction rates and the same equation of state (with Debye-Hückel correction included) as were used in computing the final model listed in Table III (see Secs. II and III).

1. Results of model calculations

The first two rows in Table VII compare the neutrino fluxes and event rates calculated with Los Alamos opacities for the two different heavy-element mixtures, the largely photospheric abundances of Grevesse (1984) and the meteoritic abundance values of Anders and Grevesse (1989). The main difference between the two sets of input data is in the assumed iron abundance. The opacities used in evolving the model for row 1 were calculated for the Grevesse (1984) tabulation, which gave the photospheric iron abundance, 7.67, whereas the opacities used in calculating row 2 were computed for the meteoritic mixture of Anders and Grevesse (1989) with an iron abundance of 7.51. The Anders and Grevesse (1989) mixture leads to lower ^{13}N and ^{15}O neutrino fluxes relative to the earlier Grevesse (1984) mixture as a result of both the different relative and total abundances of CNO elements. The differences in the computed ^{7}Be and ^{8}B neutrino fluxes that correspond to using either the Grevesse (1984) or the Anders and Grevesse (1989) mixture are smaller than the change in the total Z would lead one to expect, because the difference in total Z between the two mixtures is compensated for partially by the different relative abundances among the individual heavy elements. The difference between the two sets of abundances corresponds to 0.9 SNU for the chlorine experiment and 4 SNU for the gallium experiment. This result agrees with the change predicted by the previously computed partial derivatives of neutrino fluxes with respect to individual element abundances (see Table XIII of Bahcall *et al.*, 1982).

TABLE VI. OPAL radiative opacities.[a]

	$R=\rho/T_6$							
	$X=0.73$, $Z=0.0188$				$X=0.35$, $Z=0.0188$			
T_6	1.000E−2	2.818E−2	3.981E−2	5.623E−2	1.000E−2	2.818E−2	3.981E−2	5.623E−2
1.000	27.34	54.31	66.46	80.12	24.31	50.68	62.65	76.66
1.218	23.01	47.87	59.14	71.89	20.32	43.92	54.99	67.81
1.483	20.44	42.90	52.90	64.13	17.86	39.02	48.71	59.91
1.807	18.12	36.93	44.89	53.36	15.77	33.44	41.12	49.62
2.200	15.28	28.57	33.82	39.24	13.38	25.90	30.95	36.48
2.680	11.93	19.94	23.03	26.28	10.54	18.20	21.20	24.44
3.264	8.405	13.08	14.90	16.87	7.469	11.96	13.71	15.64
3.975	5.648	8.506	9.644	10.89	5.013	7.760	8.856	10.05
4.841	3.750	5.576	6.316	7.182	3.306	5.067	5.737	6.562
5.896	2.520	3.776	4.283	4.869	2.196	3.357	3.830	4.384
7.181	–	2.664	3.034	3.490	–	2.324	2.670	3.094
8.746	–	2.000	2.316	2.698	–	1.730	2.007	2.364
10.652	–	1.637	1.908	2.224	–	1.402	1.644	1.946
12.973	–	1.416	1.632	1.872	–	1.213	1.413	1.647
15.800	–	1.230	1.383	1.553	–	1.061	1.203	1.371
19.243	–	1.040	1.146	1.270	–	0.9014	0.9944	1.124
23.436	–	0.8684	0.9469	1.036	–	0.7517	0.8165	0.9250
	$X=0.73$, $Z=0.0195$				$X=0.35$, $Z=0.0195$			
1.000	28.15	55.89	68.44	82.45	25.00	52.15	64.44	78.77
1.218	23.67	49.29	60.86	73.97	20.88	45.12	56.52	69.69
1.483	21.03	44.15	54.44	66.00	18.34	40.11	50.07	61.60
1.807	18.64	38.03	46.24	54.98	16.20	34.41	42.32	51.10
2.200	15.73	29.46	34.90	40.50	13.76	26.69	31.91	37.63
2.680	12.29	20.58	23.78	27.14	10.86	18.79	21.88	25.23
3.264	8.670	13.50	15.38	17.41	7.704	12.34	14.15	16.14
3.975	5.823	8.771	9.942	11.22	5.169	8.002	9.131	10.36
4.841	3.859	5.738	6.497	7.384	3.403	5.216	5.905	6.748
5.896	2.585	3.875	4.394	4.992	2.255	3.447	3.932	4.498
7.181	–	2.725	3.102	3.568	–	2.380	2.733	3.165
8.746	–	2.040	2.361	2.750	–	1.765	2.048	2.412
10.652	–	1.666	1.942	2.262	–	1.428	1.674	1.981
12.973	–	1.438	1.657	1.902	–	1.233	1.436	1.674
15.800	–	1.248	1.403	1.575	–	1.077	1.221	1.391
19.243	–	1.053	1.160	1.285	–	0.9132	1.007	1.138
23.436	–	0.8770	0.9560	1.046	–	0.7597	0.8250	0.9341

[a]Computed for the Anders and Grevesse (1989) mixture of heavy elements with meteoritic iron abundance, $Z/X=0.02668$. See Iglesias and Rogers (1991a, 1991b, 1991c) and Rogers and Iglesias (1992).

Rows 3, 4, and 5 were all computed with the new Livermore opacities. For rows 3 and 4, we have used, respectively, the photospheric abundances of Grevesse (1984) and of Anders and Grevesse (1989). The difference in event rates calculated with these two sets of abundances is only 0.1 SNU for the chlorine experiment and 1 SNU for the gallium experiment, reflecting the fact that the overall best estimates for the photospheric abundances did not change significantly in the interval between these two reviews. The situation is different for the fifth row, which was obtained using the lower meteoritic abundance of iron. This model, which uses what we believe is a better estimate of the iron abundance (the meteoritic iron abundance), predicts an event rate that is about 1.3 SNU lower for the chlorine experiment and about 6 SNU lower for the gallium experiment than is obtained with the models used to generate rows 3 and 4.

For the nuclear parameters used, our best estimate of the event rates in the standard solar model without diffusion is given in row 5 of Table VII. We believe that the Livermore opacities are superior to the earlier Los Alamos opacities because of the improvements summarized in Sec. V.B and the references contained therein. We adopt the meteoritic (lower) iron abundance for the reasons described in Sec. V.A.

2. Uncertainties due to abundances and opacities

In this paper we have taken the uncertainties in neutrino fluxes caused by uncertainties in radiative opacities to be equal to the *full* fractional differences in the neutrino fluxes between models with the same compositions but

TABLE VII. Standard solar models with different opacities and heavy-element mixtures. The neutrino fluxes are given in units of $cm^{-2}\,s^{-1}$

Opacity source	Mixture	*pp* (E10)	*pep* (E8)	*hep* (E3)	^{7}Be (E9)	^{8}B (E6)	^{13}N (E8)	^{15}O (E8)	^{17}F (E6)	Cl (SNU)	Ga (SNU)
LAOL[a]	Grevesse[c] (1984)	6.03	1.42	1.26	4.51	5.10	5.49	4.64	4.52	7.3	128
LAOL[a]	AnGr[d] (1989)	6.07	1.44	1.27	4.31	4.47	4.01	3.37	4.20	6.4	124
OPAL[b]	Grevesse[c] (1984)	5.98	1.40	1.22	4.90	5.97	6.07	5.25	5.14	8.4	134
OPAL[b]	AnGr[e] (1989)	5.99	1.40	1.22	4.96	6.11	4.92	4.32	5.46	8.5	133
OPAL[b]	AnGr[d] (1989)	6.04	1.43	1.25	4.61	5.06	4.35	3.72	4.67	7.2	127

[a]Los Alamos Opacity Library.
[b]Lawrence Livermore National Laboratory opacity code, Iglesias and Rogers (1991).
[c]Grevesse (1984) mixture of heavy elements.
[d]Anders and Grevesse (1989) meteoritic mixture of heavy elements, log[Fe/H]=7.51.
[e]Anders and Grevesse (1989) photospheric mixture of heavy elements, log[Fe/H]=7.67.

different opacity codes. Symbolically, we take the fractional uncertainty in a neutrino flux, ϕ, due to radiative opacities to be

$$\left[\frac{\Delta\phi}{\phi}\right]_{\text{opacity}} = 2\frac{[\phi(\text{Livermore})-\phi(\text{Los Alamos})]}{[\phi(\text{Livermore})+\phi(\text{Los Alamos})]}\ , \quad (20)$$

where for definiteness we use in Table VII the entries for the first row (LAOL, Grevesse, 1984) and the third row (OPAL, Grevesse, 1984) in computing the right-hand side of Eq. (20). Thus we compare opacities obtained from independent computer codes and calculational techniques in order to estimate the theoretical errors from this source. This definition leads to an opacity uncertainty of 1.1 SNU in the chlorine experiment and 6 SNU in the gallium experiment. In principle, we could also have used the comparison between rows 2 and 5 in Table VII, both computed for the Anders and Grevesse (1989) meteoritic mixture. Following the guidelines described in Bahcall *et al.* (1982) and Bahcall and Ulrich (1988), we adopt for calculating the contribution to the total theoretical error the definition that leads to the larger estimated uncertainty, which is the comparison between rows 1 and 3.

It would be easy, following the reasoning outlined in Eq. (20), to underestimate the uncertainties due to composition measurements by comparing the first entry of Table VII (LAOL, Grevesse, 1984) and the second entry (LAOL, Anders and Grevesse, 1989). The fractional uncertainty in an individual neutrino flux, ϕ, caused by uncertainties in the heavy-element abundances in this approximation would be taken to be

$$\left[\frac{\Delta\phi}{\phi}\right]_{\text{heavy elements}} = 2\frac{[\phi(\text{AnGr'89})-\phi(\text{Gr'84})]}{[\phi(\text{AnGr'89})+\phi(\text{Gr'84})]}\ . \quad (21)$$

We believe that Eq. (21) would underestimate the uncertainties. In the five years between the publication of the review by Grevesse (1984) and the appearance of the Anders and Grevesse (1989) paper, there was relatively little progress in reducing the uncertainties that are most important for solar neutrino fluxes. The best-estimate value for Z/X has changed by only 3.5% during the five years that have elapsed from the publication of the Grevesse (1984) value of 0.02765 to the publication of the Anders and Grevesse (1989) value of 0.02668 for the meteoritic iron abundance; the difference would be even less, only 0.6%, if we used the photospheric iron abundance with the Anders and Grevesse (1989) composition. The results quoted in these two reviews are very similar, in part, because there have not been great advances in measurement techniques or in precision between the publication of the Grevesse (1984) paper and the publication of the Anders and Grevesse (1989) paper. Therefore we prefer the more conservative reasoning that led Bahcall and Ulrich (1988) to adopt a 19% uncertainty in the primordial ratio of Z/X [see their Sec. II.B and Eq. (1)]. This uncertainty is larger than would be obtained from the compilations of Grevesse (1984) and Anders and Grevesse (1989) if we interpret their listed uncertainties as 1σ errors and multiply by 3 in order to approximate the effective 3σ uncertainties adopted here (see Sec. VIII). The uncertainty in calculated solar neutrino rates that follows from this more conservative prescription is, for the neutrino fluxes listed in the last row of Table VII, about 1.6 SNU for the chlorine experiment and 8.4 SNU for the gallium experiment.

VI. BEST SOLAR MODEL WITHOUT ELEMENT DIFFUSION

There has been some improvement in our knowledge of nuclear physics parameters since the systematic determination of preferred values by Bahcall and Ulrich (1988). Several important experiments and calculations have been performed, and one previously outstanding

discrepancy between different measurements has been recognized as being due to a systematic error. In our choice of nuclear parameters, we have been guided generally by the review and reanalysis carried out by two senior experimentalists, Parker and Rolfs (1991). For three reactions, the *pp* reaction, the *hep* reaction, and the ^{7}Be$(p,\gamma)^8$B reaction, we have taken account in Secs. II.B.1 and II.B.2 of more recent work than was discussed by Parker and Rolfs (1991). The final column of Table I gives, for the most important nuclear parameters, the preferred values we have adopted for our best standard models, with and without diffusion. The revised values we use here correspond to multiplying, the previously standard cross-section factors for reactions 1, 3, 4, and 6 of Table I by 0.98, 0.97, 0.99, and 0.92, respectively, all constituting relatively minor changes. In addition, the cross-section factor for the rare and highly uncertain *hep* reaction has changed by a large factor (see Sec. II.B.2 and Table I), but this has no significant effect on the calculated solar structure or on the other solar neutrino fluxes. For all nuclear parameters not given in Table I, we have used the standard values adopted by Bahcall and Ulrich (1988), except for the ^{8}B and *hep* neutrino absorption cross sections for which the current adopted values are 3% and 9% larger, respectively (see Sec. III and Garcia *et al.*, 1991).

A. Some important model results

The second column of Table VIII gives some of the important overall parameters for our best standard model that was computed neglecting helium diffusion but including the preferred nuclear parameters, the Anders and Grevesse (1989) heavy-element *meteoritic* (i.e., smaller Fe) mixture, the Livermore opacities (Iglesias and Rogers, 1991a, 1991b), weak and intermediate electron screening (see Sec. II), and the Debye-Hückel correction [see Eq. (14)]. For our purposes, two of the most important numbers are the predicted event rates in the ^{37}Cl experiment (Davis, 1978, 1987; Davis *et al.*, 1990) for a currently best standard solar model,

$$\Sigma(\phi\sigma)_{\rm Cl}=7.2\pm2.7\ \text{SNU}\ , \tag{22}$$

and the calculated rate for the ^{71}Ga experiments (Kirsten, 1986; Gavrin *et al.*, 1990; Abazov *et al.*, 1991b),

$$\Sigma(\phi\sigma)_{\rm Ga}=127.5^{+19}_{-16}\ \text{SNU}\ . \tag{23}$$

The predicted ^{8}B neutrino flux, which is measured directly in the Kamiokande (Hirata *et al.*, 1989, 1990a, 1990b, 1991) and Super-Kamiokande (Totsuka, 1990), and which will be measured in the SNO (Ewan *et al.*, 1987) solar neutrino experiments, is

$$\phi(^8\text{B})=5.1(1\pm0.43)\times10^6\ \text{cm}^{-2}\text{s}^{-1}\ . \tag{24}$$

In order to predict event rates in the Kamiokande, Super-Kamiokande, and SNO experiments, the flux given in Eq. (24) must be convolved with the measured energy resolution and detection sensitivity.

The calculated values given in Eqs. (22)–(24) are well within the range estimated previously for standard solar models (see Bahcall and Ulrich, 1988). The theoretical uncertainties determined in this paper are discussed in Sec. VIII.

TABLE VIII. Some effects of helium diffusion in solar models[a]

Quantity	Best without diffusion	Best with diffusion	Percentage change
Z	0.01895	0.01958	+3.3
$Y_{\rm initial}$	0.2716	0.2727	+0.4
$Y_{\rm surface}$	0.2716	0.2466	−9.6
$Y_{\rm central}$	0.6270	0.6376	+1.7
$T_{\rm central}$	1.559	1.569	+0.6
$M_{\rm conv}$	0.0216	0.0254	+16.2
$R_{\rm conv}$	0.721	0.707	−2.0
Mixing length	1.27	1.36	+6.8
$\phi(pp)$	6.04E+10	6.00(1±0.02)E+10	−0.7
$\phi(pep)$	1.43E+8	1.43(1±0.04)E+8	0.0
$\phi(hep)$	1.25E+3	1.23E+3	−1.6
$\phi(^7\text{Be})$	4.61E+9	4.89(1±0.18)E+9	+5.9
$\phi(^8\text{B})$	5.06E+6	5.69(1±0.43)E+6	+11.7
$\phi(^{13}\text{N})$	4.35E+8	4.92(1±0.51)E+8	+12.3
$\phi(^{15}\text{O})$	3.72E+8	4.26(1±0.58)E+8	+13.5
$\phi(^{17}\text{F})$	4.67E+6	5.39(1±0.48)E+6	+14.3
$\Sigma(\phi\sigma)_{\rm Cl}$	(7.2±2.7) SNU	(8.0±3.0) SNU	+10.5
$\Sigma(\phi\sigma)_{\rm Ga}$	127^{+19}_{-16} SNU	132^{+21}_{-17} SNU	+3.1

[a]Temperatures are expressed in 10^7 K, neutrino fluxes in $\text{cm}^{-2}\text{s}^{-1}$, and $M_{\rm conv}$, $R_{\rm conv}$ in solar masses and solar radii. The values given here are computed using the preferred nuclear reaction rates (Sec. II.A, Sec. II.B, and Table I), the Anders and Grevesse (1989) heavy-element mixture with meteoritic iron, $Z/X=0.02668$, OPAL opacities (Iglesias and Rogers, 1991a, 1991b), and the Debye-Hückel equation of state [see Eq. (3) in Sec. III.B].

B. Detailed numerical models

Tables XV and XVII in the Appendix present a detailed numerical description of the solar interior of the standard model without helium diffusion. These details should be sufficient to permit accurate calculations of the effects of various proposed modifications of the weak interactions on the predicted neutrino fluxes. The first six columns of Table XV present physical variables that together help to define the model: the mass included in the current and all inner zones, the radius, the temperature (in degrees K), the density, the pressure, and the luminosity integrated up to and including the current zone. We use cgs units for density and pressure. The last five columns of Table XV give, except for helium, the principal isotopic abundances by mass. The helium abundance is determined by the relation $Y=1.0-X(^1\mathrm{H})-X(^3\mathrm{He})-Z$, where the heavy-element abundance Z is given in Table VIII.

Table XVII gives the neutrino fluxes produced in a given spherical shell, as well as the temperature, electron number density, fraction of the solar mass, and the ^{7}Be abundance by mass in the shell.

VII. BEST SOLAR MODEL WITH HELIUM DIFFUSION

Convection is the only mechanism that is usually included in standard solar models which describes material motions within a star. However, interactions between species of different mass cause heavier elements to transfer momentum to lighter elements; the heavier elements sink relative to hydrogen (gravitational settling). The presence of a temperature gradient also causes lighter elements to rise relative to heavier ones (thermal diffusion). In addition, radiation pressure can cause partially ionized or neutral species to rise relative to species with a smaller cross section (radiative levitation); this process is unimportant for the sun (Michaud *et al.*, 1976). For the remainder of this section, we concentrate on gravitational settling and thermal diffusion of the two most abundant elements, hydrogen and helium.

We summarize in Sec. VII.A the equations that describe helium diffusion in the convenient approximation developed by Bahcall and Loeb (1990) and then outline in Sec. VII.B the calculations that are performed in a separate (exportable) subroutine that computes helium diffusion. In Sec. VII.C we present the results of solar evolutionary models that include helium diffusion and compare the characteristic parameters obtained with and without diffusion. Detailed numerical models are presented in Tables XVI and XVIII of the Appendix. We note that the Bahcall-Loeb treatment of diffusion describes the same physical processes, gravitational settling and thermal diffusion, as in previous treatments (e.g., Michaud *et al.*, 1976; Noerdlinger, 1977; Paquette *et al.*, 1986; and Cox, Guzik, and Kidman, 1989). The principal difference from earlier work is that Bahcall-Loeb made systematic approximations that reduced the interactions between multiple components into a single (for helium diffusion) partial differential equation rather than a set of coupled equations.

A. Basic equations for helium diffusion

The diffusion of the helium mass fraction, Y, satisfies the equation (Bahcall and Loeb, 1990)

$$\frac{\partial Y}{\partial t}=-\frac{1}{\rho r^2}\frac{\partial}{\partial r}\left[\frac{r^2XT^{5/2}\xi_H(r)}{(\ln\Lambda/2.2)}\right], \tag{25}$$

where X is the hydrogen mass fraction and $\ln\Lambda$ is the Coulomb logarithm that has a weak dependence on the plasma characteristics (see, e.g., Braginskii, 1965). For the solar interior (and similar plasmas), one can use the approximation $\ln\Lambda\approx 2.2$ (Noerdlinger, 1977). The units have been chosen so that the numerical coefficient of the right-hand side of Eq. (25) is unity (see definition below of the dimensionless variables used here). The time rate of change of the helium mass fraction is approximately equal in magnitude and opposite in sign to the rate of change of the hydrogen mass fraction. Hydrogen diffuses slowly upward from the stellar interior while helium diffuses slowly downward.

The dimensionless function $\xi_H(r)$ that appears in Eq. (25) is (Bahcall and Loeb, 1990)

$$\xi_H(r)=\frac{5(1-X)}{4}\frac{\partial \ln P}{\partial r}+\frac{\partial}{\partial r}\ln\left\{\frac{X(1+X)}{(3+5X)^2}\right\}$$
$$+\Phi_H(X)\frac{\partial \ln T}{\partial r}\,. \tag{26}$$

The first two terms in Eq. (26) correspond to gravitational settling, and the third term represents thermal diffusion. The thermal diffusion function $\Phi(X)$ can be written in the following form:

$$\Phi(X)\approx\frac{6(1-X)(X+0.32)}{(1.8-0.9X)(3+5X)}\,. \tag{27}$$

Equations (25) and (26) are in dimensionless form. The unprimed dimensionless variables are defined in terms of primed dimensional variables by

$$r=\frac{r'}{R_\odot},\quad T=\frac{T'}{T_0},\quad \rho=\frac{\rho'}{\rho_0}\,. \tag{28}$$

Following Bahcall and Loeb, we adopt $T_0=10^7$ K and $\rho_0=100$ g cm^{-3}, representative values for the interior region of the standard solar model. The corresponding characteristic diffusion time τ_0, where we define a dimensionless time t by $t=t'/\tau_0$, yields for a density ρ_0, a temperature T_0, and $\ln\Lambda=2.2$, $\tau_0=6\times10^{13}$ yr.

In Eqs. (25) and (26) the partial time derivatives are evaluated at constant mass shells of the star. In these Lagrangian coordinates, the diffusion equations are solved with zero hydrodynamic velocity of the stellar plasma. The temporal evolution of the radius during the star's lifetime is automatically included via the changes in the

spatial positions of the different mass shells.

The results summarized in Eqs. (25), (26), and (27) are expected to be accurate to of order ±30% (total errors), which is sufficiently accurate to permit a good estimate of the small effects of diffusion in solar models and in a number of other applications. The main uncertainties arise with respect to the exact evaluation of the Coulomb logarithm and the collision integrals needed for the thermal diffusion coefficients. The effects of uncertainties in the basic equations can be estimated easily by multiplying the right-hand side of Eq. (25) by a constant equal to 1 ± 0.3 and then evolving a solar model with this altered equation for the helium diffusion rate. Uncertainties that are related to the thermal diffusion coefficient can be estimated by multiplying the right-hand side of Eq. (27) by an appropriate constant.

B. Method

In constructing solar models with helium diffusion, we used a new subroutine written by one of us (MHP) that carries out the diffusion calculations using data supplied by other parts of the Yale code, in which the thermal structure and the element abundances are calculated. We assumed that the amount of diffusion within a given time step was too small to affect significantly the changes in thermal structure, in abundances, and in nuclear reaction rates that are calculated elsewhere. We verified the correctness of this assumption by showing that decreasing the time steps by a factor of 2 produced negligible changes in the final results. Typical time steps were 9×10^7 yr.

The diffusion subroutine computes the change in hydrogen and helium abundance as a function of mass fraction. Within the subroutine, Eq. (25) was solved in two stages. The first and third terms of $\xi_H(r)$ in Eq. (26) give rise to first spatial derivatives of the hydrogen mass fraction when used in Eq. (25). The second term in Eq. (26) gives rise to a second spatial derivative of the hydrogen abundance and is typically much less important. This type of equation is most easily solved with an implicit-explicit approach (Press *et al.*, 1986).

We first solve Eq. (25) by neglecting the second derivatives of the hydrogen abundance and by using a two-step Lax-Wendroff technique (Press *et al.*, 1986). We then use this trial solution to determine the term depending upon second derivatives by a fully implicit method; we iterate the solution until the desired accuracy is achieved (usually 1 part in 10^{10}). This approach requires only a small additional amount of computer time, typically 1% extra computational time, when compared to models that were computed without diffusion.

C. Results with diffusion

The middle column in Table VIII gives the neutrino fluxes and other parameters computed from the Yale standard model including helium diffusion. The predicted event rate in the ^{37}Cl (Davis, 1978, 1987, 1989; Davis *et al.*, 1990) experiment is

$$\Sigma(\phi\sigma)_{\rm Cl}=8.0\pm3.0\ \text{SNU}\ , \tag{29}$$

and the corresponding rate for the ^{71}Ga experiments (Kirsten, 1986; Gavrin *et al.*, 1990; Abazov *et al.*, 1991b) is

$$\Sigma(\phi\sigma)_{\rm Ga}=131.5^{+21}_{-17}\ \text{SNU}\ . \tag{30}$$

The ^{8}B neutrino flux, measured in the Kamiokande (Hirata *et al.*, 1989, 1990a, 1990b, 1991), Super-Kamiokande (Totsuka, 1990), and the SNO (Ewan *et al.*, 1987) solar neutrino experiments, is

$$\phi(^8\text{B})=5.7(1\pm0.43)\times10^6\ \text{cm}^{-2}\text{s}^{-1}\ . \tag{31}$$

The estimated uncertainties are discussed in Sec. VIII.

Inclusion of helium diffusion in the stellar evolution code increases (see Table VIII) the calculated ^{8}B neutrino flux by about 12%, the ^{7}Be neutrino flux by about 6%, and the CNO fluxes by approximately 13%. The predicted event rate in the chlorine experiment is increased by 0.8 SNU, or about 11%, from 7.2 SNU to 8.0 SNU; the calculated event rate in the gallium experiment is increased correspondingly by 4 SNU, or 3%, from 127.5 SNU to 131.5 SNU.

As helium sinks, it raises the mean molecular weight in the core. This leads (see Table VIII) to a 0.6% increase in the central temperature, an increase of 0.4% in the calculated primordial helium abundance, and a slight concentration of the energy generation towards the center. The computed depth of the convection zone, $R=0.707R_\odot$, is in agreement with the value of $0.71R_\odot$ inferred from an early analysis of p-mode oscillation data by Christensen-Dalsgaard, Gough, and Toomre (1985) and with the more precise value of $(0.713\pm0.003)R_\odot$ inferred recently by Christensen-Dalsgaard, Gough, and Thompson (1991). The Christensen-Dalsgaard *et al.* (1991) analysis uses the observed p-mode oscillation frequencies reported by Duvall *et al.* (1988) and by Libbrecht and Kaufman (1988). The uncertainty in the calculated depth of the convective zone that arises from the estimated (Bahcall and Loeb, 1990) ±30% uncertainty in the helium diffusion rate is $0.004R_\odot$.

In calculating accurate solar models with helium diffusion, it is important to perform enough iterations in order to be able to precisely match the ratio of heavy elements to hydrogen, Z/X, that is observed on the solar surface at the present epoch. Since the surface abundance of hydrogen changes with time in models with diffusion, it is possible to make a factor-of-2 error in the size of diffusion-induced changes if one fails to iterate the model to achieve the correct Z/X ratio.

Figure 1 compares the temperature profiles computed with and without including helium diffusion. Figure 2 compares the profile of the hydrogen abundance computed with and without helium diffusion. In the approximation we are using, the change in the helium abundance, ΔY, that is caused by helium diffusion is related to the

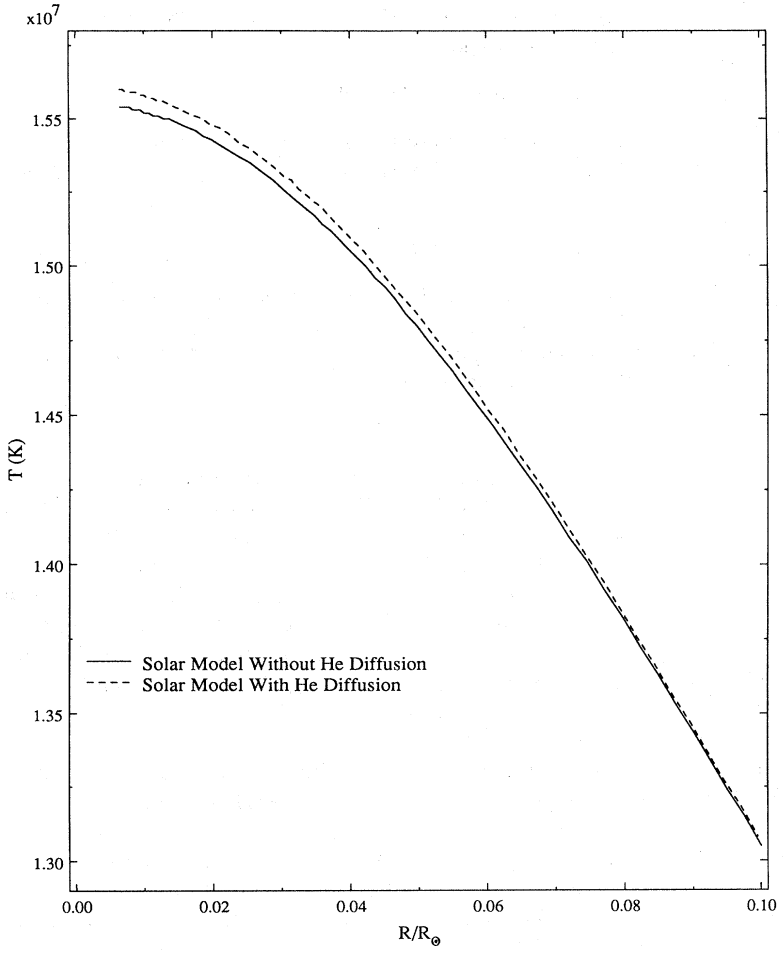

FIG. 1. Comparison of the temperature profiles computed with and without including helium diffusion.

change in the hydrogen abundance (shown in Fig. 2) by the simple equation $\Delta Y = -\Delta X$.

It is also of interest to compare our results with those of Proffitt and Michaud (1991), who have calculated the effects of helium diffusion in the sun using diffusion coefficients derived by Paquette *et al.* (1986). Table IX shows for the Proffitt and Michaud (1991) calculations (indicated by PM in the table) and for the work in this

TABLE IX. Effects of diffusion: two different approaches. The second and third columns give the percentage changes produced by diffusion as calculated by Bahcall and Pinsonneault (BP, this paper) and by Proffitt and Michaud (1991; PM). The fourth and fifth columns list the absolute changes produced by diffusion with the units, where relevant, indicated in the first column. The numbers in parentheses were obtained by holding the heavy element abundance Z constant, rather than iterating so that the model has the observed value of Z/X for the mixture.

Quantity	δ(%) BP	δ(%) PM	δ BP	δ PM
Y_{initial}	+0.4(−0.6)	(−0.7)	+0.0011(−0.0017)	(−0.0020)
Y_{surface}	−9.6(−10.2)	(−12.0)	−0.0250(−0.0278)	(−0.0338)
Y_{central}	+1.7(+1.1)	(+1.6)	+0.0106(+0.0071)	(+0.0102)
$T_{\text{central}}/10^5$ K	+0.6(+0.4)	(+0.5)	+1(+0.6)	(+0.8)
$M_{\text{conv}}/M_\odot$	+16.2(+15.7)	(+25)	+0.0038(+0.00339)	(+0.004)
$R_{\text{conv}}/R_\odot$	−2.0(−1.7)	(−2.3)	−0.014(−0.012)	(−0.017)
Mixing length	+6.8(+6.3)	(+9.4)	+0.09(+0.081)	(+0.154)

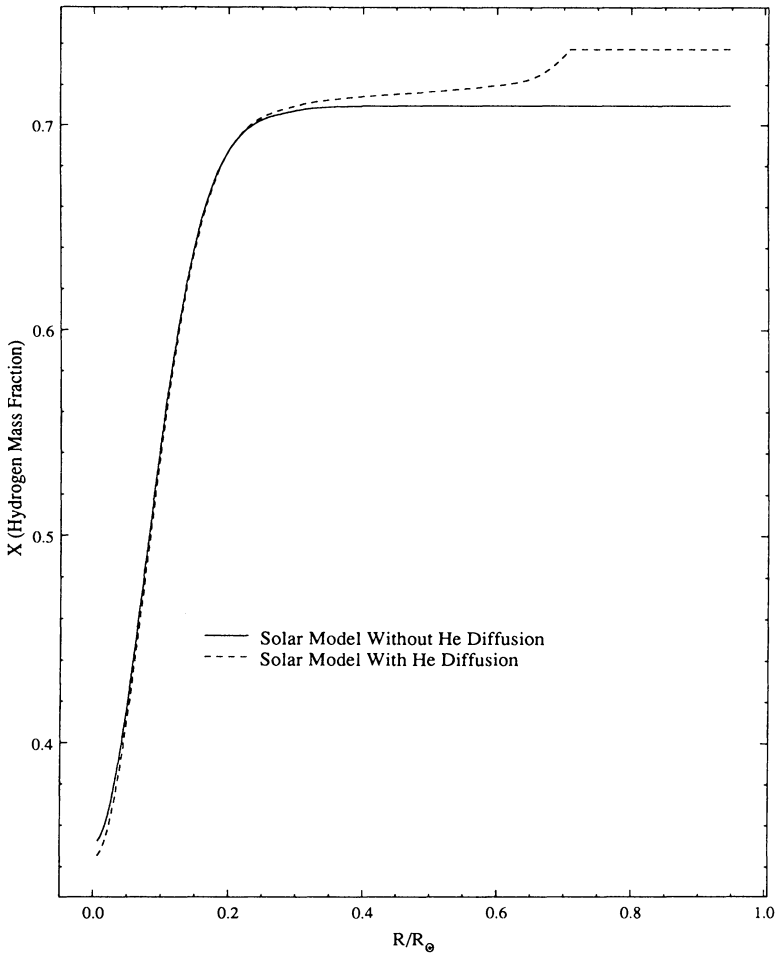

FIG. 2. Comparison of the profiles for the hydrogen mass fraction X computed with and without including helium diffusion.

paper (indicated by BP in the table) the percentage differences and the absolute changes that diffusion produces in the helium abundance, central temperature, depth and mass of the convective zone, and the mixing length. The quantities shown in parentheses were calculated by holding the heavy-element abundance Z constant, rather than keeping the heavy-element-to-hydrogen ratio Z/X constant and equal to the observed value. The differences are within the expected accuracy of the physical treatment of the diffusion process. The slightly different change in central temperature found in the two calculations corresponds to approximately 0.1 SNU in the chlorine experiment, using the approximate scaling laws described in Sec. 6.2 of Bahcall (1989).

Tables XVI and XVIII, in the Appendix, present a detailed numerical description of the interior of our best standard solar model that was calculated with the inclusion of helium diffusion.

VIII. UNCERTAINTIES

The uncertainties estimated in this paper for predicted solar neutrino fluxes and predicted event rates represent the total theoretical uncertainties as defined in Bahcall and Ulrich (1988) and in Chap. 7 of Bahcall (1989). We use, as described in these references, 3σ errors for all measured input quantities. For parameters that must be determined theoretically, we use a broad range of calculated values. The most important theoretical uncertainty relates to the radiative opacity (see discussion below).

Many experimentalists quote 1σ errors. The most comparable quantity for our theoretical calculations is obtained by dividing the theoretical errors we quote by a factor of 3. This prescription is accurate for all of the errors in our results that are determined by measurement uncertainties in input parameters and is plausibly of the right size for the errors we quote on quantities that must be calculated because they cannot be measured.

For most of the uncertainties, we have used the same estimates as those given by Bahcall and Ulrich (1988). However, we have revised some of the nuclear physics uncertainties; the revised values are given in Sec. II and in Table I. We have also determined new estimates for the uncertainties due to radiative opacities and to heavy-element abundances; these new estimates are described in Sec. V.C.2 and in Eqs. (20) and (21).

The uncertainty we estimate for the radiative opacity is approximately twice as large as we used in our earlier studies (see Bahcall *et al.*, 1982 and Bahcall and Ulrich,

1988); this increase is due to the inclusion here of the factor of 2 in the right-hand side of Eq. (20). The factor of 2 reflects the "rule-of-thumb" (see Sec. 7.1 of Bahcall, 1989) that the changes with time of the "best" estimate of a particular quantity are often the most realistic indication of the uncertainties. However, a word of caution should be included with this uncertainty estimate. Approximately half or more of the radiative opacity in the central regions of the sun in which the neutrinos are produced is caused by photon scattering on free electrons and by inverse bremsstrahlung in the presence of completely ionized hydrogen and helium, processes that occur even if the heavy-element abundance is identically zero and which can be calculated with an accuracy of better than 10%. Simple physics dominates the opacity in the central regions of the sun. It is therefore unlikely that refinements in the calculations will *reduce* the central opacity by a major factor. Moreover, opacities computed for temperatures less than the temperature (2×10^6 K) at the base of the convective zone have no influence on calculations of solar structure or neutrino production, although atmospheric opacities are important for helioseismological studies. We believe, therefore, that we may have overestimated the amount by which future improvements in opacity might decrease the ^{8}B neutrino flux.

In the same vein, we admit that we have made a very conservative error estimate (see Sec. V.C.2 for a discussion of our reasoning) for the important parameter, the ratio, Z/X, of heavy elements to hydrogen. The best-estimate value for Z/X has changed by only 3.5% from the time of publication of the Grevesse (1984) value of 0.02765 to the publication of the Anders and Grevesse (1989) value of 0.02668 (meteoritic iron abundance). In our error estimates, we have followed Bahcall and Ulrich (1988) and have assumed a total uncertainty of 19% in the value of Z/X.

Table X gives the calculated uncertainties that are caused by some of the most important individual parameters. No single parameter dominates the calculated uncertainties. The first four parameters are the low-energy cross-section factors for reactions 1, 3, 4, and 6 of Table I; the last three parameters are, respectively, the heavy-element-to-hydrogen ratio, the radiative opacity, and the neutrino absorption cross sections. We have not shown explicitly the small effect of the uncertainty in the diffusion rate, which may be estimated directly from Table VIII as a factor of 0.3 times the differences between models evolved with and without including helium diffusion. The uncertainties in Table X are given in SNU for the predicted event rates of the chlorine and gallium experiments and are given in fractions of the calculated fluxes for the ^{7}Be and ^{8}B neutrino fluxes. When expressed in SNU, the uncertainties are slightly different for the best standard model without diffusion (described in Sec. VI) and for the best standard model including helium diffusion (described in Sec. VII). The uncertainties in SNU that appear in Table X were calculated for the solar model that includes helium diffusion.

The total theoretical uncertainties in the individual neutrino fluxes are given in the third column of Table VIII.

Why are the uncertainties quoted by Turck-Chièze *et al.* (1988) larger than those given in this paper and in Bahcall and Ulrich (1988)? The reason is that Turck-Chièze *et al.* assume larger uncertainties for two important quantities: the low-energy cross-section factor for the ^{7}Be$(p,\gamma)^8$B reaction and the radiative opacities. We believe that the uncertainties assumed by Turck-Chièze *et al.* (1988) are too large.

Table XI compares the 1σ uncertainties for $S_0(^8\mathrm{B})$ and the radiative opacity used in the present work with the values used by Turck-Chièze *et al.* (1988).

For $S_0(^8\mathrm{B})$, we have adopted in the present work the 1σ uncertainty of 9.3% determined by Johnson *et al.* (1992) in their recent comprehensive reanalysis of all the

TABLE XI. Comparison of uncertainties: 1σ estimates.

Source	σ(this work)	σ(Turck-Chièze *et al.*)
$S_0(^8\mathrm{B})$	9%[a]	15%
Opacity	~2.5%[b]	≥5%

[a]Taken from Johnson *et al.* (1992).
[b]Characteristic difference between the solar interior opacities calculated with the Livermore and with the Los Alamos opacity codes (see Iglesias and Rogers, 1991a, and Sec. V.C.2).

TABLE X. Individual uncertainties in predicted capture rates and in neutrino fluxes. The uncertainties shown represent 3σ errors for measured quantities. The different detectors are listed in the first column. For the first two rows, columns 2 through 8 contain the uncertainty in SNU of the total capture rate caused by the uncertainty in the parameter shown at the top of the column. The last two rows give the calculated *fractional* uncertainties in the ^{7}Be and the ^{8}B neutrino fluxes. The total uncertainty is calculated by combining incoherently the uncertainties from each parameter shown and the smaller uncertainties estimated for less critical parameters.

Detector or flux	*pp*	^{3}He+^{3}He	^{3}He+^{4}He	^{7}Be+*p*	*Z*/*X*	Opacity	σ_{abs}	Total
^{37}Cl	0.8	0.5	0.6	1.7	1.8	1.1	0.6	3.0
^{71}Ga	3.7	2.9	3.6	3.9	9.4	5.4	16	21
^{7}Be	0.04	0.07	0.08	0.0	0.11	0.08		0.18
^{8}B	0.11	0.06	0.08	0.28	0.25	0.16		0.43

available experimental information. We use in our calculations of the total uncertainty a 3σ uncertainty of 28% for $S_0(^8B)$, consistent with our general policy of adopting for each paper in this series the contemporary 3σ error limits for all experimentally determined quantities. Turck-Chièze *et al.* (1988) have adopted a bigger 1σ uncertainty, 15%, which is about a factor of 2 larger than determined by the contemporary analyses of this reaction by experimentalists (see Filippone, 1986; Parker, 1986). The Turck-Chièze *et al.* prescription would, if applied to our calculations, increase the estimated uncertainty for the chlorine experiment from just the $S_0(^8B)$ input parameter from 1.7 SNU to 2.7 SNU.

Turck-Chièze *et al.* have adopted a large uncertainty in the radiative opacity, in excess of 5% in the solar interior. This large uncertainty lacks justification. Our policy is to estimate theoretical errors, in the absence of a specific error calculation, by comparing the differences with time of different state-of-the-art evaluations. Iglesias and Rogers (1991a) have evaluated the fractional differences between the much improved Livermore opacities and the earlier Los Alamos opacities; the typical differences are of order 2.5% in the solar interior. This result is a factor of 2 less than the minimum 1σ uncertainty assumed by Turck-Chièze *et al.* For our final error estimates, we evolved accurate solar models using the Livermore and the Los Alamos opacities and compared the differences in order to estimate the total theoretical uncertainties [see Sec. V.C.2, Eq. (20), and Table VII for details]. We believe that our method of estimating the error is preferable, since it is based upon comparing the results obtained by explicit stellar evolution calculations with different input parameters. If we had used instead the Turck-Chièze *et al.* prescription, the total theoretical uncertainty from radiative opacity for our best calculations would have been increased for the chlorine experiment by a factor of about 2.6 from 1.1 SNU (see Table X) to 2.9 SNU.

We also note that Turck-Chièze *et al.* assume a large 1σ uncertainty of 10% for the primordial ratio of heavy elements to hydrogen, Z/X. The corresponding 3σ uncertainty for Z/X is 30%, which is significantly bigger than the conservative estimate of 19% adopted in this work and by Bahcall and Ulrich (1988) and much larger than the change of 3.5% that has occurred from the time of publication of the standard Grevesse (1984) value of 0.02765 to the publication of the Anders and Grevesse (1989) value of 0.02668 (meteoritic iron abundance). Further observational improvements over the next decade will determine if all groups have overestimated the uncertainty due to Z/X. Decreasing the error estimate for Z/X by a factor of 2 would decrease the total calculated uncertainty for the chlorine experiment by a modest amount, about 15%.

Suppose we use in the Turck-Chièze *et al.* (1988) calculation the recently determined (Johnson *et al.*, 1992) uncertainty in $S_0(^8B)$ and the uncertainty in radiative opacity that results from comparing the most recent Livermore and Los Alamos solar interior opacities (see Table XI). The total uncertainty (3σ limits on experimental input data) for the Turck-Chièze *et al.* model is then in good agreement with the value of 3.0 SNU given in this paper.

IX. THE MAXIMUM RATE MODEL

Nearly all published nonstandard solar models yield, by design, a smaller ^8B neutrino flux than is predicted by the standard solar model (see Chap. 5 of Bahcall, 1989). Presumably, the explanation for this fact is that a number of imaginative scientists have concentrated on discovering what changes in various input quantities or in the physical descriptions of the solar material would "solve the solar neutrino problem," even if the changes were implausible or, as was true in many cases, apparently ruled out by independent theoretical or experimental considerations. There is a need, in addition, for a different kind of nonstandard solar model that yields as large as possible—in some well-defined sense—a ^8B neutrino flux. This Maximum Rate Model could be used together with models for changed neutrino physics, such as the MSW solution, to set limits on the maximum influence of nonstandard neutrino physics on the produced solar neutrino fluxes. For example, at present it is usually assumed that the reduction caused by neutrino oscillations could be at most a factor of 4, from the best-estimate calculated rate for Cl of about 8 SNU to the experimental value of about 2 SNU. In principle, the true production rate for the ^8B neutrino flux could be larger than predicted by the best standard solar model, and this larger rate could then be reduced to the observed value by nonstandard neutrino physics whose parameters should be inferred from the correct (larger-than-standard) production rate (cf. Chen and Cherry, 1991).

For illustrative purposes only, we give in Table XII the calculated results of a Maximum Rate Model. This model is identical to our best standard model including helium diffusion, except for the fact that we have set the rate of the ^3He-^3He reaction (reaction 4 of Table I) equal to zero. The Maximum Rate Model is a nonphysical model in which all of the terminations of the proton-proton chain occur via the ^3He-^4He reaction. The opposite limit, in which all of the terminations occur via the ^3He-^3He reaction, yields (see Chap. 11 of Bahcall, 1989) the minimum rate consistent with standard electroweak

TABLE XII. Maximum rate model.

Neutrino source	Flux ($cm^{-2}s^{-1}$)	Cl (SNU)	Ga (SNU)
pp	3.5E+10	0.0	41.4
pep	6.9E+7	0.1	1.5
hep	4.1E+4	0.2	0.3
^7Be	3.3E+10	7.8	239.4
^8B	7.4E+6	8.0	17.9
^{13}N	1.7E+8	0.03	1.0
^{15}O	9.9E+7	0.07	1.1
Total		16.3	303

theory and the assumption that the sun currently is generating nuclear energy in its core at the rate at which it is radiating energy from its surface.

The energy production in the Maximum Rate Model is dominated by reactions 4 and 5 of Table I followed by $^7\text{Li}(p,\alpha)^4\text{He}$. The changed nuclear reaction chain, taken together with the standard boundary condition that the model luminosity at the current epoch be equal to the observed solar luminosity, leads to some unusual effects that are discussed below.

The calculated neutrino fluxes and event rates for the Maximum Rate Model are shown in Table XII. For the chlorine experiment, the Maximum Rate Model predicts

$$\Sigma(\phi\sigma)_{\text{Cl}}=16.3\pm4.7 \text{ SNU} ; \quad (32)$$

the corresponding rate for the ^{71}Ga experiment is

$$\Sigma(\phi\sigma)_{\text{Ga}}=303^{+57}_{-54} \text{ SNU} . \quad (33)$$

These rates for the Maximum Rate Model are about a factor of 2 larger than the corresponding predictions of the standard solar model. As shown in Table XII, the ^{7}Be and ^{8}B neutrino fluxes contribute almost equally to the chlorine rate, while the calculated rate for the gallium experiment is dominated by the ^{7}Be neutrino flux.

Compared to standard solar models, the Maximum Rate Model has a low central temperature, $T=14.7\times10^6$ K, but a high predicted ^{8}B neutrino flux and high predicted neutrino capture rates. This combination of relatively low temperature (6% lower than in the standard solar model, see Table VIII) and high rates departs strongly from the well-known correlation between temperature and ^{8}B neutrino flux (or predicted event rate in the chlorine experiment) that exists for standard solar models (see Sec. 6.2 of Bahcall, 1989). The key to understanding this result is the distribution of ^{3}He in the solar interior, which peaks at a very large value (2% by mass at $0.16R_\odot$) in the Maximum Rate Model. The dominant mechanism for destroying ^{3}He in the standard model, the ^{3}He-^{3}He reaction (reaction 3 of Table I), is, by assumption, not operative in the Maximum Rate Model, which allows ^{3}He to build up to a large equilibrium abundance that can be burned efficiently by the ^{3}He-^{4}He reaction. The exclusive dependence upon the more temperature sensitive ^{3}He-^{4}He and CNO reactions (see Table I) to produce the solar luminosity results in a convective core that persists for 1.9×10^9 years and which contains about 9% of the mass for the first 10^9 years. These two factors, the higher ^{3}He abundance and the convective core, result in a smoother and lower temperature profile for the Maximum Rate Model as compared to the standard solar model.

X. DISCUSSION

We have shown in Sec. IV that, for the same input data, four state-of-the-art solar evolution codes all give the same event rates to within ±0.1 SNU (1%) for the chlorine experiment. The three codes that can be compared give the same result within ±0.5 SNU (better than 0.5%) for the gallium experiment. The computed ^{8}B neutrino fluxes agree to within a few percent, when the published fluxes are corrected to all refer to the same input data. These important results are made manifest by Tables III–V and by Eqs. (15)–(19). The larger differences between event rates that are occasionally found in the literature arise from different choices of input data or from programing errors; the differences do not reflect uncertainties in the equations of stellar evolution or in the numerical techniques. This point has sometimes been misunderstood by physicists not familiar with stellar evolution theory who have inferred that differences in quoted solar neutrino fluxes reflected different stellar astrophysics rather than different choices of input data.

TABLE XIII. Individual neutrino contributions to the calculated event rates in the chlorine and gallium solar neutrino experiments. The neutrino fluxes are calculated with our best solar model which includes helium diffusion.

Neutrino source	Cl (SNU)	Ga (SNU)
pp	0.0	70.8
pep	0.2	3.1
^{7}Be	1.2	35.8
^{8}B	6.2	13.8
^{13}N	0.1	3.0
^{15}O	0.3	4.9
Total	8.0±3.0	131.5^{+21}_{-17}

In new models discussed in this paper, we have included the diffusion of helium and hydrogen in the evolutionary calculations of a standard solar model according to the prescription of Bahcall and Loeb (1990). The diffusion process increases the calculated event rates for the chlorine and gallium neutrino experiments, respectively, by 0.8 SNU (i.e., 11%) and by 4 SNU (i.e., 3%) and increases by 12% the calculated ^{8}B solar neutrino flux, which is measured in the Kamiokande experiment and will be measured more precisely in the SNO and the Super-Kamiokande experiments.

For our best model including diffusion, Table XIII shows the contributions from individual neutrino branches to the calculated event rates for the chlorine and gallium experiments.

A heuristic measure of the accuracy with which the solar neutrino fluxes and event rates are calculated is the dependence upon time of the published best-estimate theoretical values. Table XIV compares the fluxes and the predicted event rates determined by Bahcall and Ulrich (1988) with the values obtained here using improved input data and improved physics (including helium diffusion). The fractional changes in the fluxes are small, less than or of order of a few percent, for all the fluxes that contribute significantly to ongoing or planned solar neutrino experiments, i.e., all but the CNO neutrinos. The change in the predicted rate for the chlorine experiment is about 1%; the change in the predicted rate for the gallium experiment is less than 1%. In all cases, the changes are less than the estimated uncertainties (see Sec. VIII and Table VIII).

The diffusion rate used in this paper is expected to be accurate to ±30% (see Bahcall and Loeb, 1990). Since

TABLE XIV. Comparison with Bahcall and Ulrich (1988).

Source	Before[a]	After[b]	% Change
pp	6.0E+10	6.0E+10	<1
pep	1.4E+8	1.4E+8	<1
hep	8E+3	1.2E+3[c]	order of mangitude[c]
^{7}Be	4.7E+9	4.9E+9	+4
^{8}B	5.8E+6	5.7E+6	−2
^{13}N	6.1E+8	4.9E+8	−22
^{15}O	5.2E+8	4.3E+8	−19
^{17}F	5.2E+6	5.4E+6	+4
$\Sigma(\phi\sigma)_{Cl}$	7.9±2.6 SNU	8.0±3.0 SNU	+1
$\Sigma(\phi\sigma)_{Ga}$	132^{+20}_{-17} SNU	131.5^{+21}_{-17} SNU	<1

[a]Bahcall and Ulrich (1988).
[b]This paper.
[c]Used new calculation of Carlson *et al.* (1991); see Sec. II.B.2.

the effects of diffusion are small for all of the quantities we have calculated, this accuracy is sufficient for studying the solar neutrino problem. The formulation used here has the advantage of being relatively simple to implement numerically.

The primordial solar helium abundance found here, $Y=0.272$ without diffusion and $Y=0.273$ including helium diffusion, agrees with the result, $Y=0.271$, of Bahcall and Ulrich (1988), who used different abundances, radiative opacities, and nuclear parameters. We conclude that the primordial solar helium abundance is robustly determined with current input parameters, although a survey of the historical record (see Bahcall *et al.*, 1982 and Bahcall and Ulrich, 1988) suggests that a plausible estimate for the overall uncertainty due to systematic errors might be as large as $\Delta Y=0.015$.

The surface abundances of hydrogen, helium, and the heavy elements are affected significantly by diffusion. For our best solar model without helium diffusion, we find the following surface abundances at the current epoch: $X=0.70945$, $Y=0.2716$, $Z=0.01895$. Including helium diffusion in our best solar model, we find the following surface abundances: $X=0.73382$, $Y=0.2466$, $Z=0.01958$. The effect of including helium diffusion is to increase the calculated hydrogen surface abundance by about 3%, to decrease the helium surface abundance by approximately 10%, and to increase the calculated heavy-element abundance by about 3%.

Finally, we note that the depth of the convective zone found here, $R=0.721R_{\odot}$ without diffusion and $R=(0.707\pm0.004)R_{\odot}$ with helium diffusion, is in agreement with the best observational determination, using *p*-mode oscillation frequencies (Christensen-Dalsgaard *et al.*, 1991), which yields $R=(0.713\pm0.003)R_{\odot}$. The precise parameters of the convective zone are unimportant for solar neutrino calculations, although they are important for the calculation of the solar oscillation frequencies. We shall therefore present in a future paper the *p*-mode and *g*-mode frequencies calculated with the series of standard solar models presented in this paper.

In connection with the work presented in this paper, we have developed two exportable FORTRAN subroutines: a subroutine that calculates nuclear energy generation and solar neutrino production and a subroutine that evaluates helium diffusion. Both subroutines have been implemented in the Yale stellar evolution code, but were written in an exportable and user-friendly style. Copies of the energy and neutrino generation routine can be obtained from J. Bahcall, and copies of the helium diffusion routine can be obtained from M. Pinsonneault.

Tables XV through XVIII give detailed numerical descriptions of our best solar models with and without helium diffusion. The first six columns of Table XV (no diffusion) and Table XVII (including helium diffusion) present the mass included in the current and all inner zones, the radius, the temperature (in degrees K), the density, the pressure, and the luminosity integrated up to and including the current zone. We use cgs units for density and pressure. The last five columns of Table XV and Table XVII give, except for helium, the principal isotopic abundances by mass. The helium abundance is determined by the relation $Y=1.0-X(^{1}\mathrm{H})-X(^{3}\mathrm{He})-Z$. Table XVI (no diffusion) and Table XVIII (including helium diffusion) give the neutrino fluxes produced in a given spherical shell, as well as the temperature, electron number density, fraction of the solar mass, and the ^{7}Be abundance by mass in the shell. Taken together with the detailed tables of a solar model presented by Bahcall and Ulrich (1988), the results given here should be sufficient to allow different workers to estimate the uncertainties in calculations of the effect of the sun on the emergent solar neutrino fluxes. We have constructed the present tables so that they contain the information required to calculate accurate results for the MSW effect (Wolfenstein, 1978, 1979, 1986; Mikheyev and Smirnov, 1986a, 1986b, 1986c). Machine-readable copies of all these tables can be obtained from J. Bahcall.

Future calculations in this series of studies of solar neutrino fluxes will take account of the diffusion of heavy elements, in which the chemical abundance and the opacity must both be adjusted after each time step and at each radial shell. We intend to implement the differential equation of Bahcall and Loeb (1990) that describes heavy-element diffusion by a relation similar to Eq. (25). We anticipate that including the diffusion of heavy elements will slightly increase the calculated central temperature and the predicted ^{8}B neutrino flux.

ACKNOWLEDGMENTS

This work was supported in part by NSF Grant No. PHY-91-06210 with the Institute for Advanced Study and by NASA Grant NAGW-777 with Yale University. It is a pleasure to acknowledge important discussions with, or suggestions from, E. Adelberger, E. Beier, A. Boothroyd, T. Bowles, J. Carlson, A. Cox, R. Davis, P. Demarque, S. Freedman, M. Fukugita, A. Garcia, V. Gavrin, A. Gould, R. Gould, C. A. Iglesias, C. Johnson, B. Kayser, T. Kirsten, S. Koonin, K. Lande, A. Loeb, A. McDonald, P. Parker, W. H. Press, H. Robertson, F. Rogers, I.-J. Sackmann, E. E. Salpeter, Y. Totsuka, S. Turck-Chièze, R. K. Ulrich, and J. Wilkerson.

APPENDIX: NUMERICAL SOLAR MODELS

TABLE XV

STANDARD SOLAR MODEL WITHOUT HE DIFFUSION

$M/M_\odot$	$R/R_\odot$	T	ρ	P	$L/L_\odot$	$X(^1H)$	$X(^3He)$	$X(^{12}C)$	$X(^{14}N)$	$X(^{16}O)$
0.0000298	0.00652	1.557E+07	1.513E+02	2.334E+17	0.00026	0.35407	8.76E-06	2.03E-05	5.09E-03	9.08E-03
0.0000431	0.00737	1.557E+07	1.512E+02	2.332E+17	0.00038	0.35445	8.79E-06	2.03E-05	5.09E-03	9.08E-03
0.0000622	0.00833	1.556E+07	1.510E+02	2.330E+17	0.00054	0.35493	8.83E-06	2.03E-05	5.09E-03	9.09E-03
0.0000899	0.00943	1.556E+07	1.508E+02	2.327E+17	0.00078	0.35555	8.87E-06	2.02E-05	5.09E-03	9.09E-03
0.0001300	0.01066	1.555E+07	1.505E+02	2.323E+17	0.00113	0.35633	8.94E-06	2.02E-05	5.08E-03	9.10E-03
0.0001563	0.01134	1.554E+07	1.503E+02	2.321E+17	0.00136	0.35680	8.97E-06	2.02E-05	5.08E-03	9.10E-03
0.0001879	0.01206	1.554E+07	1.501E+02	2.318E+17	0.00163	0.35734	9.02E-06	2.01E-05	5.08E-03	9.10E-03
0.0002259	0.01283	1.553E+07	1.499E+02	2.315E+17	0.00196	0.35794	9.06E-06	2.01E-05	5.07E-03	9.11E-03
0.0002716	0.01364	1.552E+07	1.497E+02	2.312E+17	0.00236	0.35862	9.12E-06	2.01E-05	5.07E-03	9.11E-03
0.0003266	0.01451	1.551E+07	1.494E+02	2.308E+17	0.00283	0.35939	9.18E-06	2.00E-05	5.07E-03	9.12E-03
0.0003926	0.01544	1.551E+07	1.491E+02	2.304E+17	0.00340	0.36025	9.25E-06	2.00E-05	5.06E-03	9.12E-03
0.0004721	0.01642	1.550E+07	1.487E+02	2.299E+17	0.00408	0.36123	9.33E-06	1.99E-05	5.05E-03	9.13E-03
0.0005675	0.01747	1.548E+07	1.483E+02	2.294E+17	0.00490	0.36233	9.42E-06	1.99E-05	5.05E-03	9.13E-03
0.0006823	0.01859	1.547E+07	1.479E+02	2.288E+17	0.00588	0.36358	9.52E-06	1.98E-05	5.04E-03	9.14E-03
0.0008204	0.01978	1.546E+07	1.473E+02	2.281E+17	0.00705	0.36498	9.64E-06	1.98E-05	5.04E-03	9.15E-03
0.0009863	0.02105	1.544E+07	1.468E+02	2.273E+17	0.00846	0.36656	9.78E-06	1.97E-05	5.03E-03	9.16E-03
0.0011858	0.02240	1.542E+07	1.461E+02	2.265E+17	0.01015	0.36834	9.93E-06	1.96E-05	5.02E-03	9.17E-03
0.0014256	0.02385	1.540E+07	1.454E+02	2.255E+17	0.01216	0.37035	1.01E-05	1.95E-05	5.01E-03	9.18E-03
0.0017140	0.02539	1.537E+07	1.446E+02	2.244E+17	0.01457	0.37260	1.03E-05	1.94E-05	5.00E-03	9.20E-03
0.0020606	0.02703	1.535E+07	1.437E+02	2.231E+17	0.01745	0.37514	1.05E-05	1.93E-05	4.98E-03	9.21E-03
0.0024774	0.02878	1.531E+07	1.427E+02	2.218E+17	0.02089	0.37799	1.08E-05	1.92E-05	4.97E-03	9.22E-03
0.0029785	0.03065	1.528E+07	1.415E+02	2.202E+17	0.02500	0.38119	1.11E-05	1.90E-05	4.96E-03	9.24E-03
0.0032659	0.03164	1.526E+07	1.409E+02	2.193E+17	0.02733	0.38294	1.13E-05	1.89E-05	4.95E-03	9.25E-03
0.0035810	0.03266	1.524E+07	1.403E+02	2.184E+17	0.02988	0.38479	1.14E-05	1.89E-05	4.94E-03	9.26E-03
0.0039265	0.03371	1.522E+07	1.396E+02	2.175E+17	0.03267	0.38674	1.16E-05	1.88E-05	4.93E-03	9.27E-03
0.0043053	0.03479	1.519E+07	1.389E+02	2.165E+17	0.03570	0.38883	1.18E-05	1.87E-05	4.92E-03	9.28E-03
0.0047206	0.03592	1.517E+07	1.381E+02	2.154E+17	0.03901	0.39102	1.21E-05	1.86E-05	4.92E-03	9.29E-03
0.0051761	0.03708	1.514E+07	1.373E+02	2.143E+17	0.04262	0.39335	1.23E-05	1.85E-05	4.91E-03	9.30E-03
0.0056754	0.03829	1.512E+07	1.364E+02	2.131E+17	0.04654	0.39580	1.26E-05	1.84E-05	4.90E-03	9.31E-03
0.0062230	0.03954	1.509E+07	1.355E+02	2.118E+17	0.05082	0.39839	1.28E-05	1.83E-05	4.89E-03	9.32E-03
0.0068234	0.04083	1.506E+07	1.346E+02	2.105E+17	0.05547	0.40113	1.31E-05	1.82E-05	4.88E-03	9.33E-03
0.0074817	0.04217	1.502E+07	1.336E+02	2.090E+17	0.06053	0.40403	1.35E-05	1.81E-05	4.87E-03	9.34E-03
0.0082035	0.04355	1.499E+07	1.325E+02	2.075E+17	0.06603	0.40708	1.38E-05	1.79E-05	4.86E-03	9.35E-03
0.0089950	0.04499	1.495E+07	1.314E+02	2.060E+17	0.07201	0.41031	1.42E-05	1.78E-05	4.85E-03	9.37E-03
0.0098628	0.04647	1.491E+07	1.303E+02	2.043E+17	0.07850	0.41371	1.46E-05	1.77E-05	4.84E-03	9.38E-03
0.0108143	0.04802	1.487E+07	1.291E+02	2.025E+17	0.08555	0.41730	1.50E-05	1.75E-05	4.83E-03	9.39E-03
0.0118577	0.04961	1.482E+07	1.278E+02	2.007E+17	0.09318	0.42111	1.55E-05	1.74E-05	4.82E-03	9.40E-03
0.0130017	0.05127	1.478E+07	1.265E+02	1.987E+17	0.10146	0.42509	1.61E-05	1.73E-05	4.81E-03	9.41E-03
0.0142561	0.05299	1.473E+07	1.251E+02	1.966E+17	0.11042	0.42928	1.66E-05	1.71E-05	4.80E-03	9.42E-03
0.0156315	0.05478	1.467E+07	1.236E+02	1.944E+17	0.12010	0.43369	1.73E-05	1.69E-05	4.79E-03	9.44E-03
0.0171396	0.05664	1.462E+07	1.221E+02	1.922E+17	0.13057	0.43832	1.79E-05	1.68E-05	4.78E-03	9.45E-03
0.0187932	0.05856	1.456E+07	1.205E+02	1.897E+17	0.14187	0.44319	1.87E-05	1.66E-05	4.77E-03	9.46E-03
0.0206063	0.06057	1.449E+07	1.188E+02	1.872E+17	0.15406	0.44834	1.95E-05	1.64E-05	4.76E-03	9.47E-03
0.0225944	0.06265	1.442E+07	1.171E+02	1.845E+17	0.16718	0.45370	2.04E-05	1.62E-05	4.75E-03	9.48E-03
0.0247742	0.06482	1.435E+07	1.153E+02	1.818E+17	0.18129	0.45931	2.14E-05	1.61E-05	4.74E-03	9.49E-03
0.0271644	0.06707	1.428E+07	1.134E+02	1.788E+17	0.19644	0.46518	2.25E-05	1.59E-05	4.74E-03	9.50E-03
0.0297852	0.06942	1.420E+07	1.115E+02	1.757E+17	0.21269	0.47138	2.37E-05	1.57E-05	4.73E-03	9.51E-03
0.0326588	0.07186	1.411E+07	1.094E+02	1.725E+17	0.23009	0.47779	2.51E-05	1.54E-05	4.72E-03	9.52E-03
0.0358097	0.07441	1.402E+07	1.073E+02	1.692E+17	0.24869	0.48448	2.66E-05	1.52E-05	4.71E-03	9.53E-03
0.0392645	0.07707	1.393E+07	1.052E+02	1.656E+17	0.26851	0.49144	2.82E-05	1.50E-05	4.71E-03	9.53E-03
0.0428509	0.07970	1.383E+07	1.030E+02	1.621E+17	0.28851	0.49837	3.00E-05	1.47E-05	4.70E-03	9.54E-03
0.0465450	0.08229	1.374E+07	1.009E+02	1.587E+17	0.30851	0.50510	3.19E-05	1.45E-05	4.70E-03	9.54E-03
0.0503522	0.08485	1.364E+07	9.888E+01	1.553E+17	0.32850	0.51170	3.38E-05	1.43E-05	4.69E-03	9.55E-03
0.0542780	0.08739	1.355E+07	9.688E+01	1.520E+17	0.34851	0.51818	3.59E-05	1.41E-05	4.69E-03	9.55E-03
0.0583286	0.08991	1.345E+07	9.492E+01	1.487E+17	0.36851	0.52455	3.81E-05	1.39E-05	4.69E-03	9.56E-03
0.0625107	0.09242	1.336E+07	9.298E+01	1.454E+17	0.38851	0.53086	4.04E-05	1.37E-05	4.68E-03	9.56E-03

TABLE XV—*continued*

$M/M_\odot$	$R/R_\odot$	T	ρ	P	$L/L_\odot$	$X(^1H)$	$X(^3He)$	$X(^{12}C)$	$X(^{14}N)$	$X(^{16}O)$
0.0668314	0.09493	1.326E+07	9.108E+01	1.422E+17	0.40851	0.53711	4.29E-05	1.34E-05	4.68E-03	9.56E-03
0.0712994	0.09745	1.316E+07	8.920E+01	1.390E+17	0.42852	0.54322	4.55E-05	1.32E-05	4.68E-03	9.57E-03
0.0759241	0.09997	1.307E+07	8.734E+01	1.358E+17	0.44853	0.54926	4.83E-05	1.30E-05	4.68E-03	9.57E-03
0.0807161	0.10251	1.297E+07	8.550E+01	1.326E+17	0.46854	0.55523	5.13E-05	1.28E-05	4.68E-03	9.57E-03
0.0856869	0.10507	1.287E+07	8.367E+01	1.294E+17	0.48855	0.56113	5.46E-05	1.26E-05	4.68E-03	9.57E-03
0.0908494	0.10765	1.277E+07	8.186E+01	1.262E+17	0.50856	0.56698	5.81E-05	1.24E-05	4.68E-03	9.57E-03
0.0962184	0.11027	1.266E+07	8.005E+01	1.230E+17	0.52857	0.57277	6.19E-05	1.22E-05	4.68E-03	9.57E-03
0.1018102	0.11293	1.256E+07	7.825E+01	1.198E+17	0.54859	0.57851	6.60E-05	1.20E-05	4.68E-03	9.57E-03
0.1076435	0.11564	1.245E+07	7.645E+01	1.166E+17	0.56860	0.58421	7.04E-05	1.17E-05	4.68E-03	9.58E-03
0.1137396	0.11841	1.234E+07	7.465E+01	1.134E+17	0.58862	0.58987	7.53E-05	1.15E-05	4.68E-03	9.58E-03
0.1201228	0.12124	1.223E+07	7.284E+01	1.102E+17	0.60863	0.59549	8.07E-05	1.13E-05	4.68E-03	9.58E-03
0.1268212	0.12414	1.212E+07	7.103E+01	1.069E+17	0.62865	0.60108	8.66E-05	1.10E-05	4.68E-03	9.58E-03
0.1338675	0.12712	1.200E+07	6.920E+01	1.036E+17	0.64867	0.60665	9.31E-05	1.08E-05	4.68E-03	9.58E-03
0.1412997	0.13021	1.188E+07	6.735E+01	1.003E+17	0.66869	0.61218	1.00E-04	1.07E-05	4.68E-03	9.58E-03
0.1491629	0.13341	1.176E+07	6.547E+01	9.690E+16	0.68871	0.61770	1.08E-04	1.13E-05	4.68E-03	9.58E-03
0.1575101	0.13673	1.163E+07	6.357E+01	9.346E+16	0.70873	0.62320	1.18E-04	1.47E-05	4.67E-03	9.58E-03
0.1664046	0.14021	1.150E+07	6.163E+01	8.996E+16	0.72875	0.62869	1.28E-04	2.66E-05	4.65E-03	9.58E-03
0.1759221	0.14386	1.136E+07	5.965E+01	8.638E+16	0.74876	0.63417	1.40E-04	6.01E-05	4.59E-03	9.58E-03
0.1861546	0.14771	1.121E+07	5.762E+01	8.272E+16	0.76878	0.63966	1.54E-04	1.37E-04	4.47E-03	9.58E-03
0.1971242	0.15177	1.106E+07	5.554E+01	7.898E+16	0.78863	0.64511	1.70E-04	2.84E-04	4.22E-03	9.58E-03
0.2081396	0.15578	1.091E+07	5.355E+01	7.541E+16	0.80702	0.65017	1.88E-04	5.02E-04	3.86E-03	9.58E-03
0.2191875	0.15974	1.076E+07	5.164E+01	7.200E+16	0.82402	0.65487	2.07E-04	7.77E-04	3.42E-03	9.58E-03
0.2302555	0.16365	1.062E+07	4.981E+01	6.875E+16	0.83970	0.65923	2.28E-04	1.08E-03	2.94E-03	9.58E-03
0.2413322	0.16753	1.048E+07	4.805E+01	6.564E+16	0.85413	0.66325	2.51E-04	1.39E-03	2.49E-03	9.58E-03
0.2524068	0.17136	1.035E+07	4.635E+01	6.268E+16	0.86739	0.66697	2.76E-04	1.69E-03	2.09E-03	9.58E-03
0.2634692	0.17516	1.021E+07	4.473E+01	5.985E+16	0.87954	0.67040	3.03E-04	1.95E-03	1.79E-03	9.58E-03
0.2745100	0.17892	1.008E+07	4.316E+01	5.715E+16	0.89066	0.67355	3.33E-04	2.17E-03	1.56E-03	9.58E-03
0.2855205	0.18265	9.954E+06	4.166E+01	5.456E+16	0.90083	0.67644	3.65E-04	2.36E-03	1.40E-03	9.58E-03
0.2964924	0.18634	9.829E+06	4.021E+01	5.210E+16	0.91012	0.67911	4.00E-04	2.51E-03	1.29E-03	9.58E-03
0.3074180	0.19001	9.706E+06	3.881E+01	4.975E+16	0.91860	0.68156	4.38E-04	2.63E-03	1.22E-03	9.58E-03
0.3182904	0.19364	9.587E+06	3.746E+01	4.750E+16	0.92634	0.68380	4.80E-04	2.72E-03	1.18E-03	9.58E-03
0.3291030	0.19725	9.469E+06	3.616E+01	4.536E+16	0.93339	0.68587	5.24E-04	2.80E-03	1.15E-03	9.58E-03
0.3398496	0.20083	9.355E+06	3.491E+01	4.331E+16	0.93981	0.68776	5.73E-04	2.85E-03	1.14E-03	9.58E-03
0.3505247	0.20439	9.242E+06	3.370E+01	4.136E+16	0.94565	0.68950	6.26E-04	2.90E-03	1.13E-03	9.58E-03
0.3611230	0.20792	9.132E+06	3.253E+01	3.949E+16	0.95097	0.69110	6.83E-04	2.93E-03	1.12E-03	9.58E-03
0.3716399	0.21143	9.025E+06	3.140E+01	3.771E+16	0.95581	0.69256	7.46E-04	2.96E-03	1.12E-03	9.58E-03
0.3820709	0.21492	8.919E+06	3.032E+01	3.600E+16	0.96021	0.69390	8.13E-04	2.98E-03	1.11E-03	9.58E-03
0.3924120	0.21839	8.816E+06	2.926E+01	3.438E+16	0.96420	0.69513	8.87E-04	2.99E-03	1.11E-03	9.58E-03
0.4026596	0.22184	8.714E+06	2.825E+01	3.283E+16	0.96783	0.69625	9.67E-04	3.00E-03	1.11E-03	9.58E-03
0.4128105	0.22528	8.615E+06	2.727E+01	3.135E+16	0.97113	0.69728	1.05E-03	3.01E-03	1.11E-03	9.58E-03
0.4228615	0.22869	8.518E+06	2.632E+01	2.993E+16	0.97413	0.69822	1.15E-03	3.02E-03	1.11E-03	9.58E-03
0.4328100	0.23209	8.422E+06	2.540E+01	2.858E+16	0.97685	0.69907	1.25E-03	3.02E-03	1.11E-03	9.58E-03
0.4426536	0.23548	8.329E+06	2.452E+01	2.729E+16	0.97932	0.69985	1.36E-03	3.03E-03	1.11E-03	9.58E-03
0.4523900	0.23885	8.237E+06	2.367E+01	2.606E+16	0.98156	0.70056	1.48E-03	3.03E-03	1.11E-03	9.58E-03
0.4620175	0.24221	8.147E+06	2.284E+01	2.489E+16	0.98360	0.70121	1.62E-03	3.03E-03	1.11E-03	9.58E-03
0.4715341	0.24555	8.058E+06	2.204E+01	2.376E+16	0.98545	0.70179	1.76E-03	3.03E-03	1.11E-03	9.58E-03
0.4809386	0.24888	7.971E+06	2.127E+01	2.269E+16	0.98713	0.70232	1.92E-03	3.04E-03	1.11E-03	9.58E-03
0.4902295	0.25221	7.886E+06	2.053E+01	2.167E+16	0.98866	0.70280	2.09E-03	3.04E-03	1.11E-03	9.58E-03
0.4994059	0.25552	7.802E+06	1.981E+01	2.069E+16	0.99005	0.70323	2.28E-03	3.04E-03	1.11E-03	9.58E-03
0.5084667	0.25882	7.720E+06	1.912E+01	1.976E+16	0.99131	0.70361	2.47E-03	3.04E-03	1.11E-03	9.58E-03
0.5174112	0.26212	7.639E+06	1.844E+01	1.887E+16	0.99245	0.70396	2.67E-03	3.04E-03	1.11E-03	9.58E-03
0.5262388	0.26540	7.559E+06	1.780E+01	1.801E+16	0.99348	0.70427	2.87E-03	3.04E-03	1.11E-03	9.58E-03
0.5349491	0.26868	7.481E+06	1.717E+01	1.720E+16	0.99439	0.70456	3.04E-03	3.04E-03	1.11E-03	9.58E-03
0.5435417	0.27195	7.404E+06	1.656E+01	1.643E+16	0.99518	0.70484	3.17E-03	3.04E-03	1.11E-03	9.58E-03
0.5520165	0.27521	7.328E+06	1.598E+01	1.569E+16	0.99588	0.70510	3.26E-03	3.04E-03	1.11E-03	9.58E-03
0.5603735	0.27847	7.254E+06	1.541E+01	1.498E+16	0.99647	0.70536	3.29E-03	3.04E-03	1.11E-03	9.58E-03

TABLE XV—*continued*

$M/M_\odot$	$R/R_\odot$	T	ρ	P	$L/L_\odot$	$X(^1H)$	$X(^3He)$	$X(^{12}C)$	$X(^{14}N)$	$X(^{16}O)$
0.5686126	0.28173	7.181E+06	1.487E+01	1.430E+16	0.99697	0.70561	3.27E-03	3.04E-03	1.11E-03	9.58E-03
0.5767340	0.28498	7.109E+06	1.434E+01	1.366E+16	0.99739	0.70586	3.21E-03	3.04E-03	1.11E-03	9.58E-03
0.5847380	0.28822	7.038E+06	1.383E+01	1.304E+16	0.99774	0.70610	3.11E-03	3.04E-03	1.11E-03	9.58E-03
0.5926251	0.29147	6.968E+06	1.334E+01	1.245E+16	0.99804	0.70634	2.97E-03	3.04E-03	1.11E-03	9.58E-03
0.6003955	0.29471	6.899E+06	1.286E+01	1.189E+16	0.99829	0.70657	2.82E-03	3.04E-03	1.11E-03	9.58E-03
0.6080499	0.29794	6.831E+06	1.240E+01	1.136E+16	0.99850	0.70678	2.65E-03	3.04E-03	1.11E-03	9.58E-03
0.6155887	0.30118	6.764E+06	1.196E+01	1.084E+16	0.99869	0.70699	2.49E-03	3.04E-03	1.11E-03	9.58E-03
0.6230128	0.30441	6.699E+06	1.153E+01	1.035E+16	0.99885	0.70718	2.32E-03	3.04E-03	1.11E-03	9.58E-03
0.6303227	0.30765	6.634E+06	1.112E+01	9.888E+15	0.99899	0.70736	2.16E-03	3.04E-03	1.11E-03	9.58E-03
0.6375193	0.31088	6.570E+06	1.072E+01	9.442E+15	0.99911	0.70753	2.00E-03	3.04E-03	1.11E-03	9.58E-03
0.6446033	0.31411	6.507E+06	1.034E+01	9.016E+15	0.99922	0.70768	1.86E-03	3.04E-03	1.11E-03	9.58E-03
0.6584372	0.32058	6.383E+06	9.608E+00	8.221E+15	0.99940	0.70796	1.59E-03	3.04E-03	1.11E-03	9.58E-03
0.6718318	0.32705	6.263E+06	8.929E+00	7.497E+15	0.99954	0.70819	1.36E-03	3.04E-03	1.11E-03	9.58E-03
0.6847950	0.33352	6.146E+06	8.297E+00	6.836E+15	0.99966	0.70839	1.16E-03	3.04E-03	1.11E-03	9.58E-03
0.6973350	0.34001	6.032E+06	7.709E+00	6.233E+15	0.99975	0.70855	9.97E-04	3.04E-03	1.11E-03	9.58E-03
0.7034491	0.34326	5.976E+06	7.430E+00	5.952E+15	0.99979	0.70863	9.24E-04	3.04E-03	1.11E-03	9.58E-03
0.7094607	0.34651	5.921E+06	7.161E+00	5.684E+15	0.99982	0.70870	8.56E-04	3.04E-03	1.11E-03	9.58E-03
0.7153709	0.34976	5.866E+06	6.902E+00	5.428E+15	0.99985	0.70876	7.94E-04	3.04E-03	1.11E-03	9.58E-03
0.7211809	0.35302	5.812E+06	6.652E+00	5.183E+15	0.99988	0.70882	7.37E-04	3.04E-03	1.11E-03	9.58E-03
0.7268918	0.35628	5.759E+06	6.411E+00	4.949E+15	0.99990	0.70887	6.85E-04	3.04E-03	1.11E-03	9.58E-03
0.7380213	0.36282	5.654E+06	5.954E+00	4.513E+15	0.99994	0.70896	5.92E-04	3.04E-03	1.11E-03	9.58E-03
0.7487687	0.36937	5.552E+06	5.530E+00	4.115E+15	0.99997	0.70904	5.14E-04	3.04E-03	1.11E-03	9.58E-03
0.7591436	0.37595	5.452E+06	5.135E+00	3.753E+15	1.00000	0.70910	4.49E-04	3.04E-03	1.11E-03	9.58E-03
0.7691557	0.38255	5.355E+06	4.767E+00	3.422E+15	1.00002	0.70916	3.93E-04	3.04E-03	1.11E-03	9.58E-03
0.7788146	0.38917	5.260E+06	4.426E+00	3.120E+15	1.00003	0.70921	3.47E-04	3.04E-03	1.11E-03	9.58E-03
0.7881298	0.39583	5.166E+06	4.109E+00	2.845E+15	1.00004	0.70925	3.07E-04	3.04E-03	1.11E-03	9.58E-03
0.7971111	0.40251	5.075E+06	3.814E+00	2.595E+15	1.00005	0.70928	2.74E-04	3.04E-03	1.11E-03	9.58E-03
0.8057678	0.40921	4.986E+06	3.540E+00	2.366E+15	1.00006	0.70931	2.46E-04	3.04E-03	1.11E-03	9.58E-03
0.8141093	0.41595	4.899E+06	3.286E+00	2.158E+15	1.00006	0.70933	2.23E-04	3.04E-03	1.11E-03	9.58E-03
0.8221450	0.42272	4.813E+06	3.050E+00	1.967E+15	1.00006	0.70935	2.03E-04	3.04E-03	1.11E-03	9.58E-03
0.8298841	0.42953	4.729E+06	2.830E+00	1.794E+15	1.00006	0.70937	1.87E-04	3.04E-03	1.11E-03	9.58E-03
0.8373354	0.43637	4.647E+06	2.627E+00	1.636E+15	1.00006	0.70938	1.73E-04	3.04E-03	1.11E-03	9.58E-03
0.8445080	0.44324	4.566E+06	2.438E+00	1.492E+15	1.00006	0.70939	1.61E-04	3.04E-03	1.11E-03	9.58E-03
0.8514104	0.45015	4.487E+06	2.262E+00	1.360E+15	1.00006	0.70940	1.51E-04	3.04E-03	1.11E-03	9.58E-03
0.8580512	0.45710	4.409E+06	2.099E+00	1.240E+15	1.00006	0.70941	1.43E-04	3.04E-03	1.11E-03	9.58E-03
0.8644388	0.46408	4.332E+06	1.948E+00	1.131E+15	1.00006	0.70942	1.36E-04	3.04E-03	1.11E-03	9.58E-03
0.8705812	0.47111	4.257E+06	1.808E+00	1.032E+15	1.00006	0.70942	1.30E-04	3.04E-03	1.11E-03	9.58E-03
0.8764866	0.47817	4.184E+06	1.677E+00	9.406E+14	1.00006	0.70943	1.25E-04	3.04E-03	1.11E-03	9.58E-03
0.8821626	0.48527	4.111E+06	1.556E+00	8.577E+14	1.00005	0.70943	1.21E-04	3.04E-03	1.11E-03	9.58E-03
0.8876169	0.49241	4.040E+06	1.444E+00	7.822E+14	1.00005	0.70944	1.17E-04	3.04E-03	1.11E-03	9.58E-03
0.8928567	0.49959	3.970E+06	1.340E+00	7.133E+14	1.00005	0.70944	1.15E-04	3.04E-03	1.11E-03	9.58E-03
0.8978895	0.50682	3.901E+06	1.244E+00	6.504E+14	1.00005	0.70944	1.12E-04	3.04E-03	1.11E-03	9.58E-03
0.9027220	0.51408	3.833E+06	1.154E+00	5.931E+14	1.00004	0.70944	1.10E-04	3.04E-03	1.11E-03	9.58E-03
0.9073613	0.52138	3.766E+06	1.071E+00	5.408E+14	1.00004	0.70944	1.08E-04	3.04E-03	1.11E-03	9.58E-03
0.9118138	0.52872	3.700E+06	9.942E-01	4.932E+14	1.00004	0.70945	1.07E-04	3.04E-03	1.11E-03	9.58E-03
0.9160861	0.53610	3.635E+06	9.228E-01	4.497E+14	1.00004	0.70945	1.06E-04	3.04E-03	1.11E-03	9.58E-03
0.9201843	0.54352	3.571E+06	8.565E-01	4.101E+14	1.00004	0.70945	1.05E-04	3.04E-03	1.11E-03	9.58E-03
0.9241146	0.55098	3.507E+06	7.951E-01	3.740E+14	1.00003	0.70945	1.04E-04	3.04E-03	1.11E-03	9.58E-03
0.9278829	0.55848	3.445E+06	7.382E-01	3.410E+14	1.00003	0.70945	1.03E-04	3.04E-03	1.11E-03	9.58E-03
0.9314948	0.56601	3.383E+06	6.854E-01	3.110E+14	1.00003	0.70945	1.03E-04	3.04E-03	1.11E-03	9.58E-03
0.9349559	0.57359	3.322E+06	6.365E-01	2.836E+14	1.00003	0.70945	1.02E-04	3.04E-03	1.11E-03	9.58E-03
0.9382715	0.58119	3.261E+06	5.912E-01	2.586E+14	1.00003	0.70945	1.02E-04	3.04E-03	1.11E-03	9.58E-03
0.9414468	0.58883	3.201E+06	5.492E-01	2.358E+14	1.00003	0.70945	1.02E-04	3.04E-03	1.11E-03	9.58E-03
0.9444868	0.59650	3.142E+06	5.103E-01	2.150E+14	1.00002	0.70945	1.01E-04	3.04E-03	1.11E-03	9.58E-03
0.9473964	0.60420	3.083E+06	4.742E-01	1.961E+14	1.00002	0.70945	1.01E-04	3.04E-03	1.11E-03	9.58E-03
0.9501802	0.61192	3.024E+06	4.408E-01	1.788E+14	1.00002	0.70945	1.01E-04	3.04E-03	1.11E-03	9.58E-03

TABLE XV—*continued*

$M/M_\odot$	$R/R_\odot$	T	ρ	P	$L/L_\odot$	$X(^1H)$	$X(^3He)$	$X(^{12}C)$	$X(^{14}N)$	$X(^{16}O)$
0.9528429	0.61967	2.965E+06	4.099E-01	1.631E+14	1.00002	0.70945	1.01E-04	3.04E-03	1.11E-03	9.58E-03
0.9553886	0.62744	2.907E+06	3.813E-01	1.487E+14	1.00002	0.70945	1.01E-04	3.04E-03	1.11E-03	9.58E-03
0.9578218	0.63522	2.849E+06	3.548E-01	1.356E+14	1.00002	0.70945	1.00E-04	3.04E-03	1.11E-03	9.58E-03
0.9601464	0.64302	2.791E+06	3.303E-01	1.237E+14	1.00002	0.70945	1.00E-04	3.04E-03	1.11E-03	9.58E-03
0.9623663	0.65083	2.732E+06	3.076E-01	1.128E+14	1.00002	0.70945	1.00E-04	3.04E-03	1.11E-03	9.58E-03
0.9644854	0.65864	2.674E+06	2.866E-01	1.028E+14	1.00001	0.70945	1.00E-04	3.04E-03	1.11E-03	9.58E-03
0.9665073	0.66645	2.615E+06	2.673E-01	9.377E+13	1.00001	0.70945	1.00E-04	3.04E-03	1.11E-03	9.58E-03
0.9684355	0.67424	2.555E+06	2.494E-01	8.550E+13	1.00001	0.70945	1.00E-04	3.04E-03	1.11E-03	9.58E-03
0.9702734	0.68202	2.494E+06	2.330E-01	7.797E+13	1.00001	0.70945	1.00E-04	3.04E-03	1.11E-03	9.58E-03
0.9711595	0.68590	2.464E+06	2.253E-01	7.446E+13	1.00001	0.70945	1.00E-04	3.04E-03	1.11E-03	9.58E-03
0.9736910	0.69747	2.369E+06	2.041E-01	6.484E+13	1.00001	0.70945	1.00E-04	3.04E-03	1.11E-03	9.58E-03
0.9750056	0.70379	2.314E+06	1.936E-01	6.009E+13	1.00001	0.70945	1.00E-04	3.04E-03	1.11E-03	9.58E-03
0.9755795	0.70662	2.289E+06	1.891E-01	5.806E+13	1.00001	0.70945	1.00E-04	3.04E-03	1.11E-03	9.58E-03
0.9761427	0.70944	2.263E+06	1.848E-01	5.611E+13	1.00001	0.70945	1.00E-04	3.04E-03	1.11E-03	9.58E-03
0.9766954	0.71225	2.237E+06	1.807E-01	5.422E+13	1.00001	0.70945	1.00E-04	3.04E-03	1.11E-03	9.58E-03
0.9772376	0.71504	2.210E+06	1.768E-01	5.239E+13	1.00001	0.70945	1.00E-04	3.04E-03	1.11E-03	9.58E-03
0.9777694	0.71782	2.183E+06	1.730E-01	5.063E+13	1.00001	0.70945	1.00E-04	3.04E-03	1.11E-03	9.58E-03
0.9782911	0.72058	2.154E+06	1.694E-01	4.893E+13	1.00001	0.70945	1.00E-04	3.04E-03	1.11E-03	9.58E-03
0.9788076	0.72336	2.125E+06	1.659E-01	4.726E+13	1.00001	0.70945	1.00E-04	3.04E-03	1.11E-03	9.58E-03
0.9793140	0.72611	2.096E+06	1.625E-01	4.566E+13	1.00001	0.70945	1.00E-04	3.04E-03	1.11E-03	9.58E-03
0.9798104	0.72885	2.067E+06	1.592E-01	4.410E+13	1.00001	0.70945	1.00E-04	3.04E-03	1.11E-03	9.58E-03
0.9802969	0.73156	2.039E+06	1.559E-01	4.261E+13	1.00001	0.70945	1.00E-04	3.04E-03	1.11E-03	9.58E-03
0.9807736	0.73426	2.011E+06	1.527E-01	4.116E+13	1.00001	0.70945	1.00E-04	3.04E-03	1.11E-03	9.58E-03
0.9812407	0.73694	1.984E+06	1.496E-01	3.976E+13	1.00001	0.70945	1.00E-04	3.04E-03	1.11E-03	9.58E-03
0.9821463	0.74224	1.930E+06	1.435E-01	3.710E+13	1.00001	0.70945	1.00E-04	3.04E-03	1.11E-03	9.58E-03
0.9838476	0.75262	1.827E+06	1.321E-01	3.231E+13	1.00001	0.70945	1.00E-04	3.04E-03	1.11E-03	9.58E-03
0.9854092	0.76269	1.730E+06	1.215E-01	2.814E+13	1.00000	0.70945	1.00E-04	3.04E-03	1.11E-03	9.58E-03
0.9868395	0.77245	1.637E+06	1.119E-01	2.450E+13	1.00000	0.70945	1.00E-04	3.04E-03	1.11E-03	9.58E-03
0.9881467	0.78191	1.550E+06	1.030E-01	2.134E+13	1.00000	0.70945	1.00E-04	3.04E-03	1.11E-03	9.58E-03
0.9893391	0.79106	1.467E+06	9.477E-02	1.858E+13	1.00000	0.70945	1.00E-04	3.04E-03	1.11E-03	9.58E-03
0.9904246	0.79991	1.389E+06	8.722E-02	1.618E+13	1.00000	0.70945	1.00E-04	3.04E-03	1.11E-03	9.58E-03
0.9914109	0.80845	1.315E+06	8.028E-02	1.409E+13	1.00000	0.70945	1.00E-04	3.04E-03	1.11E-03	9.58E-03
0.9923054	0.81670	1.244E+06	7.389E-02	1.227E+13	1.00000	0.70945	1.00E-04	3.04E-03	1.11E-03	9.58E-03
0.9931153	0.82465	1.178E+06	6.801E-02	1.069E+13	1.00000	0.70945	1.00E-04	3.04E-03	1.11E-03	9.58E-03
0.9938472	0.83232	1.115E+06	6.260E-02	9.310E+12	1.00000	0.70945	1.00E-04	3.04E-03	1.11E-03	9.58E-03
0.9945076	0.83969	1.056E+06	5.762E-02	8.108E+12	1.00000	0.70945	1.00E-04	3.04E-03	1.11E-03	9.58E-03
0.9951025	0.84679	9.995E+05	5.304E-02	7.061E+12	1.00000	0.70945	1.00E-04	3.04E-03	1.11E-03	9.58E-03
0.9956376	0.85361	9.462E+05	4.882E-02	6.149E+12	1.00000	0.70945	1.00E-04	3.04E-03	1.11E-03	9.58E-03
0.9961182	0.86016	8.958E+05	4.494E-02	5.356E+12	1.00000	0.70945	1.00E-04	3.04E-03	1.11E-03	9.58E-03
0.9965492	0.86645	8.480E+05	4.136E-02	4.664E+12	1.00000	0.70945	1.00E-04	3.04E-03	1.11E-03	9.58E-03
0.9969353	0.87249	8.029E+05	3.807E-02	4.062E+12	1.00000	0.70945	1.00E-04	3.04E-03	1.11E-03	9.58E-03
0.9972807	0.87827	7.601E+05	3.504E-02	3.538E+12	1.00000	0.70945	1.00E-04	3.04E-03	1.11E-03	9.58E-03
0.9975892	0.88382	7.196E+05	3.225E-02	3.081E+12	1.00000	0.70945	1.00E-04	3.04E-03	1.11E-03	9.58E-03
0.9978645	0.88913	6.813E+05	2.967E-02	2.683E+12	1.00000	0.70945	1.00E-04	3.04E-03	1.11E-03	9.58E-03
0.9981098	0.89421	6.450E+05	2.730E-02	2.337E+12	1.00000	0.70945	1.00E-04	3.04E-03	1.11E-03	9.58E-03
0.9983283	0.89908	6.106E+05	2.512E-02	2.035E+12	1.00000	0.70945	1.00E-04	3.04E-03	1.11E-03	9.58E-03
0.9985226	0.90373	5.780E+05	2.311E-02	1.773E+12	1.00000	0.70945	1.00E-04	3.04E-03	1.11E-03	9.58E-03
0.9986952	0.90818	5.472E+05	2.126E-02	1.544E+12	1.00000	0.70945	1.00E-04	3.04E-03	1.11E-03	9.58E-03
0.9988484	0.91243	5.180E+05	1.955E-02	1.345E+12	1.00000	0.70945	1.00E-04	3.04E-03	1.11E-03	9.58E-03
0.9989843	0.91649	4.904E+05	1.798E-02	1.171E+12	1.00000	0.70945	1.00E-04	3.04E-03	1.11E-03	9.58E-03
0.9992112	0.92408	4.394E+05	1.521E-02	8.883E+11	1.00000	0.70945	1.00E-04	3.04E-03	1.11E-03	9.58E-03
0.9993889	0.93098	3.938E+05	1.287E-02	6.738E+11	1.00000	0.70945	1.00E-04	3.04E-03	1.11E-03	9.58E-03
0.9995274	0.93726	3.530E+05	1.090E-02	5.111E+11	1.00000	0.70945	1.00E-04	3.04E-03	1.11E-03	9.58E-03
0.9996353	0.94295	3.165E+05	9.227E-03	3.877E+11	1.00000	0.70945	1.00E-04	3.04E-03	1.11E-03	9.58E-03
0.9997095	0.94749	2.878E+05	7.978E-03	3.045E+11	1.00000	0.70945	1.00E-04	3.04E-03	1.11E-03	9.58E-03

TABLE XVI

STANDARD SOLAR MODEL WITH HE DIFFUSION

$M/M_\odot$	$R/R_\odot$	T	ρ	P	$L/L_\odot$	$X(^1H)$	$X(^3He)$	$X(^{12}C)$	$X(^{14}N)$	$X(^{16}O)$
0.0000298	0.00648	1.567E+07	1.542E+02	2.365E+17	0.00026	0.34279	7.99E-06	2.14E-05	5.30E-03	9.34E-03
0.0000431	0.00733	1.567E+07	1.541E+02	2.363E+17	0.00038	0.34316	8.02E-06	2.14E-05	5.30E-03	9.34E-03
0.0000622	0.00829	1.566E+07	1.539E+02	2.361E+17	0.00055	0.34364	8.05E-06	2.14E-05	5.30E-03	9.34E-03
0.0000899	0.00937	1.566E+07	1.536E+02	2.358E+17	0.00079	0.34425	8.10E-06	2.13E-05	5.29E-03	9.35E-03
0.0001300	0.01060	1.565E+07	1.533E+02	2.354E+17	0.00115	0.34503	8.16E-06	2.13E-05	5.29E-03	9.36E-03
0.0001563	0.01127	1.564E+07	1.532E+02	2.351E+17	0.00138	0.34550	8.19E-06	2.12E-05	5.28E-03	9.36E-03
0.0001879	0.01199	1.564E+07	1.530E+02	2.349E+17	0.00165	0.34603	8.23E-06	2.12E-05	5.28E-03	9.36E-03
0.0002259	0.01275	1.563E+07	1.527E+02	2.346E+17	0.00199	0.34662	8.28E-06	2.12E-05	5.28E-03	9.37E-03
0.0002716	0.01356	1.562E+07	1.525E+02	2.342E+17	0.00239	0.34730	8.33E-06	2.11E-05	5.27E-03	9.37E-03
0.0003266	0.01443	1.561E+07	1.522E+02	2.339E+17	0.00287	0.34806	8.39E-06	2.11E-05	5.27E-03	9.38E-03
0.0003926	0.01535	1.561E+07	1.519E+02	2.334E+17	0.00344	0.34892	8.45E-06	2.11E-05	5.26E-03	9.38E-03
0.0004721	0.01633	1.559E+07	1.515E+02	2.329E+17	0.00413	0.34989	8.53E-06	2.10E-05	5.26E-03	9.39E-03
0.0005675	0.01737	1.558E+07	1.511E+02	2.324E+17	0.00496	0.35099	8.61E-06	2.10E-05	5.25E-03	9.40E-03
0.0006823	0.01848	1.557E+07	1.506E+02	2.318E+17	0.00595	0.35223	8.71E-06	2.09E-05	5.24E-03	9.41E-03
0.0008204	0.01967	1.555E+07	1.501E+02	2.311E+17	0.00714	0.35362	8.82E-06	2.08E-05	5.24E-03	9.42E-03
0.0009863	0.02093	1.554E+07	1.495E+02	2.303E+17	0.00856	0.35519	8.95E-06	2.07E-05	5.23E-03	9.43E-03
0.0011858	0.02228	1.552E+07	1.488E+02	2.294E+17	0.01027	0.35696	9.10E-06	2.06E-05	5.22E-03	9.44E-03
0.0014256	0.02371	1.549E+07	1.481E+02	2.284E+17	0.01230	0.35896	9.26E-06	2.05E-05	5.20E-03	9.45E-03
0.0017140	0.02524	1.547E+07	1.473E+02	2.273E+17	0.01474	0.36121	9.45E-06	2.04E-05	5.19E-03	9.47E-03
0.0020606	0.02687	1.544E+07	1.463E+02	2.260E+17	0.01765	0.36374	9.67E-06	2.03E-05	5.18E-03	9.48E-03
0.0024774	0.02862	1.541E+07	1.453E+02	2.246E+17	0.02112	0.36659	9.92E-06	2.01E-05	5.16E-03	9.50E-03
0.0029785	0.03048	1.537E+07	1.441E+02	2.230E+17	0.02526	0.36978	1.02E-05	2.00E-05	5.15E-03	9.52E-03
0.0032659	0.03146	1.535E+07	1.435E+02	2.221E+17	0.02762	0.37153	1.04E-05	1.99E-05	5.14E-03	9.53E-03
0.0035810	0.03247	1.533E+07	1.428E+02	2.212E+17	0.03020	0.37338	1.05E-05	1.98E-05	5.13E-03	9.54E-03
0.0039265	0.03352	1.531E+07	1.421E+02	2.202E+17	0.03300	0.37533	1.07E-05	1.97E-05	5.12E-03	9.55E-03
0.0043053	0.03460	1.529E+07	1.414E+02	2.192E+17	0.03606	0.37741	1.09E-05	1.96E-05	5.11E-03	9.56E-03
0.0047206	0.03572	1.526E+07	1.406E+02	2.181E+17	0.03940	0.37960	1.11E-05	1.95E-05	5.10E-03	9.57E-03
0.0051761	0.03688	1.524E+07	1.397E+02	2.169E+17	0.04303	0.38193	1.14E-05	1.94E-05	5.09E-03	9.58E-03
0.0056754	0.03808	1.521E+07	1.389E+02	2.157E+17	0.04699	0.38438	1.16E-05	1.93E-05	5.08E-03	9.59E-03
0.0062230	0.03932	1.518E+07	1.379E+02	2.144E+17	0.05130	0.38698	1.19E-05	1.92E-05	5.07E-03	9.61E-03
0.0068234	0.04060	1.515E+07	1.370E+02	2.130E+17	0.05598	0.38973	1.22E-05	1.91E-05	5.06E-03	9.62E-03
0.0074817	0.04193	1.511E+07	1.359E+02	2.115E+17	0.06108	0.39264	1.25E-05	1.90E-05	5.05E-03	9.63E-03
0.0082035	0.04331	1.508E+07	1.349E+02	2.100E+17	0.06662	0.39571	1.28E-05	1.88E-05	5.04E-03	9.65E-03
0.0089950	0.04474	1.504E+07	1.337E+02	2.084E+17	0.07263	0.39895	1.32E-05	1.87E-05	5.03E-03	9.66E-03
0.0098628	0.04622	1.500E+07	1.325E+02	2.067E+17	0.07916	0.40238	1.36E-05	1.86E-05	5.02E-03	9.67E-03
0.0108143	0.04775	1.495E+07	1.313E+02	2.049E+17	0.08625	0.40599	1.40E-05	1.84E-05	5.00E-03	9.68E-03
0.0118577	0.04934	1.491E+07	1.300E+02	2.030E+17	0.09392	0.40980	1.45E-05	1.82E-05	4.99E-03	9.70E-03
0.0130017	0.05100	1.486E+07	1.286E+02	2.009E+17	0.10224	0.41381	1.50E-05	1.81E-05	4.98E-03	9.71E-03
0.0142561	0.05271	1.481E+07	1.272E+02	1.988E+17	0.11124	0.41804	1.55E-05	1.79E-05	4.97E-03	9.72E-03
0.0156315	0.05449	1.476E+07	1.257E+02	1.966E+17	0.12097	0.42250	1.61E-05	1.78E-05	4.96E-03	9.74E-03
0.0171396	0.05633	1.470E+07	1.241E+02	1.943E+17	0.13148	0.42718	1.68E-05	1.76E-05	4.95E-03	9.75E-03
0.0187932	0.05825	1.464E+07	1.224E+02	1.918E+17	0.14283	0.43211	1.75E-05	1.74E-05	4.94E-03	9.76E-03
0.0206063	0.06025	1.457E+07	1.207E+02	1.892E+17	0.15505	0.43728	1.83E-05	1.72E-05	4.93E-03	9.78E-03
0.0225944	0.06232	1.450E+07	1.189E+02	1.865E+17	0.16821	0.44271	1.91E-05	1.70E-05	4.92E-03	9.79E-03
0.0247742	0.06448	1.443E+07	1.171E+02	1.836E+17	0.18237	0.44841	2.01E-05	1.68E-05	4.91E-03	9.80E-03
0.0271644	0.06673	1.435E+07	1.151E+02	1.806E+17	0.19756	0.45437	2.11E-05	1.66E-05	4.90E-03	9.81E-03
0.0297852	0.06907	1.427E+07	1.131E+02	1.775E+17	0.21385	0.46062	2.23E-05	1.64E-05	4.89E-03	9.82E-03
0.0326588	0.07151	1.419E+07	1.110E+02	1.742E+17	0.23128	0.46714	2.36E-05	1.61E-05	4.88E-03	9.83E-03
0.0358097	0.07405	1.410E+07	1.088E+02	1.707E+17	0.24991	0.47395	2.51E-05	1.59E-05	4.87E-03	9.84E-03
0.0392645	0.07670	1.400E+07	1.066E+02	1.671E+17	0.26976	0.48105	2.67E-05	1.57E-05	4.87E-03	9.85E-03
0.0428469	0.07932	1.390E+07	1.044E+02	1.636E+17	0.28976	0.48805	2.84E-05	1.54E-05	4.86E-03	9.85E-03
0.0465377	0.08190	1.381E+07	1.022E+02	1.601E+17	0.30976	0.49491	3.02E-05	1.52E-05	4.86E-03	9.86E-03
0.0503418	0.08445	1.371E+07	1.001E+02	1.566E+17	0.32976	0.50164	3.20E-05	1.49E-05	4.85E-03	9.87E-03
0.0542649	0.08699	1.361E+07	9.808E+01	1.532E+17	0.34976	0.50827	3.40E-05	1.47E-05	4.85E-03	9.87E-03
0.0583130	0.08950	1.352E+07	9.605E+01	1.499E+17	0.36976	0.51479	3.62E-05	1.45E-05	4.84E-03	9.87E-03
0.0624930	0.09201	1.342E+07	9.406E+01	1.465E+17	0.38976	0.52122	3.84E-05	1.43E-05	4.84E-03	9.88E-03

TABLE XVI—*continued*

$M/M_\odot$	$R/R_\odot$	T	ρ	P	$L/L_\odot$	$X(^1H)$	$X(^3He)$	$X(^{12}C)$	$X(^{14}N)$	$X(^{16}O)$
0.0668124	0.09451	1.332E+07	9.210E+01	1.432E+17	0.40977	0.52756	4.08E-05	1.40E-05	4.84E-03	9.88E-03
0.0712795	0.09702	1.322E+07	9.017E+01	1.400E+17	0.42977	0.53383	4.34E-05	1.38E-05	4.84E-03	9.88E-03
0.0759036	0.09954	1.313E+07	8.826E+01	1.367E+17	0.44978	0.54002	4.61E-05	1.36E-05	4.84E-03	9.88E-03
0.0806953	0.10208	1.303E+07	8.637E+01	1.334E+17	0.46979	0.54615	4.90E-05	1.34E-05	4.83E-03	9.89E-03
0.0856661	0.10464	1.292E+07	8.449E+01	1.302E+17	0.48980	0.55221	5.22E-05	1.31E-05	4.83E-03	9.89E-03
0.0908289	0.10723	1.282E+07	8.263E+01	1.270E+17	0.50981	0.55822	5.56E-05	1.29E-05	4.83E-03	9.89E-03
0.0961984	0.10985	1.272E+07	8.077E+01	1.237E+17	0.52982	0.56418	5.93E-05	1.27E-05	4.83E-03	9.89E-03
0.1017912	0.11251	1.261E+07	7.892E+01	1.205E+17	0.54983	0.57009	6.33E-05	1.25E-05	4.83E-03	9.89E-03
0.1076259	0.11522	1.250E+07	7.707E+01	1.172E+17	0.56985	0.57596	6.76E-05	1.22E-05	4.83E-03	9.89E-03
0.1137238	0.11798	1.239E+07	7.522E+01	1.140E+17	0.58986	0.58180	7.23E-05	1.20E-05	4.83E-03	9.89E-03
0.1201094	0.12082	1.228E+07	7.337E+01	1.107E+17	0.60988	0.58760	7.76E-05	1.17E-05	4.83E-03	9.89E-03
0.1268110	0.12372	1.217E+07	7.151E+01	1.074E+17	0.62989	0.59337	8.33E-05	1.15E-05	4.83E-03	9.89E-03
0.1338614	0.12672	1.205E+07	6.963E+01	1.040E+17	0.64991	0.59912	8.97E-05	1.13E-05	4.83E-03	9.89E-03
0.1412988	0.12981	1.193E+07	6.774E+01	1.006E+17	0.66993	0.60485	9.68E-05	1.11E-05	4.83E-03	9.89E-03
0.1491686	0.13301	1.180E+07	6.583E+01	9.719E+16	0.68995	0.61056	1.05E-04	1.15E-05	4.83E-03	9.89E-03
0.1575242	0.13635	1.167E+07	6.388E+01	9.370E+16	0.70996	0.61626	1.14E-04	1.43E-05	4.83E-03	9.90E-03
0.1664296	0.13984	1.154E+07	6.190E+01	9.015E+16	0.72998	0.62196	1.24E-04	2.47E-05	4.81E-03	9.90E-03
0.1759612	0.14350	1.140E+07	5.988E+01	8.652E+16	0.74999	0.62766	1.36E-04	5.53E-05	4.76E-03	9.90E-03
0.1862118	0.14737	1.125E+07	5.780E+01	8.281E+16	0.77001	0.63336	1.50E-04	1.29E-04	4.64E-03	9.90E-03
0.1970741	0.15140	1.109E+07	5.571E+01	7.906E+16	0.78963	0.63897	1.65E-04	2.71E-04	4.40E-03	9.90E-03
0.2079824	0.15538	1.095E+07	5.370E+01	7.549E+16	0.80782	0.64419	1.82E-04	4.85E-04	4.05E-03	9.90E-03
0.2189238	0.15932	1.080E+07	5.177E+01	7.208E+16	0.82465	0.64904	2.01E-04	7.61E-04	3.60E-03	9.90E-03
0.2298863	0.16321	1.066E+07	4.993E+01	6.882E+16	0.84018	0.65356	2.21E-04	1.07E-03	3.11E-03	9.90E-03
0.2408586	0.16707	1.052E+07	4.815E+01	6.571E+16	0.85449	0.65774	2.44E-04	1.39E-03	2.64E-03	9.90E-03
0.2518303	0.17088	1.038E+07	4.645E+01	6.274E+16	0.86764	0.66162	2.68E-04	1.70E-03	2.22E-03	9.90E-03
0.2627914	0.17466	1.025E+07	4.481E+01	5.991E+16	0.87970	0.66521	2.94E-04	1.97E-03	1.89E-03	9.90E-03
0.2737327	0.17841	1.012E+07	4.324E+01	5.720E+16	0.89075	0.66852	3.23E-04	2.21E-03	1.64E-03	9.90E-03
0.2846456	0.18212	9.987E+06	4.172E+01	5.462E+16	0.90086	0.67157	3.54E-04	2.41E-03	1.47E-03	9.90E-03
0.2955221	0.18581	9.862E+06	4.026E+01	5.215E+16	0.91010	0.67439	3.88E-04	2.57E-03	1.35E-03	9.90E-03
0.3063546	0.18946	9.739E+06	3.886E+01	4.980E+16	0.91854	0.67698	4.25E-04	2.70E-03	1.28E-03	9.90E-03
0.3171361	0.19309	9.619E+06	3.750E+01	4.755E+16	0.92624	0.67938	4.65E-04	2.80E-03	1.23E-03	9.90E-03
0.3278602	0.19669	9.502E+06	3.620E+01	4.540E+16	0.93326	0.68159	5.09E-04	2.88E-03	1.20E-03	9.90E-03
0.3385209	0.20026	9.387E+06	3.494E+01	4.335E+16	0.93966	0.68362	5.56E-04	2.94E-03	1.18E-03	9.90E-03
0.3491125	0.20381	9.274E+06	3.372E+01	4.139E+16	0.94549	0.68550	6.08E-04	2.99E-03	1.17E-03	9.90E-03
0.3596300	0.20734	9.164E+06	3.255E+01	3.952E+16	0.95080	0.68723	6.63E-04	3.02E-03	1.16E-03	9.90E-03
0.3700686	0.21085	9.056E+06	3.142E+01	3.774E+16	0.95563	0.68882	7.24E-04	3.05E-03	1.15E-03	9.90E-03
0.3804240	0.21433	8.950E+06	3.032E+01	3.604E+16	0.96002	0.69029	7.89E-04	3.07E-03	1.15E-03	9.90E-03
0.3906921	0.21780	8.846E+06	2.927E+01	3.441E+16	0.96402	0.69164	8.61E-04	3.09E-03	1.15E-03	9.90E-03
0.4008695	0.22125	8.745E+06	2.825E+01	3.286E+16	0.96765	0.69289	9.38E-04	3.10E-03	1.15E-03	9.90E-03
0.4109526	0.22468	8.645E+06	2.727E+01	3.137E+16	0.97094	0.69404	1.02E-03	3.11E-03	1.15E-03	9.90E-03
0.4209387	0.22810	8.548E+06	2.631E+01	2.996E+16	0.97394	0.69510	1.11E-03	3.12E-03	1.15E-03	9.90E-03
0.4308248	0.23150	8.452E+06	2.540E+01	2.861E+16	0.97667	0.69607	1.21E-03	3.12E-03	1.15E-03	9.90E-03
0.4406087	0.23489	8.358E+06	2.451E+01	2.731E+16	0.97914	0.69697	1.32E-03	3.13E-03	1.14E-03	9.90E-03
0.4502880	0.23826	8.266E+06	2.365E+01	2.608E+16	0.98139	0.69779	1.44E-03	3.13E-03	1.14E-03	9.90E-03
0.4598609	0.24162	8.176E+06	2.283E+01	2.490E+16	0.98343	0.69855	1.57E-03	3.13E-03	1.14E-03	9.90E-03
0.4693256	0.24497	8.087E+06	2.203E+01	2.378E+16	0.98529	0.69924	1.71E-03	3.14E-03	1.14E-03	9.90E-03
0.4786806	0.24831	8.000E+06	2.125E+01	2.271E+16	0.98697	0.69988	1.86E-03	3.14E-03	1.14E-03	9.90E-03
0.4879245	0.25164	7.914E+06	2.051E+01	2.168E+16	0.98851	0.70046	2.03E-03	3.14E-03	1.14E-03	9.90E-03
0.4970564	0.25496	7.830E+06	1.979E+01	2.071E+16	0.98990	0.70099	2.21E-03	3.14E-03	1.14E-03	9.90E-03
0.5060751	0.25827	7.748E+06	1.909E+01	1.977E+16	0.99117	0.70147	2.40E-03	3.14E-03	1.14E-03	9.90E-03
0.5149799	0.26157	7.667E+06	1.842E+01	1.888E+16	0.99232	0.70191	2.60E-03	3.14E-03	1.14E-03	9.90E-03
0.5237701	0.26486	7.587E+06	1.777E+01	1.803E+16	0.99335	0.70231	2.79E-03	3.14E-03	1.14E-03	9.90E-03
0.5324453	0.26815	7.508E+06	1.714E+01	1.721E+16	0.99427	0.70268	2.97E-03	3.14E-03	1.14E-03	9.90E-03
0.5410050	0.27143	7.431E+06	1.654E+01	1.644E+16	0.99508	0.70303	3.11E-03	3.14E-03	1.14E-03	9.90E-03
0.5494491	0.27470	7.355E+06	1.595E+01	1.570E+16	0.99579	0.70336	3.21E-03	3.14E-03	1.14E-03	9.90E-03
0.5577775	0.27797	7.281E+06	1.539E+01	1.499E+16	0.99639	0.70368	3.26E-03	3.14E-03	1.14E-03	9.90E-03

TABLE XVI—*continued*

$M/M_\odot$	$R/R_\odot$	T	ρ	P	$L/L_\odot$	$X(^1H)$	$X(^3He)$	$X(^{12}C)$	$X(^{14}N)$	$X(^{16}O)$
0.5659901	0.28124	7.207E+06	1.484E+01	1.431E+16	0.99690	0.70400	3.26E-03	3.14E-03	1.14E-03	9.90E-03
0.5740871	0.28450	7.135E+06	1.431E+01	1.367E+16	0.99734	0.70431	3.21E-03	3.14E-03	1.14E-03	9.90E-03
0.5820687	0.28776	7.064E+06	1.380E+01	1.305E+16	0.99770	0.70462	3.12E-03	3.14E-03	1.14E-03	9.90E-03
0.5899351	0.29101	6.994E+06	1.331E+01	1.246E+16	0.99801	0.70493	3.00E-03	3.14E-03	1.14E-03	9.90E-03
0.5976869	0.29426	6.925E+06	1.284E+01	1.190E+16	0.99827	0.70523	2.85E-03	3.14E-03	1.14E-03	9.90E-03
0.6053244	0.29751	6.857E+06	1.238E+01	1.136E+16	0.99849	0.70553	2.69E-03	3.14E-03	1.14E-03	9.90E-03
0.6128482	0.30076	6.790E+06	1.193E+01	1.085E+16	0.99868	0.70581	2.53E-03	3.14E-03	1.14E-03	9.90E-03
0.6202589	0.30401	6.724E+06	1.151E+01	1.036E+16	0.99884	0.70608	2.36E-03	3.14E-03	1.14E-03	9.90E-03
0.6275572	0.30726	6.659E+06	1.109E+01	9.893E+15	0.99898	0.70635	2.20E-03	3.14E-03	1.14E-03	9.90E-03
0.6347438	0.31051	6.595E+06	1.070E+01	9.447E+15	0.99911	0.70660	2.04E-03	3.14E-03	1.14E-03	9.90E-03
0.6418194	0.31376	6.531E+06	1.031E+01	9.021E+15	0.99922	0.70684	1.89E-03	3.14E-03	1.14E-03	9.90E-03
0.6556412	0.32026	6.408E+06	9.582E+00	8.226E+15	0.99940	0.70728	1.63E-03	3.14E-03	1.14E-03	9.90E-03
0.6690296	0.32676	6.287E+06	8.903E+00	7.501E+15	0.99955	0.70768	1.39E-03	3.14E-03	1.14E-03	9.90E-03
0.6819922	0.33327	6.169E+06	8.272E+00	6.839E+15	0.99966	0.70804	1.19E-03	3.14E-03	1.14E-03	9.90E-03
0.6945369	0.33980	6.055E+06	7.684E+00	6.236E+15	0.99976	0.70837	1.02E-03	3.14E-03	1.14E-03	9.90E-03
0.7006552	0.34307	5.999E+06	7.406E+00	5.955E+15	0.99979	0.70853	9.48E-04	3.14E-03	1.14E-03	9.90E-03
0.7066722	0.34634	5.943E+06	7.138E+00	5.687E+15	0.99983	0.70868	8.79E-04	3.14E-03	1.14E-03	9.90E-03
0.7125890	0.34961	5.889E+06	6.879E+00	5.430E+15	0.99986	0.70882	8.16E-04	3.14E-03	1.14E-03	9.90E-03
0.7184067	0.35289	5.834E+06	6.629E+00	5.185E+15	0.99989	0.70896	7.57E-04	3.14E-03	1.14E-03	9.90E-03
0.7241265	0.35618	5.781E+06	6.389E+00	4.951E+15	0.99991	0.70909	7.03E-04	3.14E-03	1.14E-03	9.90E-03
0.7352768	0.36276	5.676E+06	5.933E+00	4.515E+15	0.99995	0.70934	6.09E-04	3.14E-03	1.14E-03	9.90E-03
0.7460489	0.36937	5.573E+06	5.509E+00	4.117E+15	0.99998	0.70958	5.29E-04	3.14E-03	1.14E-03	9.90E-03
0.7564523	0.37599	5.473E+06	5.114E+00	3.754E+15	1.00001	0.70980	4.61E-04	3.14E-03	1.14E-03	9.90E-03
0.7664962	0.38265	5.375E+06	4.748E+00	3.423E+15	1.00003	0.71000	4.04E-04	3.14E-03	1.14E-03	9.90E-03
0.7761902	0.38933	5.280E+06	4.407E+00	3.121E+15	1.00004	0.71020	3.56E-04	3.14E-03	1.14E-03	9.90E-03
0.7855434	0.39604	5.186E+06	4.091E+00	2.846E+15	1.00005	0.71039	3.15E-04	3.14E-03	1.14E-03	9.90E-03
0.7945654	0.40278	5.095E+06	3.797E+00	2.595E+15	1.00006	0.71058	2.81E-04	3.14E-03	1.14E-03	9.90E-03
0.8032653	0.40955	5.005E+06	3.524E+00	2.367E+15	1.00007	0.71076	2.52E-04	3.14E-03	1.14E-03	9.90E-03
0.8116523	0.41635	4.917E+06	3.271E+00	2.158E+15	1.00007	0.71093	2.28E-04	3.14E-03	1.14E-03	9.90E-03
0.8197356	0.42319	4.831E+06	3.035E+00	1.968E+15	1.00007	0.71111	2.08E-04	3.14E-03	1.14E-03	9.90E-03
0.8275241	0.43007	4.747E+06	2.816E+00	1.794E+15	1.00007	0.71128	1.90E-04	3.14E-03	1.14E-03	9.90E-03
0.8350266	0.43698	4.664E+06	2.613E+00	1.636E+15	1.00007	0.71145	1.76E-04	3.14E-03	1.14E-03	9.90E-03
0.8422518	0.44393	4.583E+06	2.425E+00	1.492E+15	1.00007	0.71162	1.64E-04	3.14E-03	1.14E-03	9.90E-03
0.8492083	0.45091	4.503E+06	2.250E+00	1.361E+15	1.00007	0.71180	1.53E-04	3.14E-03	1.14E-03	9.90E-03
0.8559043	0.45794	4.425E+06	2.088E+00	1.241E+15	1.00007	0.71197	1.45E-04	3.14E-03	1.14E-03	9.90E-03
0.8623482	0.46501	4.348E+06	1.937E+00	1.131E+15	1.00007	0.71214	1.38E-04	3.14E-03	1.14E-03	9.90E-03
0.8685478	0.47211	4.272E+06	1.797E+00	1.032E+15	1.00006	0.71232	1.31E-04	3.14E-03	1.14E-03	9.90E-03
0.8745111	0.47926	4.198E+06	1.668E+00	9.407E+14	1.00006	0.71250	1.26E-04	3.14E-03	1.14E-03	9.90E-03
0.8802457	0.48645	4.125E+06	1.547E+00	8.578E+14	1.00006	0.71268	1.22E-04	3.14E-03	1.14E-03	9.90E-03
0.8857590	0.49369	4.053E+06	1.436E+00	7.822E+14	1.00006	0.71286	1.18E-04	3.14E-03	1.14E-03	9.90E-03
0.8910584	0.50096	3.983E+06	1.332E+00	7.133E+14	1.00005	0.71305	1.15E-04	3.14E-03	1.14E-03	9.90E-03
0.8961508	0.50828	3.913E+06	1.236E+00	6.504E+14	1.00005	0.71323	1.13E-04	3.14E-03	1.14E-03	9.90E-03
0.9010433	0.51565	3.845E+06	1.147E+00	5.931E+14	1.00005	0.71343	1.11E-04	3.14E-03	1.14E-03	9.90E-03
0.9057424	0.52305	3.777E+06	1.065E+00	5.408E+14	1.00005	0.71363	1.09E-04	3.14E-03	1.14E-03	9.90E-03
0.9102548	0.53050	3.711E+06	9.880E-01	4.932E+14	1.00004	0.71383	1.07E-04	3.14E-03	1.14E-03	9.90E-03
0.9145868	0.53799	3.645E+06	9.170E-01	4.497E+14	1.00004	0.71404	1.06E-04	3.14E-03	1.14E-03	9.90E-03
0.9187446	0.54552	3.580E+06	8.511E-01	4.101E+14	1.00004	0.71425	1.05E-04	3.14E-03	1.14E-03	9.90E-03
0.9227341	0.55309	3.516E+06	7.901E-01	3.740E+14	1.00004	0.71448	1.04E-04	3.14E-03	1.14E-03	9.90E-03
0.9265611	0.56070	3.453E+06	7.335E-01	3.410E+14	1.00004	0.71471	1.03E-04	3.14E-03	1.14E-03	9.90E-03
0.9302313	0.56836	3.390E+06	6.811E-01	3.109E+14	1.00003	0.71495	1.03E-04	3.14E-03	1.14E-03	9.90E-03
0.9337500	0.57605	3.328E+06	6.326E-01	2.835E+14	1.00003	0.71520	1.02E-04	3.14E-03	1.14E-03	9.90E-03
0.9371227	0.58377	3.266E+06	5.876E-01	2.586E+14	1.00003	0.71545	1.02E-04	3.14E-03	1.14E-03	9.90E-03
0.9403543	0.59153	3.205E+06	5.459E-01	2.358E+14	1.00003	0.71573	1.02E-04	3.14E-03	1.14E-03	9.90E-03
0.9434498	0.59933	3.144E+06	5.073E-01	2.150E+14	1.00003	0.71601	1.01E-04	3.14E-03	1.14E-03	9.90E-03
0.9464140	0.60715	3.084E+06	4.715E-01	1.961E+14	1.00002	0.71632	1.01E-04	3.14E-03	1.14E-03	9.90E-03
0.9492514	0.61500	3.023E+06	4.385E-01	1.788E+14	1.00002	0.71665	1.01E-04	3.14E-03	1.14E-03	9.90E-03

TABLE XVI—*continued*

$M/M_\odot$	$R/R_\odot$	T	ρ	P	$L/L_\odot$	$X(^1H)$	$X(^3He)$	$X(^{12}C)$	$X(^{14}N)$	$X(^{16}O)$
0.9519666	0.62287	2.963E+06	4.078E-01	1.630E+14	1.00002	0.71703	1.01E-04	3.14E-03	1.14E-03	9.90E-03
0.9545639	0.63076	2.902E+06	3.795E-01	1.487E+14	1.00002	0.71749	1.01E-04	3.14E-03	1.14E-03	9.90E-03
0.9570473	0.63867	2.842E+06	3.533E-01	1.356E+14	1.00002	0.71806	1.00E-04	3.14E-03	1.14E-03	9.90E-03
0.9594209	0.64659	2.781E+06	3.290E-01	1.236E+14	1.00002	0.71879	1.00E-04	3.14E-03	1.14E-03	9.90E-03
0.9616886	0.65451	2.719E+06	3.066E-01	1.127E+14	1.00002	0.71975	1.00E-04	3.14E-03	1.14E-03	9.90E-03
0.9638540	0.66243	2.657E+06	2.859E-01	1.028E+14	1.00002	0.72099	1.00E-04	3.14E-03	1.14E-03	9.90E-03
0.9659208	0.67035	2.593E+06	2.668E-01	9.374E+13	1.00001	0.72253	1.00E-04	3.14E-03	1.14E-03	9.90E-03
0.9678923	0.67824	2.528E+06	2.493E-01	8.548E+13	1.00001	0.72438	1.00E-04	3.14E-03	1.14E-03	9.90E-03
0.9697719	0.68611	2.460E+06	2.332E-01	7.795E+13	1.00001	0.72652	1.00E-04	3.14E-03	1.14E-03	9.90E-03
0.9702672	0.68824	2.442E+06	2.291E-01	7.602E+13	1.00001	0.72715	1.00E-04	3.14E-03	1.14E-03	9.90E-03
0.9709324	0.69114	2.416E+06	2.236E-01	7.347E+13	1.00001	0.72803	1.00E-04	3.14E-03	1.14E-03	9.90E-03
0.9715858	0.69404	2.389E+06	2.184E-01	7.100E+13	1.00001	0.72895	1.00E-04	3.14E-03	1.14E-03	9.90E-03
0.9722273	0.69693	2.362E+06	2.133E-01	6.861E+13	1.00001	0.72990	1.00E-04	3.14E-03	1.14E-03	9.90E-03
0.9728573	0.69980	2.334E+06	2.084E-01	6.631E+13	1.00001	0.73089	1.00E-04	3.14E-03	1.14E-03	9.90E-03
0.9734757	0.70267	2.306E+06	2.038E-01	6.408E+13	1.00001	0.73192	1.00E-04	3.14E-03	1.14E-03	9.90E-03
0.9740827	0.70552	2.276E+06	1.993E-01	6.192E+13	1.00001	0.73301	1.00E-04	3.14E-03	1.14E-03	9.90E-03
0.9746808	0.70837	2.246E+06	1.951E-01	5.984E+13	1.00001	0.73381	1.00E-04	3.14E-03	1.14E-03	9.90E-03
0.9752722	0.71123	2.215E+06	1.911E-01	5.780E+13	1.00001	0.73381	1.00E-04	3.14E-03	1.14E-03	9.90E-03
0.9758524	0.71406	2.185E+06	1.872E-01	5.584E+13	1.00001	0.73381	1.00E-04	3.14E-03	1.14E-03	9.90E-03
0.9764214	0.71688	2.155E+06	1.833E-01	5.394E+13	1.00001	0.73381	1.00E-04	3.14E-03	1.14E-03	9.90E-03
0.9769795	0.71968	2.126E+06	1.796E-01	5.211E+13	1.00001	0.73381	1.00E-04	3.14E-03	1.14E-03	9.90E-03
0.9775267	0.72246	2.097E+06	1.759E-01	5.033E+13	1.00001	0.73381	1.00E-04	3.14E-03	1.14E-03	9.90E-03
0.9780632	0.72523	2.068E+06	1.723E-01	4.862E+13	1.00001	0.73381	1.00E-04	3.14E-03	1.14E-03	9.90E-03
0.9796093	0.73340	1.985E+06	1.619E-01	4.383E+13	1.00001	0.73381	1.00E-04	3.14E-03	1.14E-03	9.90E-03
0.9815287	0.74404	1.879E+06	1.490E-01	3.817E+13	1.00001	0.73381	1.00E-04	3.14E-03	1.14E-03	9.90E-03
0.9832937	0.75437	1.779E+06	1.371E-01	3.324E+13	1.00000	0.73381	1.00E-04	3.14E-03	1.14E-03	9.90E-03
0.9849131	0.76439	1.684E+06	1.262E-01	2.895E+13	1.00000	0.73381	1.00E-04	3.14E-03	1.14E-03	9.90E-03
0.9863958	0.77411	1.594E+06	1.161E-01	2.521E+13	1.00000	0.73381	1.00E-04	3.14E-03	1.14E-03	9.90E-03
0.9877504	0.78352	1.509E+06	1.069E-01	2.195E+13	1.00000	0.73381	1.00E-04	3.14E-03	1.14E-03	9.90E-03
0.9889855	0.79262	1.428E+06	9.840E-02	1.912E+13	1.00000	0.73381	1.00E-04	3.14E-03	1.14E-03	9.90E-03
0.9901095	0.80142	1.352E+06	9.057E-02	1.665E+13	1.00000	0.73381	1.00E-04	3.14E-03	1.14E-03	9.90E-03
0.9911304	0.80992	1.280E+06	8.336E-02	1.450E+13	1.00000	0.73381	1.00E-04	3.14E-03	1.14E-03	9.90E-03
0.9920559	0.81812	1.211E+06	7.673E-02	1.263E+13	1.00000	0.73381	1.00E-04	3.14E-03	1.14E-03	9.90E-03
0.9928936	0.82603	1.147E+06	7.062E-02	1.100E+13	1.00000	0.73381	1.00E-04	3.14E-03	1.14E-03	9.90E-03
0.9936504	0.83364	1.086E+06	6.501E-02	9.578E+12	1.00000	0.73381	1.00E-04	3.14E-03	1.14E-03	9.90E-03
0.9943331	0.84098	1.028E+06	5.984E-02	8.342E+12	1.00000	0.73381	1.00E-04	3.14E-03	1.14E-03	9.90E-03
0.9949479	0.84803	9.730E+05	5.508E-02	7.265E+12	1.00000	0.73381	1.00E-04	3.14E-03	1.14E-03	9.90E-03
0.9955008	0.85480	9.211E+05	5.070E-02	6.327E+12	1.00000	0.73381	1.00E-04	3.14E-03	1.14E-03	9.90E-03
0.9959972	0.86131	8.720E+05	4.666E-02	5.510E+12	1.00000	0.73381	1.00E-04	3.14E-03	1.14E-03	9.90E-03
0.9964423	0.86756	8.256E+05	4.295E-02	4.799E+12	1.00000	0.73381	1.00E-04	3.14E-03	1.14E-03	9.90E-03
0.9968409	0.87355	7.816E+05	3.953E-02	4.179E+12	1.00000	0.73381	1.00E-04	3.14E-03	1.14E-03	9.90E-03
0.9971973	0.87929	7.400E+05	3.638E-02	3.640E+12	1.00000	0.73381	1.00E-04	3.14E-03	1.14E-03	9.90E-03
0.9975157	0.88480	7.006E+05	3.348E-02	3.170E+12	1.00000	0.73381	1.00E-04	3.14E-03	1.14E-03	9.90E-03
0.9977997	0.89007	6.633E+05	3.081E-02	2.761E+12	1.00000	0.73381	1.00E-04	3.14E-03	1.14E-03	9.90E-03
0.9980527	0.89511	6.279E+05	2.835E-02	2.405E+12	1.00000	0.73381	1.00E-04	3.14E-03	1.14E-03	9.90E-03
0.9982780	0.89994	5.945E+05	2.608E-02	2.094E+12	1.00000	0.73381	1.00E-04	3.14E-03	1.14E-03	9.90E-03
0.9984783	0.90456	5.628E+05	2.399E-02	1.824E+12	1.00000	0.73381	1.00E-04	3.14E-03	1.14E-03	9.90E-03
0.9986563	0.90898	5.328E+05	2.207E-02	1.588E+12	1.00000	0.73381	1.00E-04	3.14E-03	1.14E-03	9.90E-03
0.9988142	0.91320	5.043E+05	2.030E-02	1.383E+12	1.00000	0.73381	1.00E-04	3.14E-03	1.14E-03	9.90E-03
0.9989542	0.91723	4.774E+05	1.867E-02	1.205E+12	1.00000	0.73381	1.00E-04	3.14E-03	1.14E-03	9.90E-03
0.9991881	0.92475	4.278E+05	1.580E-02	9.139E+11	1.00000	0.73381	1.00E-04	3.14E-03	1.14E-03	9.90E-03
0.9993710	0.93160	3.834E+05	1.337E-02	6.933E+11	1.00000	0.73381	1.00E-04	3.14E-03	1.14E-03	9.90E-03
0.9995137	0.93782	3.437E+05	1.132E-02	5.259E+11	1.00000	0.73381	1.00E-04	3.14E-03	1.14E-03	9.90E-03
0.9996247	0.94347	3.082E+05	9.582E-03	3.989E+11	1.00000	0.73381	1.00E-04	3.14E-03	1.14E-03	9.90E-03
0.9997095	0.94850	2.770E+05	8.136E-03	3.041E+11	1.00000	0.73381	1.00E-04	3.14E-03	1.14E-03	9.90E-03

TABLE XVII

STANDARD SOLAR MODEL (NO HE DIFFUSION) ^{7}BE MASS FRACTION AND RATES OF NEUTRINO PRODUCTION

$R/R_\odot$	T6	log ρ_e	d(Mass)	X(^{7}Be)	dϕ(pp)	dϕ(^{8}B)	dϕ(^{13}N)	dϕ(^{15}O)	dϕ(^{17}F)	dϕ(^{7}Be)	dϕ(pep)	dϕ(hep)
0.00652	15.571	2.011	3.274E-05	1.668E-11	2.074E-04	2.534E-03	1.922E-03	2.253E-03	2.348E-03	1.026E-03	3.259E-04	8.778E-05
0.00693	15.569	2.010	6.622E-06	1.666E-11	4.195E-05	5.112E-04	3.877E-04	4.545E-04	4.738E-04	2.072E-04	6.590E-05	1.777E-05
0.00737	15.567	2.010	7.961E-06	1.665E-11	5.044E-05	6.130E-04	4.648E-04	5.449E-04	5.680E-04	2.488E-04	7.922E-05	2.138E-05
0.00784	15.565	2.010	9.571E-06	1.663E-11	6.064E-05	7.348E-04	5.569E-04	6.530E-04	6.809E-04	2.987E-04	9.522E-05	2.573E-05
0.00834	15.562	2.010	1.151E-05	1.661E-11	7.292E-05	8.804E-04	6.673E-04	7.823E-04	8.157E-04	3.586E-04	1.144E-04	3.096E-05
0.00887	15.559	2.010	1.383E-05	1.658E-11	8.768E-05	1.054E-03	7.988E-04	9.367E-04	9.768E-04	4.303E-04	1.376E-04	3.727E-05
0.00943	15.556	2.009	1.663E-05	1.656E-11	1.054E-04	1.262E-03	9.559E-04	1.121E-03	1.169E-03	5.162E-04	1.653E-04	4.487E-05
0.01003	15.552	2.009	2.000E-05	1.653E-11	1.268E-04	1.510E-03	1.144E-03	1.341E-03	1.399E-03	6.192E-04	1.987E-04	5.403E-05
0.01067	15.547	2.009	2.404E-05	1.649E-11	1.525E-04	1.805E-03	1.367E-03	1.602E-03	1.672E-03	7.424E-04	2.388E-04	6.507E-05
0.01134	15.542	2.009	2.890E-05	1.645E-11	1.833E-04	2.156E-03	1.632E-03	1.913E-03	1.997E-03	8.899E-04	2.869E-04	7.837E-05
0.01206	15.537	2.008	3.475E-05	1.641E-11	2.205E-04	2.573E-03	1.947E-03	2.283E-03	2.384E-03	1.066E-03	3.448E-04	9.443E-05
0.01283	15.530	2.008	4.178E-05	1.636E-11	2.652E-04	3.068E-03	2.321E-03	2.721E-03	2.842E-03	1.277E-03	4.142E-04	1.138E-04
0.01365	15.523	2.007	5.023E-05	1.630E-11	3.189E-04	3.655E-03	2.763E-03	3.240E-03	3.385E-03	1.528E-03	4.977E-04	1.372E-04
0.01452	15.515	2.007	6.039E-05	1.624E-11	3.835E-04	4.348E-03	3.285E-03	3.853E-03	4.027E-03	1.828E-03	5.978E-04	1.655E-04
0.01544	15.506	2.006	7.260E-05	1.617E-11	4.613E-04	5.165E-03	3.902E-03	4.575E-03	4.783E-03	2.186E-03	7.180E-04	1.996E-04
0.01643	15.495	2.005	8.729E-05	1.608E-11	5.548E-04	6.126E-03	4.626E-03	5.424E-03	5.673E-03	2.611E-03	8.623E-04	2.409E-04
0.01748	15.484	2.004	1.049E-04	1.599E-11	6.672E-04	7.252E-03	5.474E-03	6.418E-03	6.716E-03	3.116E-03	1.035E-03	2.909E-04
0.01860	15.470	2.003	1.262E-04	1.589E-11	8.025E-04	8.568E-03	6.464E-03	7.579E-03	7.935E-03	3.715E-03	1.243E-03	3.514E-04
0.01979	15.455	2.002	1.517E-04	1.577E-11	9.653E-04	1.010E-02	7.615E-03	8.929E-03	9.353E-03	4.424E-03	1.492E-03	4.247E-04
0.02106	15.438	2.001	1.824E-04	1.564E-11	1.161E-03	1.187E-02	8.948E-03	1.049E-02	1.099E-02	5.261E-03	1.790E-03	5.136E-04
0.02241	15.419	2.000	2.193E-04	1.548E-11	1.396E-03	1.391E-02	1.048E-02	1.229E-02	1.289E-02	6.247E-03	2.147E-03	6.215E-04
0.02386	15.397	1.998	2.636E-04	1.531E-11	1.679E-03	1.624E-02	1.224E-02	1.435E-02	1.505E-02	7.405E-03	2.574E-03	7.526E-04
0.02540	15.373	1.997	3.169E-04	1.511E-11	2.020E-03	1.888E-02	1.423E-02	1.668E-02	1.751E-02	8.760E-03	3.084E-03	9.121E-04
0.02704	15.345	1.995	3.810E-04	1.490E-11	2.429E-03	2.186E-02	1.648E-02	1.932E-02	2.029E-02	1.034E-02	3.694E-03	1.106E-03
0.02879	15.314	1.993	4.581E-04	1.465E-11	2.920E-03	2.518E-02	1.898E-02	2.226E-02	2.338E-02	1.218E-02	4.421E-03	1.343E-03
0.03067	15.279	1.990	5.508E-04	1.437E-11	3.510E-03	2.881E-02	2.175E-02	2.550E-02	2.679E-02	1.429E-02	5.287E-03	1.632E-03
0.03267	15.239	1.987	6.622E-04	1.406E-11	4.218E-03	3.275E-02	2.477E-02	2.904E-02	3.050E-02	1.671E-02	6.317E-03	1.984E-03
0.03481	15.194	1.984	7.961E-04	1.370E-11	5.066E-03	3.692E-02	2.799E-02	3.282E-02	3.446E-02	1.947E-02	7.538E-03	2.415E-03
0.03710	15.143	1.981	9.571E-04	1.330E-11	6.082E-03	4.125E-02	3.139E-02	3.680E-02	3.861E-02	2.257E-02	8.983E-03	2.941E-03
0.03955	15.086	1.977	1.151E-03	1.286E-11	7.295E-03	4.560E-02	3.487E-02	4.088E-02	4.283E-02	2.604E-02	1.069E-02	3.586E-03
0.04218	15.022	1.972	1.383E-03	1.237E-11	8.742E-03	4.981E-02	3.833E-02	4.494E-02	4.699E-02	2.985E-02	1.269E-02	4.375E-03
0.04500	14.949	1.967	1.663E-03	1.182E-11	1.046E-02	5.364E-02	4.164E-02	4.882E-02	5.089E-02	3.396E-02	1.503E-02	5.340E-03
0.04803	14.868	1.961	2.000E-03	1.121E-11	1.250E-02	5.681E-02	4.462E-02	5.232E-02	5.431E-02	3.831E-02	1.774E-02	6.518E-03
0.05129	14.776	1.955	2.404E-03	1.056E-11	1.491E-02	5.908E-02	4.709E-02	5.521E-02	5.700E-02	4.281E-02	2.088E-02	7.961E-03
0.05480	14.672	1.948	2.890E-03	9.839E-12	1.773E-02	6.011E-02	4.884E-02	5.725E-02	5.868E-02	4.730E-02	2.446E-02	9.717E-03
0.05859	14.556	1.939	3.475E-03	9.066E-12	2.101E-02	5.964E-02	4.963E-02	5.818E-02	5.908E-02	5.158E-02	2.851E-02	1.185E-02
0.06267	14.425	1.930	4.178E-03	8.243E-12	2.480E-02	5.749E-02	4.929E-02	5.778E-02	5.799E-02	5.541E-02	3.303E-02	1.443E-02
0.06710	14.278	1.920	5.023E-03	7.384E-12	2.913E-02	5.360E-02	4.769E-02	5.590E-02	5.527E-02	5.850E-02	3.797E-02	1.754E-02
0.07189	14.113	1.908	6.039E-03	6.498E-12	3.400E-02	4.806E-02	4.475E-02	5.246E-02	5.094E-02	6.051E-02	4.326E-02	2.125E-02
0.07710	13.928	1.894	6.994E-03	5.600E-12	3.796E-02	3.994E-02	3.928E-02	4.604E-02	4.373E-02	5.908E-02	4.703E-02	2.470E-02
0.08233	13.738	1.881	7.506E-03	4.779E-12	3.905E-02	3.000E-02	3.134E-02	3.675E-02	3.409E-02	5.278E-02	4.705E-02	2.647E-02
0.08742	13.548	1.867	7.982E-03	4.059E-12	3.963E-02	2.207E-02	2.462E-02	2.887E-02	2.610E-02	4.644E-02	4.640E-02	2.797E-02
0.09246	13.357	1.852	8.509E-03	3.427E-12	4.013E-02	1.609E-02	1.923E-02	2.255E-02	1.985E-02	4.071E-02	4.567E-02	2.949E-02
0.09748	13.164	1.838	9.100E-03	2.875E-12	4.059E-02	1.160E-02	1.491E-02	1.750E-02	1.497E-02	3.554E-02	4.485E-02	3.106E-02
0.10255	12.968	1.823	9.772E-03	2.392E-12	4.099E-02	8.252E-03	1.147E-02	1.346E-02	1.117E-02	3.088E-02	4.394E-02	3.268E-02

TABLE XVII—*continued*

$R/R_\odot$	T6	log ρ_e	d(Mass)	X(^{7}Be)	dϕ(pp)	dϕ(^{8}B)	dϕ(^{13}N)	dϕ(^{15}O)	dϕ(^{17}F)	dϕ(^{7}Be)	dϕ(pep)	dϕ(hep)
0.10770	12.767	1.807	1.054E-02	1.972E-12	4.135E-02	5.778E-03	8.712E-03	1.023E-02	8.232E-03	2.668E-02	4.295E-02	3.438E-02
0.11298	12.560	1.791	1.144E-02	1.608E-12	4.167E-02	3.969E-03	6.530E-03	7.676E-03	5.972E-03	2.290E-02	4.189E-02	3.619E-02
0.11845	12.345	1.773	1.250E-02	1.294E-12	4.195E-02	2.665E-03	4.811E-03	5.662E-03	4.251E-03	1.949E-02	4.073E-02	3.813E-02
0.12419	12.121	1.755	1.377E-02	1.025E-12	4.221E-02	1.741E-03	3.471E-03	4.092E-03	2.957E-03	1.643E-02	3.948E-02	4.026E-02
0.13026	11.884	1.735	1.532E-02	7.970E-13	4.244E-02	1.100E-03	2.513E-03	2.882E-03	1.999E-03	1.369E-02	3.812E-02	4.262E-02
0.13679	11.631	1.713	1.728E-02	6.042E-13	4.263E-02	6.651E-04	2.668E-03	1.962E-03	1.302E-03	1.123E-02	3.664E-02	4.527E-02
0.14392	11.358	1.688	1.978E-02	4.445E-13	4.272E-02	3.806E-04	7.428E-03	1.259E-03	8.086E-04	9.029E-03	3.495E-02	4.827E-02
0.15183	11.060	1.660	2.182E-02	3.143E-13	4.049E-02	1.948E-04	1.967E-02	6.886E-04	4.527E-04	6.742E-03	3.134E-02	4.894E-02
0.15980	10.765	1.631	2.212E-02	2.206E-13	3.489E-02	8.818E-05	2.953E-02	2.985E-04	2.250E-04	4.551E-03	2.549E-02	4.524E-02
0.16759	10.483	1.602	2.215E-02	1.556E-13	2.960E-02	3.953E-05	2.962E-02	1.147E-04	1.105E-04	3.043E-03	2.039E-02	4.115E-02
0.17523	10.213	1.572	2.210E-02	1.103E-13	2.495E-02	1.777E-05	2.317E-02	4.297E-05	5.431E-05	2.035E-03	1.621E-02	3.716E-02
0.18272	9.954	1.543	2.198E-02	7.851E-14	2.092E-02	8.015E-06	1.565E-02	1.737E-05	2.671E-05	1.363E-03	1.281E-02	3.336E-02
0.19008	9.706	1.514	2.180E-02	5.617E-14	1.746E-02	3.631E-06	9.708E-03	7.832E-06	1.316E-05	9.140E-04	1.008E-02	2.979E-02
0.19733	9.469	1.484	2.156E-02	4.039E-14	1.451E-02	1.653E-06	5.742E-03	3.826E-06	6.502E-06	6.141E-04	7.891E-03	2.649E-02
0.20447	9.242	1.454	2.128E-02	2.918E-14	1.203E-02	7.564E-07	3.308E-03	1.950E-06	3.220E-06	4.135E-04	6.158E-03	2.347E-02
0.21151	9.025	1.424	2.095E-02	2.118E-14	9.939E-03	3.480E-07	1.879E-03	1.013E-06	1.600E-06	2.790E-04	4.791E-03	2.073E-02
0.21848	8.816	1.395	2.059E-02	1.545E-14	8.194E-03	1.610E-07	1.060E-03	5.313E-07	7.975E-07	1.887E-04	3.717E-03	1.827E-02
0.22536	8.615	1.364	2.021E-02	1.132E-14	6.742E-03	7.492E-08	5.964E-04	2.800E-07	3.988E-07	1.279E-04	2.877E-03	1.607E-02
0.23218	8.422	1.334	1.980E-02	8.339E-15	5.538E-03	3.507E-08	3.352E-04	1.482E-07	2.001E-07	8.697E-05	2.221E-03	1.412E-02
0.23894	8.237	1.304	1.937E-02	6.169E-15	4.541E-03	1.651E-08	1.885E-04	7.858E-08	1.006E-07	5.931E-05	1.712E-03	1.240E-02
0.24565	8.058	1.273	1.893E-02	4.588E-15	3.719E-03	7.817E-09	1.061E-04	4.180E-08	5.077E-08	4.058E-05	1.317E-03	1.090E-02
0.25231	7.886	1.243	1.847E-02	3.428E-15	3.042E-03	3.722E-09	5.977E-05	2.229E-08	2.568E-08	2.784E-05	1.012E-03	9.577E-03
0.25892	7.720	1.212	1.801E-02	2.559E-15	2.485E-03	1.773E-09	3.373E-05	1.191E-08	1.302E-08	1.906E-05	7.764E-04	8.370E-03
0.26550	7.559	1.181	1.754E-02	1.878E-15	2.028E-03	8.320E-10	1.906E-05	6.376E-09	6.620E-09	1.281E-05	5.948E-04	7.165E-03
0.27206	7.404	1.150	1.707E-02	1.322E-15	1.654E-03	3.759E-10	1.079E-05	3.420E-09	3.372E-09	8.267E-06	4.552E-04	5.869E-03
0.27858	7.254	1.119	1.660E-02	8.734E-16	1.348E-03	1.601E-10	6.115E-06	1.838E-09	1.721E-09	5.016E-06	3.480E-04	4.510E-03
0.28509	7.109	1.087	1.613E-02	5.459E-16	1.098E-03	6.444E-11	3.470E-06	9.890E-10	8.801E-10	2.873E-06	2.658E-04	3.265E-03
0.29158	6.968	1.056	1.566E-02	3.243E-16	8.941E-04	2.467E-11	1.971E-06	5.329E-10	4.507E-10	1.563E-06	2.028E-04	2.242E-03
0.29806	6.831	1.025	1.520E-02	1.861E-16	7.274E-04	9.111E-12	1.121E-06	2.874E-10	2.311E-10	8.197E-07	1.546E-04	1.483E-03
0.30453	6.699	0.993	1.474E-02	1.047E-16	5.914E-04	3.293E-12	6.374E-07	1.552E-10	1.186E-10	4.206E-07	1.178E-04	9.594E-04
0.31100	6.570	0.962	1.429E-02	5.829E-17	4.806E-04	1.177E-12	3.628E-07	8.380E-11	6.090E-11	2.132E-07	8.967E-05	6.124E-04
0.31747	6.445	0.930	1.384E-02	3.227E-17	3.902E-04	4.178E-13	2.065E-07	4.528E-11	3.129E-11	1.073E-07	6.819E-05	3.881E-04
0.32394	6.323	0.898	1.340E-02	1.785E-17	3.167E-04	1.481E-13	1.176E-07	2.447E-11	1.608E-11	5.391E-08	5.182E-05	2.454E-04
0.33041	6.204	0.866	1.297E-02	9.875E-18	2.568E-04	5.250E-14	6.692E-08	1.322E-11	8.265E-12	2.707E-08	3.934E-05	1.550E-04
0.33690	6.089	0.835	1.254E-02	5.467E-18	2.082E-04	1.861E-14	3.809E-08	7.143E-12	4.247E-12	1.359E-08	2.985E-05	9.785E-05
0.34339	5.976	0.803	1.213E-02	3.033E-18	1.686E-04	6.608E-15	2.167E-08	3.857E-12	2.181E-12	6.833E-09	2.263E-05	6.186E-05
0.34990	5.866	0.771	1.172E-02	1.687E-18	1.365E-04	2.350E-15	1.232E-08	2.082E-12	1.120E-12	3.442E-09	1.714E-05	3.917E-05
0.35642	5.759	0.739	1.133E-02	9.406E-19	1.104E-04	8.378E-16	7.000E-09	1.123E-12	5.746E-13	1.738E-09	1.298E-05	2.486E-05
0.36296	5.654	0.707	1.094E-02	5.263E-19	8.927E-05	1.172E-16	3.975E-09	6.054E-13	2.947E-13	8.796E-10	9.817E-06	1.583E-05
0.36952	5.552	0.674	1.056E-02	2.956E-19	7.213E-05	0.000E+00	2.256E-09	3.261E-13	1.510E-13	4.467E-10	7.420E-06	1.010E-05
0.37610	5.452	0.642	1.020E-02	1.666E-19	5.825E-05	0.000E+00	1.279E-09	1.755E-13	7.727E-14	2.276E-10	5.605E-06	6.476E-06
0.38270	5.355	0.610	9.838E-03	9.438E-20	4.701E-05	0.000E+00	7.245E-10	9.436E-14	3.951E-14	1.165E-10	4.230E-06	4.168E-06
0.38933	5.260	0.578	9.489E-03	5.372E-20	3.791E-05	0.000E+00	4.099E-10	5.067E-14	2.018E-14	5.985E-11	3.191E-06	2.695E-06
0.39598	5.166	0.546	9.150E-03	3.073E-20	3.056E-05	0.000E+00	2.317E-10	2.717E-14	1.029E-14	3.090E-11	2.405E-06	1.752E-06
0.40266	5.075	0.513	8.821E-03	1.768E-20	2.462E-05	0.000E+00	1.308E-10	1.455E-14	5.239E-15	1.604E-11	1.811E-06	1.145E-06

TABLE XVIII

STANDARD SOLAR MODEL (WITH HE DIFFUSION) ^{7}BE MASS FRACTION AND RATES OF NEUTRINO PRODUCTION

$R/R_\odot$	T6	log ρ_e	d(Mass)	X(^{7}Be)	dϕ(pp)	dϕ(^{8}B)	dϕ(^{13}N)	dϕ(^{15}O)	dϕ(^{17}F)	dϕ(^{7}Be)	dϕ(pep)	dϕ(hep)
0.00648	15.672	2.015	3.274E-05	1.739E-11	2.044E-04	2.519E-03	1.976E-03	2.287E-03	2.367E-03	1.016E-03	3.234E-04	8.426E-05
0.00689	15.671	2.015	6.622E-06	1.738E-11	4.135E-05	5.083E-04	3.988E-04	4.614E-04	4.777E-04	2.052E-04	6.541E-05	1.706E-05
0.00733	15.668	2.015	7.961E-06	1.736E-11	4.973E-05	6.095E-04	4.781E-04	5.531E-04	5.728E-04	2.464E-04	7.862E-05	2.053E-05
0.00779	15.666	2.015	9.571E-06	1.734E-11	5.979E-05	7.306E-04	5.729E-04	6.629E-04	6.865E-04	2.958E-04	9.450E-05	2.470E-05
0.00829	15.663	2.014	1.151E-05	1.732E-11	7.190E-05	8.754E-04	6.863E-04	7.940E-04	8.225E-04	3.551E-04	1.136E-04	2.973E-05
0.00881	15.660	2.014	1.383E-05	1.730E-11	8.645E-05	1.048E-03	8.216E-04	9.506E-04	9.849E-04	4.261E-04	1.365E-04	3.579E-05
0.00937	15.657	2.014	1.663E-05	1.727E-11	1.040E-04	1.255E-03	9.830E-04	1.137E-03	1.179E-03	5.113E-04	1.641E-04	4.309E-05
0.00997	15.653	2.014	2.000E-05	1.724E-11	1.250E-04	1.501E-03	1.176E-03	1.360E-03	1.410E-03	6.133E-04	1.972E-04	5.190E-05
0.01060	15.648	2.013	2.404E-05	1.721E-11	1.503E-04	1.795E-03	1.405E-03	1.626E-03	1.686E-03	7.355E-04	2.370E-04	6.251E-05
0.01127	15.643	2.013	2.890E-05	1.717E-11	1.808E-04	2.144E-03	1.678E-03	1.941E-03	2.013E-03	8.817E-04	2.848E-04	7.531E-05
0.01199	15.637	2.013	3.475E-05	1.713E-11	2.174E-04	2.560E-03	2.002E-03	2.316E-03	2.403E-03	1.056E-03	3.422E-04	9.075E-05
0.01275	15.631	2.012	4.178E-05	1.708E-11	2.615E-04	3.052E-03	2.386E-03	2.760E-03	2.865E-03	1.265E-03	4.112E-04	1.094E-04
0.01356	15.623	2.012	5.023E-05	1.702E-11	3.145E-04	3.636E-03	2.841E-03	3.286E-03	3.412E-03	1.515E-03	4.941E-04	1.319E-04
0.01443	15.615	2.011	6.039E-05	1.696E-11	3.783E-04	4.326E-03	3.377E-03	3.907E-03	4.059E-03	1.812E-03	5.935E-04	1.591E-04
0.01535	15.605	2.010	7.260E-05	1.688E-11	4.550E-04	5.140E-03	4.009E-03	4.638E-03	4.821E-03	2.167E-03	7.129E-04	1.920E-04
0.01633	15.595	2.010	8.729E-05	1.680E-11	5.473E-04	6.097E-03	4.751E-03	5.497E-03	5.718E-03	2.589E-03	8.562E-04	2.318E-04
0.01737	15.583	2.009	1.049E-04	1.671E-11	6.583E-04	7.220E-03	5.622E-03	6.504E-03	6.768E-03	3.090E-03	1.028E-03	2.800E-04
0.01848	15.569	2.008	1.262E-04	1.660E-11	7.919E-04	8.530E-03	6.636E-03	7.678E-03	7.995E-03	3.685E-03	1.234E-03	3.383E-04
0.01967	15.554	2.007	1.517E-04	1.649E-11	9.526E-04	1.006E-02	7.817E-03	9.043E-03	9.423E-03	4.390E-03	1.482E-03	4.091E-04
0.02093	15.536	2.006	1.824E-04	1.635E-11	1.146E-03	1.182E-02	9.180E-03	1.062E-02	1.108E-02	5.222E-03	1.778E-03	4.950E-04
0.02228	15.517	2.004	2.193E-04	1.620E-11	1.378E-03	1.386E-02	1.075E-02	1.244E-02	1.298E-02	6.204E-03	2.133E-03	5.994E-04
0.02371	15.495	2.003	2.636E-04	1.603E-11	1.658E-03	1.619E-02	1.255E-02	1.452E-02	1.516E-02	7.357E-03	2.557E-03	7.263E-04
0.02524	15.470	2.001	3.169E-04	1.583E-11	1.995E-03	1.883E-02	1.458E-02	1.687E-02	1.764E-02	8.707E-03	3.065E-03	8.808E-04
0.02687	15.442	1.999	3.810E-04	1.561E-11	2.399E-03	2.180E-02	1.688E-02	1.953E-02	2.042E-02	1.028E-02	3.672E-03	1.069E-03
0.02862	15.410	1.997	4.581E-04	1.536E-11	2.885E-03	2.512E-02	1.944E-02	2.249E-02	2.353E-02	1.211E-02	4.395E-03	1.299E-03
0.03048	15.374	1.994	5.508E-04	1.507E-11	3.469E-03	2.875E-02	2.225E-02	2.575E-02	2.696E-02	1.422E-02	5.258E-03	1.579E-03
0.03247	15.333	1.992	6.622E-04	1.475E-11	4.170E-03	3.269E-02	2.532E-02	2.929E-02	3.068E-02	1.664E-02	6.283E-03	1.922E-03
0.03460	15.287	1.988	7.961E-04	1.440E-11	5.011E-03	3.690E-02	2.860E-02	3.309E-02	3.466E-02	1.941E-02	7.501E-03	2.343E-03
0.03688	15.236	1.985	9.571E-04	1.399E-11	6.017E-03	4.124E-02	3.204E-02	3.707E-02	3.881E-02	2.252E-02	8.941E-03	2.857E-03
0.03932	15.178	1.981	1.151E-03	1.353E-11	7.222E-03	4.560E-02	3.556E-02	4.114E-02	4.303E-02	2.598E-02	1.064E-02	3.488E-03
0.04193	15.112	1.976	1.383E-03	1.302E-11	8.658E-03	4.983E-02	3.906E-02	4.518E-02	4.718E-02	2.980E-02	1.264E-02	4.261E-03
0.04474	15.038	1.971	1.663E-03	1.246E-11	1.037E-02	5.368E-02	4.238E-02	4.903E-02	5.107E-02	3.394E-02	1.498E-02	5.209E-03
0.04775	14.955	1.965	2.000E-03	1.183E-11	1.240E-02	5.690E-02	4.537E-02	5.248E-02	5.447E-02	3.832E-02	1.769E-02	6.371E-03
0.05099	14.861	1.959	2.404E-03	1.115E-11	1.479E-02	5.919E-02	4.782E-02	5.531E-02	5.711E-02	4.285E-02	2.083E-02	7.794E-03
0.05449	14.756	1.951	2.890E-03	1.040E-11	1.761E-02	6.024E-02	4.951E-02	5.727E-02	5.873E-02	4.738E-02	2.442E-02	9.532E-03
0.05825	14.637	1.943	3.475E-03	9.591E-12	2.089E-02	5.981E-02	5.024E-02	5.811E-02	5.907E-02	5.172E-02	2.848E-02	1.165E-02
0.06232	14.504	1.933	4.178E-03	8.727E-12	2.468E-02	5.765E-02	4.981E-02	5.762E-02	5.790E-02	5.558E-02	3.301E-02	1.422E-02
0.06673	14.355	1.923	5.023E-03	7.823E-12	2.902E-02	5.373E-02	4.809E-02	5.563E-02	5.510E-02	5.869E-02	3.797E-02	1.732E-02
0.07150	14.187	1.911	6.039E-03	6.890E-12	3.390E-02	4.818E-02	4.504E-02	5.210E-02	5.069E-02	6.074E-02	4.329E-02	2.103E-02
0.07670	13.999	1.897	6.990E-03	5.939E-12	3.787E-02	3.998E-02	3.944E-02	4.561E-02	4.342E-02	5.927E-02	4.707E-02	2.448E-02
0.08190	13.806	1.883	7.500E-03	5.072E-12	3.899E-02	3.001E-02	3.140E-02	3.632E-02	3.376E-02	5.295E-02	4.710E-02	2.628E-02
0.08698	13.613	1.869	7.977E-03	4.308E-12	3.960E-02	2.206E-02	2.462E-02	2.848E-02	2.581E-02	4.658E-02	4.649E-02	2.782E-02
0.09201	13.420	1.855	8.506E-03	3.638E-12	4.015E-02	1.607E-02	1.920E-02	2.222E-02	1.959E-02	4.083E-02	4.578E-02	2.939E-02
0.09702	13.224	1.840	9.099E-03	3.051E-12	4.064E-02	1.157E-02	1.486E-02	1.720E-02	1.474E-02	3.564E-02	4.497E-02	3.100E-02
0.10208	13.025	1.825	9.771E-03	2.538E-12	4.108E-02	8.217E-03	1.140E-02	1.320E-02	1.098E-02	3.094E-02	4.408E-02	3.267E-02
0.10722	12.822	1.809	1.054E-02	2.091E-12	4.147E-02	5.743E-03	8.643E-03	1.002E-02	8.070E-03	2.671E-02	4.310E-02	3.441E-02

TABLE XVIII—*continued*

$R/R_\odot$	T6	log ρ_c	d(Mass)	X(^{7}Be)	dϕ(pp)	dϕ(^{8}B)	dϕ(^{13}N)	dϕ(^{15}O)	dϕ(^{17}F)	dϕ(^{7}Be)	dϕ(pep)	dϕ(hep)
0.11251	12.612	1.792	1.144E-02	1.704E-12	4.181E-02	3.936E-03	6.462E-03	7.495E-03	5.839E-03	2.289E-02	4.203E-02	3.626E-02
0.11798	12.395	1.774	1.250E-02	1.370E-12	4.212E-02	2.636E-03	4.749E-03	5.515E-03	4.145E-03	1.946E-02	4.087E-02	3.825E-02
0.12372	12.167	1.756	1.377E-02	1.084E-12	4.240E-02	1.717E-03	3.417E-03	3.975E-03	2.874E-03	1.638E-02	3.961E-02	4.043E-02
0.12980	11.927	1.735	1.534E-02	8.410E-13	4.264E-02	1.081E-03	2.447E-03	2.791E-03	1.936E-03	1.362E-02	3.824E-02	4.284E-02
0.13635	11.672	1.713	1.730E-02	6.368E-13	4.285E-02	6.513E-04	2.421E-03	1.894E-03	1.257E-03	1.115E-02	3.674E-02	4.555E-02
0.14350	11.395	1.688	1.978E-02	4.672E-13	4.289E-02	3.703E-04	6.437E-03	1.211E-03	7.762E-04	8.930E-03	3.497E-02	4.852E-02
0.15140	11.095	1.659	2.163E-02	3.302E-13	4.033E-02	1.876E-04	1.738E-02	6.598E-04	4.300E-04	6.604E-03	3.110E-02	4.883E-02
0.15931	10.800	1.630	2.190E-02	2.320E-13	3.475E-02	8.495E-05	2.679E-02	2.887E-04	2.138E-04	4.454E-03	2.528E-02	4.512E-02
0.16706	10.517	1.601	2.195E-02	1.637E-13	2.952E-02	3.818E-05	2.744E-02	1.120E-04	1.053E-04	2.981E-03	2.025E-02	4.109E-02
0.17466	10.246	1.572	2.190E-02	1.161E-13	2.492E-02	1.720E-05	2.179E-02	4.204E-05	5.185E-05	1.995E-03	1.612E-02	3.716E-02
0.18212	9.987	1.542	2.179E-02	8.270E-14	2.092E-02	7.772E-06	1.486E-02	1.691E-05	2.556E-05	1.337E-03	1.275E-02	3.340E-02
0.18946	9.739	1.513	2.162E-02	5.919E-14	1.748E-02	3.528E-06	9.283E-03	7.575E-06	1.262E-05	8.971E-04	1.004E-02	2.986E-02
0.19668	9.502	1.483	2.139E-02	4.257E-14	1.455E-02	1.609E-06	5.518E-03	3.690E-06	6.246E-06	6.031E-04	7.875E-03	2.658E-02
0.20381	9.274	1.454	2.111E-02	3.076E-14	1.207E-02	7.373E-07	3.190E-03	1.880E-06	3.100E-06	4.062E-04	6.153E-03	2.358E-02
0.21084	9.056	1.424	2.080E-02	2.234E-14	9.991E-03	3.397E-07	1.817E-03	9.773E-07	1.543E-06	2.742E-04	4.792E-03	2.085E-02
0.21780	8.846	1.394	2.045E-02	1.629E-14	8.247E-03	1.574E-07	1.028E-03	5.130E-07	7.706E-07	1.855E-04	3.721E-03	1.839E-02
0.22468	8.645	1.364	2.007E-02	1.194E-14	6.793E-03	7.337E-08	5.794E-04	2.709E-07	3.861E-07	1.258E-04	2.883E-03	1.619E-02
0.23150	8.452	1.333	1.967E-02	8.789E-15	5.586E-03	3.437E-08	3.263E-04	1.436E-07	1.941E-07	8.552E-05	2.229E-03	1.423E-02
0.23826	8.266	1.303	1.926E-02	6.503E-15	4.586E-03	1.620E-08	1.838E-04	7.629E-08	9.781E-08	5.834E-05	1.719E-03	1.251E-02
0.24497	8.087	1.272	1.882E-02	4.836E-15	3.759E-03	7.683E-09	1.036E-04	4.066E-08	4.943E-08	3.993E-05	1.324E-03	1.100E-02
0.25163	7.914	1.241	1.838E-02	3.613E-15	3.078E-03	3.662E-09	5.846E-05	2.172E-08	2.505E-08	2.740E-05	1.018E-03	9.671E-03
0.25826	7.748	1.211	1.793E-02	2.699E-15	2.518E-03	1.748E-09	3.305E-05	1.162E-08	1.273E-08	1.877E-05	7.819E-04	8.467E-03
0.26486	7.587	1.180	1.747E-02	1.988E-15	2.057E-03	8.243E-10	1.871E-05	6.233E-09	6.480E-09	1.267E-05	5.996E-04	7.281E-03
0.27142	7.431	1.149	1.701E-02	1.412E-15	1.679E-03	3.757E-10	1.060E-05	3.349E-09	3.306E-09	8.245E-06	4.593E-04	6.016E-03
0.27797	7.281	1.118	1.655E-02	9.423E-16	1.370E-03	1.619E-10	6.019E-06	1.802E-09	1.690E-09	5.056E-06	3.514E-04	4.673E-03
0.28449	7.135	1.086	1.608E-02	5.946E-16	1.117E-03	6.584E-11	3.421E-06	9.713E-10	8.658E-10	2.923E-06	2.686E-04	3.417E-03
0.29100	6.994	1.055	1.562E-02	3.561E-16	9.099E-04	2.545E-11	1.946E-06	5.242E-10	4.441E-10	1.605E-06	2.051E-04	2.368E-03
0.29751	6.857	1.023	1.517E-02	2.056E-16	7.410E-04	9.470E-12	1.108E-06	2.832E-10	2.281E-10	8.471E-07	1.565E-04	1.577E-03
0.30400	6.724	0.992	1.471E-02	1.161E-16	6.030E-04	3.442E-12	6.310E-07	1.531E-10	1.172E-10	4.366E-07	1.193E-04	1.025E-03
0.31050	6.595	0.960	1.427E-02	6.484E-17	4.904E-04	1.235E-12	3.596E-07	8.281E-11	6.030E-11	2.220E-07	9.092E-05	6.565E-04
0.31700	6.469	0.929	1.383E-02	3.598E-17	3.986E-04	4.399E-13	2.050E-07	4.481E-11	3.103E-11	1.121E-07	6.920E-05	4.174E-04
0.32350	6.347	0.897	1.339E-02	1.992E-17	3.238E-04	1.563E-13	1.169E-07	2.425E-11	1.597E-11	5.639E-08	5.263E-05	2.644E-04
0.33001	6.228	0.865	1.297E-02	1.103E-17	2.628E-04	5.552E-14	6.661E-08	1.312E-11	8.221E-12	2.835E-08	4.000E-05	1.673E-04
0.33653	6.112	0.833	1.255E-02	6.116E-18	2.132E-04	1.973E-14	3.795E-08	7.098E-12	4.231E-12	1.425E-08	3.037E-05	1.058E-04
0.34306	5.999	0.801	1.214E-02	3.394E-18	1.729E-04	7.016E-15	2.162E-08	3.838E-12	2.176E-12	7.173E-09	2.304E-05	6.699E-05
0.34961	5.889	0.769	1.174E-02	1.888E-18	1.401E-04	2.499E-15	1.231E-08	2.074E-12	1.119E-12	3.617E-09	1.747E-05	4.249E-05
0.35617	5.781	0.737	1.135E-02	1.053E-18	1.134E-04	8.921E-16	7.001E-09	1.120E-12	5.748E-13	1.827E-09	1.324E-05	2.700E-05
0.36275	5.676	0.705	1.096E-02	5.895E-19	9.177E-05	1.249E-16	3.980E-09	6.047E-13	2.951E-13	9.254E-10	1.002E-05	1.720E-05
0.36936	5.573	0.673	1.059E-02	3.311E-19	7.422E-05	0.000E+00	2.261E-09	3.261E-13	1.514E-13	4.701E-10	7.581E-06	1.099E-05
0.37599	5.473	0.641	1.023E-02	1.866E-19	5.999E-05	0.000E+00	1.283E-09	1.757E-13	7.758E-14	2.396E-10	5.731E-06	7.051E-06
0.38264	5.375	0.608	9.871E-03	1.057E-19	4.845E-05	0.000E+00	7.278E-10	9.457E-14	3.971E-14	1.226E-10	4.329E-06	4.540E-06
0.38932	5.280	0.576	9.526E-03	6.010E-20	3.911E-05	0.000E+00	4.122E-10	5.083E-14	2.030E-14	6.298E-11	3.268E-06	2.937E-06
0.39603	5.186	0.544	9.190E-03	3.434E-20	3.155E-05	0.000E+00	2.332E-10	2.729E-14	1.036E-14	3.250E-11	2.465E-06	1.909E-06
0.40277	5.095	0.512	8.863E-03	1.973E-20	2.544E-05	0.000E+00	1.317E-10	1.463E-14	5.283E-15	1.685E-11	1.858E-06	1.247E-06
0.40954	5.005	0.479	8.545E-03	1.140E-20	2.049E-05	0.000E+00	7.429E-11	7.828E-15	2.688E-15	8.786E-12	1.400E-06	8.197E-07

REFERENCES

Aardsma, G., *et al.*, 1987, Phys. Lett. B **194**, 321.
Abazov, A. I., *et al.*, 1991a, Nucl. Phys. B (Proc. Suppl.) **19**, 84.
Abazov, A. I., *et al.*, 1991b, Phys. Rev. Lett. **67**, 3332.
Akhmedov, E. Kh., and M. Yu. Khlopov, 1988, Mod. Phys. Lett. A **3**, 451.
Aller, L. H., and S. Chapman, 1960, Astrophys. J. **132**, 461.
Anders, E., and N. Grevesse, 1989, Geochim. Cosmochim. Acta **53**, 197.
Andreasen, G. K., 1988, Astron. Astrophys. **201**, 72.
Andreasen, G. K., and J. O. Petersen, 1988, Astron. Astrophys. **192**, L4.
Anselmann, P., *et al.* 1992, Phys. Lett. B **285**, 390.
Arpasella, C., *et al.*, 1991, in "Borexino at Gran Sasso: Proposal for a real time detector for low energy solar neutrinos," Vols. I and II (University of Milan), INFN Report.
Assenbaum, H. J., K. Langanke, and C. Rolfs, 1987, Z. Phys. A **327**, 461.
Bahcall, J. N., 1978, Rev. Mod. Phys. **50**, 881.
Bahcall, J. N., 1987, Rev. Mod. Phys. **59**, 505.
Bahcall, J. N., 1989, *Neutrino Astrophysics* (Cambridge University, Cambridge, England).
Bahcall, J. N., 1991, Phys. Rev. D **44**, 1644.
Bahcall, J. N., N. A. Bahcall, and G. Shaviv, 1968, Phys. Rev. Lett. **20**, 1209.
Bahcall, J. N., N. A. Bahcall, and R. K. Ulrich, 1969, Astrophys. J. **156**, 559.
Bahcall, J. N., and H. A. Bethe, 1990, Phys. Rev. Lett. **65**, 2233.
Bahcall, J. N., and S. C. Frautschi, 1969, Phys. Lett. B **29**, 263.
Bahcall, J. N., W. F. Huebner, S. H. Lubow, P. D. Parker, and R. K. Ulrich, 1982, Rev. Mod. Phys. **54**, 767.
Bahcall, J. N., and A. Loeb, 1990, Astrophys. J. **360**, 267.
Bahcall, J. N., and R. M. May, 1969, Astrophys. J. **155**, 501.
Bahcall, J. N., and R. L. Sears, 1972, Annu. Rev. Astron. Astrophys. **10**, 25.
Bahcall, J. N., and R. K. Ulrich, 1988, Rev. Mod. Phys. **60**, 297.
Bargholtz, C., 1979, Astrophys. J. Lett. **233**, 161.
Bethe, H. A., 1986, Phys. Rev. Lett. **56**, 1305.
Bethe, H., and C. L. Critchfield, 1938, Phys. Rev. **54**, 248.
Blin-Stoyle, R. J., and S. Papageorgiou, 1965, Nucl. Phys. **64**, 1.
Boothroyd, A. I., and I.-J. Sackmann, 1988, Astrophys. J. **328**, 653.
Boothroyd, A. I., 1992, private communication.
Braginskii, S. I., 1965, in *Reviews on Plasma Physics,* edited by M. A. Leontovich (Consultants Bureau, New York), Vol. 1, p. 205.
Brolley, J. E., 1971, Sol. Phys. **20**, 249.
Carlson, J., 1991, private communication.
Carlson, J., D. O. Riska, R. Schiavilla, and R. B. Wiringa, 1991, Phys. Rev. C **44**, 619.
Caughlan, G. R., and W. A. Fowler, 1988, At. Data Nucl. Data Tables **40**, 283.
Chen, C. X., and M. L. Cherry, 1991, Astrophys. J. Lett. **377**, 105.
Christensen-Dalsgaard, J., D. O. Gough, and M. J. Thompson, 1991, Astrophys. J. **378**, 413.
Christensen-Dalsgaard, J., D. O. Gough, and J. Toomre, 1985, Science **229**, 923.
Cox, A., 1990, in *Inside the Sun,* IAU Symposium 121, edited by G. Berthomieu and M. Cribier (Kluwer, Dordrecht), p. 61.
Cox, A., 1991, Astrophys. J. Lett. **381**, 71.
Cox, A., J. A. Guzik, and R. B. Kidman, 1989, Astrophys. J. **342**, 1187.
Cox, A., S. M. Morgan, F. J. Rogers, and C. A. Iglesias, 1992, Astrophys. J., in press.
Cox, A., and J. N. Stewart, 1970, Astrophys. J. **19**, 243.
Cox, A., J. N. Stewart, and D. D. Eilers, 1965, Astrophys. J. Suppl. Ser. **11**, 1.
Dautry, F., M. Rho, and D. O. Riska, 1976, Nucl. Phys. A **264**, 507.
Davis, R., Jr., 1964, Phys. Rev. Lett. **12**, 303.
Davis, R., Jr., 1978, in *Proceedings of Informal Conference on Status and Future of Solar Neutrino Research,* edited by G. Friedlander (Brookhaven National Laboratory, Upton), Report No. 50879, Vol. 1, p. 1.
Davis, R., Jr., 1987, in *Proceedings of Seventh Workshop on Grand Unification, ICOBAN'86, Toyama, Japan,* edited by J. Arafune (World Scientific, Singapore), p. 237.
Davis, R., Jr., 1989, in *Proceedings of the Thirteenth International Conference on Neutrino Physics and Astrophysics,* Boston, Massachusetts, 5–11 June 1988, edited by J. Schneps *et al.* (World Scientific, Singapore), p. 518.
Davis, R., Jr., D. S. Harmer, and K. C. Hoffman, 1968, Phys. Rev. Lett. **20**, 1205.
Davis, R., Jr., *et al.*, 1990, in *Proceedings of the 21st International Cosmic Ray Conference,* Vol. 12, edited by R. J. Protheroe (University of Adelaide, Adelaide), p. 143.
DeWitt, H. E., H. C. Graboske, and M. S. Cooper, 1973, Astrophys. J. **181**, 439.
Duvall, T. L., J. W. Harvey, K. G. Libbrecht, B. D. Popp, and M. A. Pomerantz, 1988, Astrophys. J. **324**, 1158.
Eddington, A. S., 1926, *The Internal Constitution of the Stars* (Cambridge University, Cambridge), p. 272.
Ewan, G. T., *et al.*, 1987, in "Sudbury Neutrino Observatory Proposal" (Sudbury Neutrino Observatory Collaboration, Queen's University at Kingston), Pub. No. SNO-87-12.
Faulkner, J., and F. J. Swenson, 1992, Astrophys. J. Lett. **386**, 55.
Filippone, B., 1986, Annu. Rev. Nucl. Part. Sci. **36**, 717.
Fontaine, G., and G. Michaud, 1979a, Astrophys. J. **231**, 826.
Fontaine, G., and G. Michaud, 1979b, in *White Dwarfs and Variable Degenerate Stars,* IAU Colloquium 53, edited by H. M. Van Horn and V. Weidmann (University of Rochester, Rochester), p. 192.
Fowler, W. A., G. R. Caughlan, and B. A. Zimmerman, 1975, Annu. Rev. Astron. Astrophys. **13**, 69.
Garcia, A., E. G. Adelberger, P. V. Magnus, H. E. Swanson, O. Tengblad and the Osolde Collaboration, and D. M. Motz, 1991, Phys. Rev. Lett. **67**, 3654.
Gari, M., 1978, in "Proceedings of Informal Conference on Status and Future of Solar Neutrino Research," edited by G. Friedlander (Brookhaven National Laboratory, Upton), Report No. 50879, Vol. 1, p. 137.
Gari, M., and A. H. Huffman, 1972, Astrophys. J. **178**, 543.
Gavrin, V. N., *et al.*, 1990, in *Inside the Sun,* IAU Symposium 121, edited by G. Berthomieu and M. Cribier (Kluwer, Dordrecht), p. 201.
Gavrin, V., *et al.*, 1992, in Proceedings of the XXVIth Internation Conference on High Energy Physics, Dallas, TX (to be published).
Glashow, S., 1961, Nucl. Phys. **22**, 579.
Glashow, S. L., and L. M. Krauss, 1987, Phys. Lett. B **190**, 199.
Gough, D., and J. Toomre, 1991, Annu. Rev. Astron. Astrophys. **29**, 627.
Gould, R. J., 1990, Astrophys. J. **363**, 574.
Gould, R. J., and N. Guessoum, 1990, Astrophys. J. Lett. **359**, 67.

Graboske, H. C., H. E. DeWitt, A. S. Grossman, and M. S. Cooper, 1973, Astrophys. J. **181**, 457.
Grevesse, N., 1984, Phys. Scr. **T8**, 49.
Grevesse, N., 1984, private communication.
Gribov, V., and B. Pontecorvo, 1969, Phys. Lett. B **28**, 493.
Guenther, D. B., A. Jaffe, and P. Demarque, 1989, Astrophys. J. **345**, 1022.
Haxton, W. C., 1986, Phys. Lett. **57**, 1271.
Hernández, J. J., *et al.*, 1990, Phys. Lett. B **239**, 1.
Hirata, K. S., *et al.*, 1989, Phys. Rev. Lett. **63**, 16.
Hirata, K. S., *et al.*, 1990a, Phys. Rev. Lett. **65**, 1297.
Hirata, K. S., *et al.*, 1990b, Phys. Rev. Lett. **65**, 1301.
Hirata, K. S., *et al.*, 1991, Phys. Rev. D **44**, 2241.
Holweger, H., A. Bard, A. Kock, and M. Kock, 1991, Astron. Astrophys. **249**, 545.
Holweger, H., C. Heise, and M. Kock, 1990, Astron. Astrophys. **232**, 510.
Hubbard, W. B., and M. Lampe, 1969, Astrophys. J. Suppl. Ser. **18**, 297.
Huebner, W. F., 1986, in *Physics of the Sun,* edited by P. A. Sturrock, T. E. Holzer, D. M. Mihalas, and R. K. Ulrich (Reidel, Dordrecht), Vol. I, p. 33.
Huebner, W. F., A. L. Merts, N. H. Magee, Jr., and M. F. Argo, 1977, "Astrophysical Opacity Library" (Los Alamos Scientific Laboratory), Report LA-6760-M.
Iglesias, C. A., and F. J. Rogers, 1991a, Astrophys. J. **371**, 408.
Iglesias, C. A., and F. J. Rogers, 1991b, Astrophys. J. Lett. **371**, 73.
Iglesias, C. A., and F. J. Rogers, 1991c, private communication.
Iglesias, C. A., F. J. Rogers, and B. G. Wilson, 1987, Astrophys. J. Lett. **322**, 45.
Iglesias, C. A., F. J. Rogers, and B. G. Wilson, 1990, Astrophys. J. **360**, 221.
Johnson, C. W., E. Kolbe, S. E. Koonin, and K. Langanke, 1992, Astrophys. J. **392**, 320.
Kamionkowski, M. P., and J. N. Bahcall, 1992, work in progress.
Kirsten, T., 1986, in *'86 Massive Neutrinos in Astrophysics and Particle Physics,* Proceedings of the Sixth Moriond Workshop, edited by O. Fackler and J. Tran Thanh Van (Editions Frontiéres, Gif-sur-Yvette), p. 119.
Kirsten, T., 1991, Nucl. Phys. B (Proc. Suppl.) **19**, 77.
Kolb, E. W., M. S. Turner, and T. P. Walker, 1986, Phys. Lett. B **175**, 478.
Krauss, A. H., H. W. Becker, H. P. Trautvetter, and A. Rolfs, 1987, Nucl. Phys. A **467**, 273.
Kuo, T. K., and J. Pantaleone, 1989, Rev. Mod. Phys. **61**, 937.
Lanou, R. E., H. J. Maris, and G. M. Seidel, 1987, Phys. Rev. Lett. **58**, 2498.
Leibacher, J. W., R. W. Noyes, J. Toomre, and R. K. Ulrich, 1985, Sci. Am. **253**, 48.
Libbrecht, K. G., 1988, Space Sci. Rev. **47**, 275.
Libbrecht, K. G., and J. M. Kaufman, 1988, Astrophys. J. **324**, 1172.
Lim, C.-S., and W. J. Marciano, 1988, Phys. Rev. D **37**, 1368.
Magee, N. H., A. L. Merts, and W. F. Huebner, 1984, Astrophys. J. **283**, 264.
Michaud, G., Y. Charland, S. Vauclair, and G. Vauclair, 1976, Astrophys. J. **210**, 447.
Mikheyev, S. P., and A. Yu. Smirnov, 1986a, Sov. J. Nucl. Phys. **42**, 913.
Mikheyev, S. P., and A. Yu. Smirnov, 1986b, Sov. Phys. JETP **64**, 4.
Mikheyev, S. P., and A. Yu. Smirnov, 1986c, Nuovo Cimento **C9**, 17.
Mikheyev, S. P., and A. Yu. Smirnov, 1989, Prog. Part. Nucl. Phys. **23**, 41.
Montmerle, T., and G. Michaud, 1976, Astrophys. J. Suppl. Ser. **31**, 489.
Moskalik, P., and W. A. Dziembowski, 1992, Astron. Astrophys. Lett. in press.
Noerdlinger, P. S., 1977, Astron. Astrophys. **57**, 407.
Noerdlinger, P. S., 1978, Astrophys. J. Suppl. Ser. **36**, 259.
O'Brian, T. R., M. E. Wickliffe, J. E. Lawler, W. Whaling, and J. W. Brault, 1991, J. Opt. Soc. Am. B **8**, 1185.
Paczyński, B., 1969, Acta Astron. **19**, 1.
Paczyński, B., 1970, Acta. Astron. **20**, 47.
Paczyński, B., 1974, Astrophys. J. **192**, 483.
Paquette, C., C. Pelletier, G. Fontaine, and G. Michaud, 1986, Astrophys. J. Suppl. Ser. **61**, 177.
Parke, S. J., 1986, Phys. Rev. Lett. **57**, 1275.
Parker, P. D., 1986, in *Physics of the Sun,* edited by P. A. Sturrock, T. E. Holzer, D. M. Mihalas, and R. K. Ulrich (Reidel, Dordrecht), Vol. I. p. 15.
Parker, P. D., and C. Rolfs, 1991, in *The Solar Interior and Atmosphere,* edited by A. Cox, W. C. Livingston, and M. S. Matthews (University of Arizona, Tucson), p. 31.
Pinsonneault, M. H., S. D. Kawaler, S. Sofia, and P. Demarque, 1989, Astrophys. J. **338**, 424.
Pontecorvo, B., 1946, Chalk River Report PD-205.
Prather, M. J., 1976, Ph.D. thesis (Yale University).
Press, W. H., B. P. Flannery, S. A. Teukolsky, and W. T. Vetterling, 1986, *Numerical Recipes* (Cambridge University, Cambridge, England).
Proffitt, C. R, and G. Michaud, 1991, Astrophys. J. **380**, 238.
Raghavan, R. S., 1990, in *Proceedings of the 25th International Conference on High Energy Physics, Singapore,* edited by K. K. Phua and Y. Yamaguchi (World Scientific, Singapore), Vol. I, p. 482.
Rogers, F. J., and C. A. Iglesias, 1991, private communication.
Rogers, F. J., and C. A. Iglesias, 1992, Astrophys. J. Suppl. Ser. **79**, 507.
Rosen, S. P., and J. M. Gelb, 1986, Phys. Rev. D **34**, 969.
Rosznyai, B., 1980 (quoted in Bahcall *et al.*, 1982).
Rowley, J. K., B. T. Cleveland, and R. Davis, Jr., 1985, in *Solar Neutrinos and Neutrino Astronomy,* AIP Conference Proceedings No. 126, edited by M. L. Cherry, W. A. Fowler, and K. Lande (American Institute of Physics, New York), p. 1.
Rozenblit, M., 1970, Phys. Lett. B **31**, 266.
Sackmann, I.-J., A. I. Boothroyd, and W. A. Fowler, 1990, Astrophys. J. **360**, 727.
Salam, A., 1968, in *Elementary Particle Theory,* edited by N. Svartholm (Almqvist and Wiksells, Stockholm), p. 367.
Salpeter, E. E., 1952, Phys. Rev. **88**, 547.
Schiavilla, R., R. B. Wiringa, V. R. Pandharipande, and J. Carlson, 1992, Phys. Rev.
Sienkiewicz, R., J. N. Bahcall, and B. Paczyński, 1990, Astrophys. J. **349**, 641.
Sienkiewicz, R., B. Paczyński, and S. J. Ratcliff, 1988, Astrophys. J. **326**, 392.
Stellingwerf, R. F., 1978, Astron. J. **83**, 1184.
Stothers, R. B., and C. Chin, 1991, Astrophys. J. Lett. **381**, 67.
Swenson, F. J., G. Stringfellow, and J. Faulkner, 1990, Astrophys. J. Lett. **348**, 33.
Totsuka, Y., 1990, in "Proceedings of the International Symposium on Underground Physics Experiments," edited by K. Nakamura (ICRR, University of Tokyo, unpublished), p. 129.
Turck-Chièze, S., 1990, in *Inside the Sun,* IAU Symposium 121,

edited by G. Berthomieu and M. Cribier (Kluwer, Dordrecht), p. 125.
Turck-Chièze, S., 1992, private communication.
Turck-Chièze, S., S. Cahen, M. Cassé, and C. Doom, 1988, Astrophys. J. **335**, 415.
Ulrich, R. K., and A. N. Cox, 1991, in *The Solar Interior and Atmosphere,* edited by A. Cox, W. C. Livingston, and M. S. Matthews (University of Arizona, Tucson), p. 162.
Vauclair, G., S. Vauclair, and G. Michaud, 1978, Astrophys. J. **223**, 920.
Vauclair, G., S. Vauclair, and A. Pamjatnikh, 1974, Astron. Astrophys. **31**, 63.
Voloshin, M. B., M. I. Vysotskii, and L. B. Okun, 1986a, Sov. J. Nucl. Phys. **44**, 440.
Voloshin, M. B., M. I. Vysotskii, and L. B. Okun, 1986b, Sov. Phys. JETP **64**, 446.
Wambsganss, J., 1988, Astron. Astrophys. **205**, 125.
Weinberg, S., 1967, Phys. Rev. Lett. **19**, 1264.
Wervelman, R., K. Abrahams, H. Postma, J. G. L. Booten, and A. G. M. Van Hees, 1991, Nucl. Phys. A **526**, 265.
Wolfenstein, L., 1978, Phys. Rev. D **17**, 2369.
Wolfenstein, L., 1979, Phys. Rev. D **20**, 2634.
Wolfenstein, L., 1986, in *Proceedings of the Twelfth International Conference on Neutrino Physics and Astrophysics, Sendai, Japan,* edited by T. Kitagaki and H. Yuta (World Scientific, Singapore), p. 1.
Wolfs, F. L. H., S. J. Freedman, J. E. Nelson, M. S. Dewey, and G. L. Greene, 1989, Phys. Rev. Lett. **63**, 2721.